2019-9

Laser-Induced Breakdown Spectroscopy (LIBS): a Potential Quality Tool for Infant Formula Manufacture

Xavier Cama Moncunill
Technological University Dublin

Laser-induced breakdown spectroscopy (LIBS): a potential quality tool for infant formula manufacture

Xavier Cama Moncunill

Technological University Dublin
School of Food Science & Environmental Health

PhD

Supervisors:
Dr. Carl Sullivan
Dr. Patrick J. Cullen

September, 2019

Abstract

Breast milk is considered the ideal food for infants. However, breastfeeding is at times supplemented or replaced with suitable alternatives. Infant formula (IF) is an industrially produced food intended as a breast milk substitute, which needs to satisfy, by itself, all nutritional requirements of infants. For this reason, it is of critical importance that IF provides the adequate amounts of nutrients including carbohydrates, fats, proteins, minerals and vitamins. Laser-induced breakdown spectroscopy (LIBS) is a promising emission spectroscopic technique for elemental analysis, which can provide real-time measurements with little to no sample preparation. Hence, the main goal of this thesis was to investigate the feasibility of LIBS as a quality tool for mineral analysis in infant formula manufacture. Experiments conducted in this work encompassed the determination of calcium and sodium contents in powdered IF samples, pelletising samples as the only sample preparation procedure; and ready-to-feed IF formula samples, by direct analysis of liquids without sample preparation. Partial least squares regression (PLSR) was utilised to develop suitable linear regression models to predict calcium and sodium contents. Suitable fits for the regressions were obtained rendering coefficients of determination for cross-validation (R^2_{cv}) of 0.89–0.90 depending on the experiment, and low root-mean-square errors of validation (RMSEP), e.g. 0.68 mg g^{-1} for calcium determination of powdered IF in an assessed range of approx. 1–6 mg g^{-1}. Furthermore, chemical elemental maps for the pelletised powdered samples were generated to study the homogeneity of the sample surface. The studies conducted in this work substantiated the potential of this technology for mineral quantification and monitoring of powdered and liquid IF samples.

Declaration

I certify that this thesis which I now submit for examination for the award of Doctor of Philosophy, is entirely my own work and has not been taken from the work of others, save and to the extent that such work has been cited and acknowledged within the text of my work.

This thesis was prepared according to the regulations for graduate study by research of the Technological University Dublin and has not been submitted in whole or in part for another award in any other third level institution. The work reported on in this thesis conforms to the principles and requirements of the TU Dublin's guidelines for ethics in research.

TU Dublin has permission to keep, lend or copy this thesis in whole or in part, on condition that any such use of the material of the thesis be duly acknowledged.

Signature:

Date:

Acknowledgements

Firstly, I wish to express my gratitude to my supervisor Dr. Carl Sullivan for his continuous, inestimable guidance and support throughout my PhD work. I would like to thank him as well for his willingness to help as a friend. This thesis would not have been possible without him.

My sincere thanks also goes to Dr. P.J. Cullen for his advice, help and encouragement during my research.

I am very grateful to Dr. Maria Markiewicz-Keszyckca for sharing her knowledge with me, and for her help and support during all the years. I also want thank Dr. Maria Casado for sharing her experience and insights with me. To both of them I am grateful for not only being a point of reference, but also friends.

I would also like to take this opportunity to thank my colleagues and friends: Agata, Anna, Yash, Chaitanya, Eva, Laurence, Apurva, Shashi, Kompal, Sebnem, Kim, Lu, Daniela and Toufic, for all the fun and laughs we have had in the last four years. Besides my friends in TU Dublin, I want to thank as well my friends who have accompanied me all this time: Masó, Quimi, Pablo, Faulon, Llinàs, Tristan, Tommy, Ot, Paula, Stephanie, Lutz.

Last but not least, I would like to thank my parents and my sister, Raquel, to whom I am deeply grateful. Their unending love and support has been indispensable for me to come so far.

This work was supported by the Food Institutional Research Measure, administered by the Department of Agriculture, Food and the Marine of Ireland (Grant agreement: 14/F/866).

Contents

List of Figures

List of Tables

Abbreviations and nomenclature

σ	Standard deviation
g	Gram
Hz	Hertz
L	Litre
M	Molar
mg	Milligram
mJ	Millijoule
mL	Millilitre
ms	Millisecond
nm	Nanometre
ppm	Parts per million
R^2	Coefficient of determination
R^2_{cv}	Coefficient of determination for cross-validation
R^2_c	Coefficient of determination for calibration

R_p^2 Coefficient of determination for prediction

W Watt

μs Microsecond

AAS Atomic absorption spectroscopy

ANN Artificial neural networks

AOAC Association of official analytical chemists

CCD Charged coupled device

CF-LIBS Calibration free laser-induced breakdown spectroscopy

CV Cross-validation

EEA European economic area

FAO Food and agriculture organization of the United Nations

FDA Food and drug administration

FOF Follow-on formula

FSAI Food Safety Authority of Ireland

FSANZ Food standards Australia New Zealand

ICP-MS Inductively coupled plasma mass spectroscopy

ICP-OES Inductively coupled plasma optical emission spectroscopy

IF Infant formula

IUPAC International union of pure and applied chemistry

LIBS Laser-induced breakdown spectroscopy

LOD Limit of detection

LOO Leave-one-out

LOQ Limit of quantification

LTE Local thermodynamic equilibrium

LV Latent variable

MSC Multiple scatter correction

Nd:YAG Neodymium-doped yttrium aluminium garnet

PAT Process analytical technology

PC Principal component

PCA Principal component analysis

PDO Protected designation of origin

PFOF Powdered follow-on formula

PIF Powdered infant formula

PLS Partial least squares

PLS-DA Partial least squares discriminant analysis

PLSR Partial least squares regression

QbD Quality by design

RMSE Root-mean-square error

RMSEC Root-mean-square error of calibration

RMSECV Root-mean-square error of cross-validation

RMSEP Root-mean-square error of prediction

RSD Relative standard deviation

RTF-FOF Ready-to-feed follow-on formula

RTF-IF Ready-to-feed infant formula

SD Standard deviation

SLR Simple linear regression

SNV Standard normal variate

WHO World health organization

Chapter 1

Introduction

1.1 Infant formula and mineral analysis

Milk and dairy products often play an important role in the human diet, especially with regard to infants and children. Breast milk is considered the ideal food for infants since it provides a well-balanced nutrition and other biological properties with added health benefits (Lesniewicz, Wroz, Wojcik, & Zyrnicki, 2010). However, there are circumstances in which a breast milk substitute is needed. Infant formula (IF) is an industrially produced food designed to satisfy by itself all nutritional requirements of infants (Codex, 2007). Therefore, IFs must provide adequate amounts of nutrients such as carbohydrates, fats, and proteins (macronutrients); as well as minerals and vitamins (micronutrients), which also play an indispensable role in infant nutrition (Montagne, Van Dael, Skanderby, & Hugelshofer, 2009). Minerals are inorganic substances found in relatively low concentrations in the human body; nevertheless, involved in numerous functions. Calcium, for instance, is an essential mineral with functions primarily related to growth and maintenance of bones (Vavrusova & Skibsted, 2014). Since it is of crit-

ical importance to ensure the quality and nutritional profile of IF for the safety and well-being of children, manufacturers need reliable and efficient analytical methods.

Conventional well-established methods for mineral analysis in infant formula and milk powders include atomic absorption spectroscopy (AAS), inductively coupled plasma optical emission spectroscopy (ICP-OES) and inductively coupled plasma mass spectroscopy (ICP-MS) (Poitevin, 2016). These methods, despite their high sensitivity and accuracy, generally require time-consuming and laborious sampling procedures and the use of chemical reagents such as acids and gases, as well as an associated high cost of consumables (e.g. argon) (G. Kim, Kwak, Choi, & Park, 2012).

Laser-induced Breakdown Spectroscopy (LIBS), yet recent in the area of food analysis, has gained remarkable popularity in the last few years with an increase in the number of publications and extensive reviews concerning food samples (Markiewicz-Keszycka et al., 2017; Sezer, Bilge, & Boyaci, 2017). The advantages that LIBS offers compared to the conventional methods are its speed (with typical LIBS setups allowing laser repetition rates in the range of 1–10 Hz; hence, as a reference, at the speed of 1 Hz 100 measurements take 1 min and 40 s); a relatively low cost concerning the instrumentation, as well as its operating cost; little to no sample preparation; and elemental surface mapping capabilities (Casado-Gavalda et al., 2017; Dixit, Casado-Gavalda, Cama-Moncunill, Cama-Moncunill, et al., 2017). Further attractive features include: remote sensing, as it constitutes an entirely optical technique, and suitability for on-/at-line applications, allowing the technology to be considered a potential process analytical technology (PAT) for qualitative and quantitative chemical analysis (Cullen, Bakalis, & Sullivan, 2017).

The new paradigm in the food industry, inspired by the concepts of process analytical technology (PAT) and quality by design (QbD), is that the quality of food products should not be tested post-production, instead quality should be built-in or by process design. With the goal of improving the robustness and efficiency of manufacturing processes and final product quality, this paradigm aims to shift from a post-problem process control (off-line product testing) to an active, continuous process control (at-line, on-line or in-line analysis), where process adjustments can be performed during manufacturing. To achieve this, PAT and QbD encourage the adoption of real-time analytical tools and chemometrics for the continuous monitoring and control of core quality parameters (FDA, 2004; van den Berg, Lyndgaard, Sørensen, & Engelsen, 2013). Therefore, the development of new analytical techniques with real-time capabilities is an opportunity for the IF industry to boost its competitiveness and productivity.

Despite the advantages of LIBS and its potential as a PAT, this analytical method also has limitations or drawbacks, especially concerning quantitative analysis. Some of these limitations include signal fluctuations on a shot-to-shot basis (Tognoni & Cristoforetti, 2016) and difficulties in establishing good calibration curves due to strong matrix effects (Ferreira et al., 2010; Lei et al., 2011). Matrix effects are caused by changes in the physical and chemical properties among samples and standards, which can lead to differences in the LIBS signal and, consequently, differences in the analyte concentration (Babos, Barros, Nóbrega, & Pereira-Filho, 2019). Several publications evaluating and discussing strategies with the goal of overcoming such problems can be found in the literature (dos Santos Augusto, Barsanelli, Pereira, & Pereira-Filho, 2017; El Haddad, Canioni, & Bousquet, 2014; Jantzi et al., 2016). Some of these strategies include the use of spectral pre-processing techniques, e.g. normalisation, baseline correction; multivariate analysis techniques, e.g. partial least square regression, artificial neural

networks; and sample preparation procedures, e.g. dilution of the matrix with the use of materials that do not produce strong matrix effects.

1.2 Objectives and overview of the thesis

The main objective of this thesis is to demonstrate the feasibility of LIBS as a quality tool for IF manufacture. As previously mentioned, LIBS offers a range of advantages which could benefit the IF industry. For instance, its real-time feature could be used to monitor manufacturing processes such as mixing of raw materials with the aim of improving manufacturing efficiency and final product quality. However, LIBS also has disadvantages such as high detection and quantification limits. For this reason, this work not only explored the possibility of LIBS for mineral analysis of IF products, but also studied strategies and different methodologies for overcoming these drawbacks and obtaining accurate results.

The present work is divided into eight chapters, which covered an introduction, a review of literature, the main experiments of this research, conclusions and recommendation for future studies. A concise explanation of the contents of each chapter is provided below:

- **Chapter 1 – Introduction**

  Brief introduction and contextualisation of the work in the thesis. In this chapter the main objectives of the thesis are also provided.

- **Chapter 2 – Literature review**

  Review of the main concepts related to the conducted research, especially regarding infant formula, LIBS and data analysis.

- **Chapter 3 – Material and methods**

Summary of the materials, instrumentation and methodologies used in the experiments.

- **Chapter 4 – LIBS as an at-line validation tool for calcium determination in IF**

  Evaluation of the potential of LIBS as an at-line tool for calcium quantification in powdered IF, as well as chemical mapping of calcium distribution on the sample surface as a means of assessing sample homogeneity.

- **Chapter 5 – Sampling effects on the quantification of sodium in IF**

  Study of strategies concerning sampling and pre-processing techniques for mineral analysis and assessment of the performance of LIBS for sodium analysis of powdered IF.

- **Chapter 6 – Direct analysis of calcium in liquid IF**

  Evaluation of LIBS feasibility for calcium quantification in liquid (ready-to-feed) IF samples with the use of a sample chamber especially designed for liquid experimentation.

- **Chapter 7 – Concluding remarks and future recommendations**

  Summary of the main conclusions of the developed research and recommendations for further related work.

Chapter 2

Literature review

2.1 Infant formula

Infancy is a crucial growth period, in which an adequate nutrition is decisive for a child's normal development. Breast milk is regarded as the ideal food for infants since it not only contains all the essential nutrients to satisfy their requirements, but also contains biological components which provide additional benefits ensuring proper development (Guo & Ahmad, 2014b). The World Health Organization (WHO) recommends exclusive breastfeeding for the first 6 months of life. Thereafter, infants should receive complementary foods while breastfeeding for up to 2 years (WHO, 2018). There are circumstances, nonetheless, in which breastfeeding is not possible or not preferable and, thus, a breast milk substitute is needed.

Infant formula is an industrially produced food intended to supplement or act as a substitute for human milk, and it is the only other food considered nutritionally acceptable for children less than 1 year of age (Guo, 2014a). Typically, IFs are based on cow's milk with subsequent adjustments with the addition of ingredients

to make them suitable for infant consumption (Jiang, 2014). Table 2.1 shows a comparison of the macro and micro nutrient contents in human milk and cow's milk.

Table 2.1: Gross composition in human and cow's milk.

Gross composition (%)	**Human milk**	**Cow's milk**
Protein	1.0	3.4
Casein	0.3	2.6
Whey	0.7	0.8
Fat	3.8	3.5
Lactose	7.0	5.0
Total solids	12.4	12.5
Ash	0.2	0.7

As observed in Table 2.1, cow's milk cannot be given directly to infants and several modifications are needed to meet the nutritional profile of human milk. Some of the typical adjustments include: the addition of whey protein in order to meet the casein/whey ratio in human milk, the addition of lactose (carbohydrates), and the adjustment of the calcium/phosphorus ratio, among other changes. The goal is to match the human milk nutrient profile and, hence, that it can fulfil the nutritional requirements of infants (Jiang, 2014; Sola-Larrañaga & Navarro-Blasco, 2006).

Despite the efforts in making IF as suitable as possible for infants, some of its components may pose a threat when given in excess or may cause difficulties when not provided in sufficient amounts. Moreover, the presence of contaminants such as heavy metals, pesticides or other substances can cause adverse health effects even in low concentrations (Ikem, Nwankwoala, Odueyungbo, Nyavor, & Egiebor, 2002; Pandelova, Lopez, Michalke, & Schramm, 2012). For instance, in 2007 powdered IF adulterated with melamine, a by-product of the coal industry

with numerous industrial uses, caused the hospitalization of more than 50,000 children in China (WHO, 2009). For these reasons, it is imperative to ensure that IF complies with all standards of quality.

2.1.1 Definition and classification of infant formula

The definition of IF according to the Codex Alimentarius Commission is *"a breast-milk substitute specially manufactured to satisfy, by itself, the nutritional requirements of infants during the first months of life up to the introduction of appropriate complementary feeding"* (Codex, 2007). Formulas intended for children from 6 to 12–36 months of age receive the name of follow-on formulas (FOF) and are regarded as foodstuffs designed for particular nutritional purposes when adequate complementary foods are introduced into the infant's diet (Montagne et al., 2009).

IFs are typically commercialised in a powder form (powdered infant formula, PIF) or in a sterilised liquid form (ready-to-feed infant formula, RTF-IF). The former (PIF) is generally cheaper, easier to transport and store, but must be mixed with water prior to its use, which can lead to errors in reconstituting the formula (Blanchard, Zhu, & Schuck, 2013; Guo & Ahmad, 2014a). Sterilised liquid formulas may be more convenient due to their ready to feed characteristic, i.e., they do not need preparation before their use. Moreover, sterile RTF-IF are the predominant choice for feeding pre-term, low-birth-weight or immunocompromised infants. However, they are generally found in the market at a relatively higher price (Happe & Gambelli, 2015; Marino, Meyer, & Cooke, 2013).

When considering the origin of the raw ingredients used, infant formulas can be classified into three major classes:

- **Milk-based formula:** The most common commercially available infant

formula, prepared from cow's milk with added vegetable oils, vitamins, and minerals, suitable for most healthy infants.

- **Soy-based formula:** Formulas based on soy protein as the sole protein source with added vegetable oils, corn syrup and/or sucrose. These formulas are suitable for those infants who are lactose intolerant or allergic to proteins in cow's milk.

- **Specialized formula:** A small percentage of infants require specialised formulas due to medical problems such as metabolic diseases, intestinal malformations or low-birth weight. These formulas may be based on protein hydrolysates, which are intended for infants allergic or intolerant to whole proteins (casein and whey) in cow's milk, or they may also be low-sodium formulas, for infants with restricted salt intake requirements, among other examples (Guo & Ahmad, 2014a; Montagne et al., 2009).

2.1.2 Regulations of infant formula

Manufacturers must comply with their local legislation on formulation and manufacturing practices of IFs. At national (or supranational) level, regulatory bodies such as the Food and Drug Administration (FDA) in the United States or the Food Standards Australia New Zealand (FSANZ) have issued regulations on legal requirements, manufacturing practices, and formulation guidelines for infant formulas. The role of such regulatory bodies is to set a normative framework for IF and to protect the customer (Jiang, 2014; Montagne et al., 2009). At international level, the Codex Alimentarius Commission, in collaboration with the Food and Agricultural Organisation (FAO) of the United Nations and the WHO, elaborates international food standards as a regulatory guidance to national authorities with the purpose of protecting consumers globally. Moreover, the Codex

Alimentarius Commission standards serve as the legal basis for international trade disputes (Montagne et al., 2009).

In Europe, the member countries of the European Economic Area (EEA) abide by the European Commission regulations on infant formulas and follow-on formulas. The Commission Directive 2006/141/EC law[1] (European Commission, 2006) provides a compositional criterion to be followed by the manufacturers, as well as for a list of permitted ingredients in order to satisfy the requirements on minerals, vitamins, amino acids, nitrogen compounds and other substances having a particular nutritional purpose. Furthermore, it lays down manufacturing practices such as labelling and packaging of the infant products. On a national level, in the Republic of Ireland, the Food Safety Authority of Ireland (FSAI) is the body responsible for food law enforcement to protect consumers.

2.1.3 Composition

The compositional criterion for IFs based on cow's milk established by the European Commission is shown in Table 2.2, which shows the permitted maximum and minimum values of energy, macro nutrients, micro nutrients and other compounds with a particular nutritional purpose.

Table 2.2: European Commission regulations on infant formulas made from cow's milk showing the permitted minimum and maximum contents of energy, macro nutrients, micro nutrients, and other compounds with a particular nutritional purpose.

Nutrient	Units	Minimum	Maximum
Energy	kJ/100 mL	250	295

continued

[1]This law will be replaced by the Commission Delegated Regulation (EU) 2016/127 which will start to apply in 2020.

Table 2.2: *(cont.)*

Nutrient	Units	Minimum	Maximum
Proteins	g/100 kJ	0.45	0.70
Lipids	g/100 kJ	1.05	1.40
Lauric acid and mystiric acid	% total fats	Not specified	20
Linoleic acid	mg/100 kJ	70	285
α-Linoleic acid	mg/100 kJ	12	Not specified
Carbohydrates	g/100 kJ	2.2	3.4
FOS[a] and GOS[b]	mg/mL	Not specified	0.8
Minerals			
Sodium	mg/100 kJ	5	14
Potassium	mg/100 kJ	15	38
Chloride	mg/100 kJ	12	38
Calcium	mg/100 kJ	12	33
Phosphorous	mg/100 kJ	6	22
Calcium: Phosphorous	ratio	1	2
Magnesium	mg/100 kJ	1.2	3.6
Iron	mg/100 kJ	0.07	0.3
Zinc	mg/100 kJ	0.12	0.36
Copper	μg/100 kJ	8.4	25
Iodine	μg/100 kJ	2.5	12
Selenium	μg/100 kJ	0.25	2.2
Manganese	μg/100 kJ	0.25	25
Fluoride	μg/100 kJ	Not specified	25
Vitamins			
Vitamin A	μg/100 kJ	14	43
Vitamin D	μg/100 kJ	0.25	0.65
Vitamin B1 (thiamin)	μg/100 kJ	14	72
Vitamin B2 (riboflavin)	μg/100 kJ	19	95
Vitamin B3 (niacin)	μg/100 kJ	72	375
Vitamin B5 (pantothenic acid)	μg/100 kJ	95	475
Vitamin B6	μg/100 kJ	9	42
Vitamin H (biotin)	μg/100 kJ	0.4	1.8
Vitamin B9 (folic acid)	μg/100 kJ	2.5	12
Vitamin B12	μg/100 kJ	0.025	0.12
Vitamin C	μg/100 kJ	2.5	7.5

continued

Table 2.2: *(cont.)*

Nutrient	Units	Minimum	Maximum
Vitamin K	μg/100 kJ	1	6
Vitamin E	mg/100 kJ	0.1	1.2

[a] Fructo-oligosaccharides
[b] Galacto-oligosaccharides

Proteins

Proteins are essential during early life, as they satisfy the need for nitrogen and provide necessary amino acids for body maintenance and growth. Cow's milk and human milk differ in their protein and amino acid profile. The main differences are, the total protein content, which in cow's milk is 2 to 3 times higher, and the whey to casein ratio, which in human milk is approx. 70:30 while in cow's milk is 20:80. Moreover, the amino acid profile also differs, human milk is richer in cysteine, and lower in tyrosine, phenylalanine and tryptophan (Blanchard et al., 2013; Montagne et al., 2009). For this reason, some modifications are needed:

- Reduction of the total protein content.
- Addition of whey protein.
- Enrichment with certain essential and semi-essential amino acids.

According to the European Commission regulations the protein content in cow's milk-based IF must be in the range of 0.45–0.70 g per 100 kJ.

Lipids

Lipids constitute a major energy source for infants providing 40–50 % of the daily energy intake of infants. Lipids also provide essential fatty acids such as linoleic

acid and α-linolenic, which are critical for optimal brain development, and fat-soluble vitamins (e.g. vitamins A, D, E, and K). Moreover, some lipids, especially long-chain polyunsaturated fatty acids (LC-PUFA), have important structural and functional roles for growth and development (Blanchard et al., 2013).

The lipid and fatty acid composition of human milk and cow's milk differs significantly and, therefore, some modifications are needed. To this end, different blends of vegetable oils are commonly added to IF, e.g. soya, sunflower, rapeseed, and palm, which are especially selected in order to meet the required lipid and fatty acid criteria. Also, IFs are often enriched with LC-PUFA such as arachidonic acid and docosahexaenoic acid, which are naturally present in breast milk and are involved in brain and visual development (Blanchard et al., 2013; Montagne et al., 2009).

The European Commission regulations on cow's milk-based IFs establishes a total lipid content in the range of 1.05–1.40 g per 100 kJ.

Carbohydrates

The main carbohydrates in human milk are lactose and oligosaccharides. The former is the main digestible carbohydrate in human milk and serves as a source of energy and plays an important role in growth and development. Oligosaccharides are indigestible carbohydrates which promote the development of intestinal flora and have an inhibitory function for certain pathogens. However, in cow's milk, the content of these carbohydrates is lower and their concentration is enhanced during manufacture of IF to meet the infant's nutritional lactose requirements, and benefit from the biological properties of oligosaccharides (Blanchard et al., 2013; Montagne et al., 2009).

According to the European Commission regulations the total carbohydrate content in cow's milk-based IF must be in the range of 2.2–3.4 g per 100 kJ, and a minimum lactose content of 1.1 g per 100 kJ.

Minerals and trace elements

Minerals and trace elements are essential nutrients for human health which have numerous functions in the human body. For instance, calcium and iron are essential for healthy growth. Iron is necessary for the red blood cells in order to transfer oxygen from the lungs to the blood, and calcium is essential for bone maintenance and growth, among other functions (Pehrsson, Patterson, & Khan, 2014). Therefore, infants must receive adequate amounts of minerals and trace elements so that they can grow and develop correctly.

Commonly, the following six elements are referred to as minerals: potassium, sodium, calcium, magnesium, phosphorous and chloride. These elements are present in IF with concentrations in the scale of mg per 100 kJ. For instance, the European Commission regulations establish a calcium content in IF in the range of 12–33 mg per 100 kJ. Whereas iron, copper, zinc, selenium, manganese and iodine are referred to as micro minerals or trace elements and are present in lower concentrations (μg per 100 kJ) (Montagne et al., 2009).

The studies presented in this thesis (Chapters 4 to 6) involved the determination of calcium and sodium in IF. Calcium, in cow's milk, is mostly found as part of colloidal particles, i.e. microscopic solid particles suspended in a fluid, which are composed of casein proteins and nanoclusters of calcium phosphate, forming the large structures known as casein micelles (de Kruif, Huppertz, Urban, & Petukhovb, 2012). Caseins constitute one of the most abundant type of proteins in cow's milk (around 80 % of total protein). It is important to note, however,

that calcium is also present in the serum phase of the milk. In the serum phase, calcium can be found in the form of free calcium (Ca^{2+}), or partially complexed to amino acids, peptides and whey proteins. In human milk, casein proteins are not as abundant as in cow's milk as seen in Table 2.1 (Section 2.1) having a higher proportion of whey proteins. The content of calcium in human milk is as well lower than that of cow's milk (Guo, 2014b; Vavrusova & Skibsted, 2014). Sodium is mainly found as a free ion (Na^{+}) in cow's milk in a higher concentration than that of human milk (Guo, 2014b; Masotti, Erba, De Noni, & Pellegrino, 2012). Although a minimum intake is indispensable for human health, excessive consumption of sodium is related to higher blood pressure and an increased risk of developing cardiovascular diseases (Masotti et al., 2012; Tamm, Bolumar, Bajovic, & Toepfl, 2016).

Partially demineralised whey is added to infant formula in order to match the casein to whey ratio in breast milk. Also, the addition of demineralised whey dilutes the remaining milk solids so that specific essential nutrients have to be added and brought to the optimum safe levels (Guo & Ahmad, 2014b). Therefore, after overall mineral and micro mineral content dilution, manufacturers need to enhance the content of minerals and micro minerals, which is accomplished by the addition of different salts (e.g. calcium carbonate) often in the form of carbonates, chlorides or citrates (Codex, 2007). Manufacturers, however, need to carefully select which salts to use since depending on their chemical form, the bioavailabity of the minerals may change drastically (Montagne et al., 2009).

2.1.4 Manufacture of powdered infant formula

PIF (powdered infant formula) is generally manufactured using either one of these two processes: dry mixing or wet mixing-spray process. The dry mixing process

involves blending the ingredients in a powdered form, while in the wet mixing-spray process ingredients are blended in a liquid phase (Jiang & Guo, 2014).

Dry blending

In the dry blending process, ingredients are received in a dehydrated powdered form and are mixed together in large batches until the nutrients are uniformly distributed throughout the batch. The final product is evaluated and tested to ensure it conforms to specifications and that no microbiological contamination has occurred during the process (Blanchard et al., 2013; Montagne et al., 2009).

The advantages of using the dry blending process are that it is more energy efficient and requires less investment for equipment, building, and maintenance. Also, since water is not involved in the dry blending process, the risk of microbiological contamination is significantly reduced (Jiang & Guo, 2014). However, the microbiological quality of a dry-blended product strongly depends on the microbiological quality of the powdered raw ingredients. In the dry blending process, there is no heat treatment to remove possible microbiological contamination, and as a consequence, if there are harmful bacteria present in one or more of the raw ingredients, these bacteria are likely to be present in the final product. Furthermore, differences in the densities of the raw ingredients may result in inhomogeneity in composition and appearance of the final product (Blanchard et al., 2013).

Wet blending-spray drying

The wet blending process is currently the most widely used method of producing PIF as it offers some advantages over the dry blending process (Montagne et al., 2009). Wet blending provides better uniformity of nutrient distribution, resulting in a more homogeneous PIF. Moreover, all quality aspects in the process, includ-

ing mixing of the PIF ingredients, evaporation and spray drying, can be more effectively controlled than those in the dry blending process (Blanchard et al., 2013; Jiang & Guo, 2014).

The manufacturing stages of PIF using the wet blending process can be observed in Figure 2.1. Wet blending consists of four main stages: preparation of the mix, high heat treatment, evaporation and drying. First, in the preparation of the mix, ingredients are blend together in a liquid form in order to achieve a uniform emulsion. The preparation of the mix can be carried out continuously or batch-wise. Water-soluble ingredients in a dry powder form are blended together with milk using a high shear mixer. The mix is then stored in a hydration tank to ensure full hydration of the ingredients. Water-soluble minerals previously dissolved in hot water are then added to the mix (Jiang & Guo, 2014; Montagne et al., 2009). At this point, the pH of the liquid mix can be adjusted as necessary with the addition of a base (such as sodium hydroxide) or citric acid solution. The liquid mix is then pasteurised to eliminate any possible pathogenic bacteria present in the raw materials or contamination during the process (Blanchard et al., 2013).

Due to differences in sensitivity to heat, oils and vitamins are normally mixed with the liquid preparation after pasteurisation. Fat-soluble ingredients are pre-heated and added to the pasteurised liquid mix. Fat-soluble vitamins are generally solubilised in oil separately in a small tank before being circulated into the main fat-soluble ingredient tank. After the pre-heating and addition of oils, a homogenisation and cooling step is carried out to obtain a stable and uniform liquid preparation (Blanchard et al., 2013; Montagne et al., 2009).

After blending of all ingredients, with the exception of encapsulated or heat sensitive ingredients, a high heat treatment is applied to the product mix either

before or after evaporation to destroy all pathogenic organisms (Blanchard et al., 2013; Jiang & Guo, 2014). The following step in the production of PIF is evaporation, which is an important process for water removal in the mix and solid content concentration. Moreover, PIF produced using evaporation prior to spray drying have a longer shelf life. The product is then commonly dried using a spray dryer. This process involves spraying the PIF product into a chamber filled with circulating hot air in the form of small droplets, which increases the surface area and allows a rapid mass transfer of heat and moisture (Jiang & Guo, 2014). The spray dried powder are then passed through a sifter and transferred to bags or silo for storage. Encapsulated ingredients or temperature sensitive ingredients are added to the final storage tank before the dry mixing process or mixed with the preparation prior to spray drying. At this point, the quality of the product is checked and evaluated. If the product conforms to the PIF specifications, the product is then prepared for packaging. PIF is usually packed with nitrogen gas in order to prevent the oxidation of the fat components (Jiang & Guo, 2014; Montagne et al., 2009).

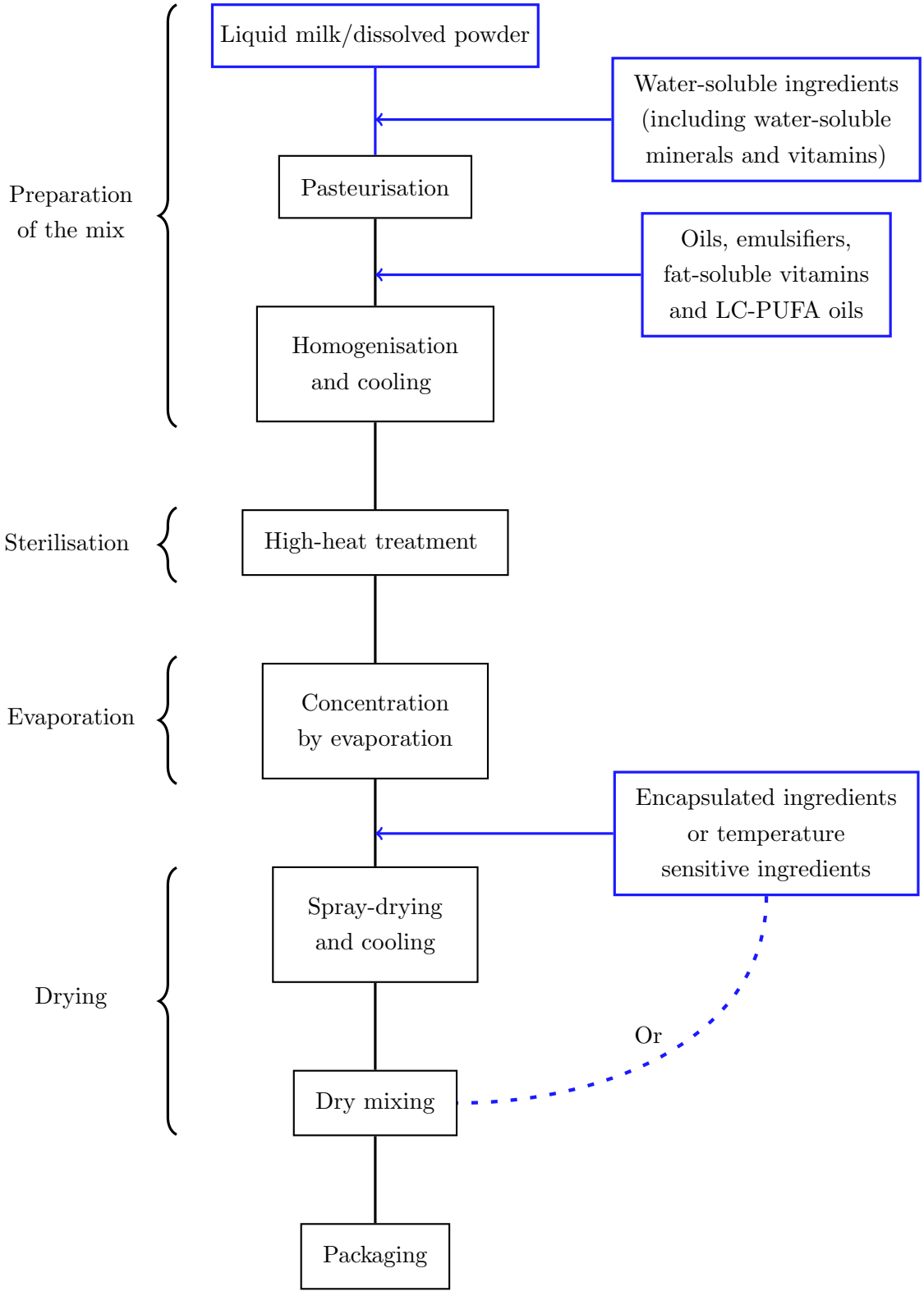

Figure 2.1: Manufacturing stages of PIF using the wet blending process. Source: adapted from Jiang and Guo (2014).

2.2 Process analytical technology and quality by design

Traditional quality assessment generally involves laboratory post-production testing on collected samples. Although this approach has been successful in providing quality products, scientific and technological advancements allow for new opportunities which can help improve manufacturing efficiency and final product quality. Process analytical technology is an initiative which originated in the early 2000's in the pharmaceutical field with the aim of improving the robustness of pharmaceutical manufacturing and quality assurance (Misra, Sullivan, & Cullen, 2015). The concept is that manufacturing processes should be controlled and assessed though timely measurements (i.e. real-time monitoring) of critical quality attributes of materials and processes (FDA, 2004). The implementation of PAT involves the application of real-time analytical techniques and chemometrics in order to gain process understanding by continuously monitoring and controlling core quality parameters. This knowledge can be subsequently utilised to modify the process to deal with incoming sources of variability (e.g. variability in raw materials) that affect final product quality, leading to a more robust and consistent manufacturing (Rathore, Chopda, & Gomes, 2016).

In the food industry, the new paradigm is quality by design (QbD). This paradigm, inspired by the PAT initiative, aims at ensuring the quality of food products by process design, i.e. real-time analysis of critical quality parameters, instead of relying only on post-production quality testing. QbD intends to shift from a post-problem process control (off-line product testing) to an active during-problem process control (at-line, on-line or in-line analysis), where process adjustments can be performed during manufacturing (van den Berg et al., 2013).

In manufacturing process control, depending on the location and speed at which chemical or physical information is provided by the sensors, it is possible to distinguish between the concepts: in-line, on-line, at-line and off-line. In-line and on-line measurements provide data continuously on a process line, which requires that the data collected at the measurement point are available in real-time or with only a short delay. In-line sensors are located in the main process line or accessed through a transparent material. On-line measurement points are located in a bypass stream line. In contrast, at-line and off-line measurements are not directly conducted in the process line. Instead, samples are taken from the line, and are analysed with instruments located in the production area: at-line analysis. If this is not possible, samples are taken to a laboratory for off-line testing (e.g. sample preparation and/or complex and expensive instrumentation required) (Kress-Rogers & Brimelow, 2001).

As for the food and pharmaceutical industries, with regard to infant formula there is also an increasing trend for the development of analytical methods suitable within the scope of QbD and PAT (including the use of at-line, on-line or in-line analysis). These methods need to be rapid, reliable and capable of effectively demonstrating control and confidence in the specifications and properties required by the infant formula industry.

2.3 Laser-induced breakdown spectroscopy

The invention of the laser in the 1960s led to the emergence of a new analytical technology known as laser-induced breakdown spectroscopy (LIBS) or sometimes laser-induced plasma spectroscopy (LIPS). Since its appearance, the technique has seen several applications and many improvements have been made in terms

of instrumentation (El Haddad et al., 2014). However, it has not been until the last decade that LIBS has gained notable popularity and it is now established as an analytical tool in various fields (Hahn & Omenetto, 2010). Probably one of the most recent well-known achievements has been the development of a portable LIBS system which landed on Mars in 2012 as part of a NASA expedition for the remote analysis of soils and rocks (Figure 2.2) (Cremers & Radziemski, 2013).

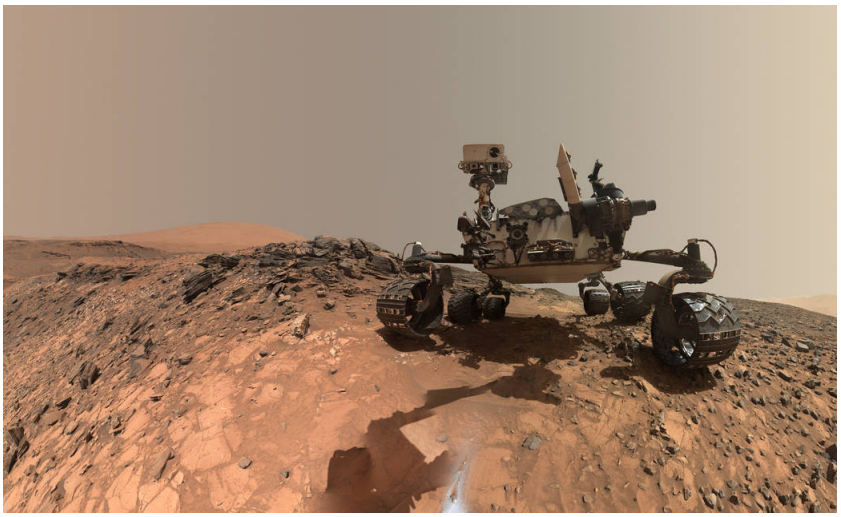

Figure 2.2: Photograph of the NASA's Curiosity Mars rover. Source: Jet Propulsion Laboratory (NASA) (2015).

In the area of food analysis, LIBS represents an emerging analytical technique for mineral assessment which offers advantages such as being a real-time method with little to no sample preparation. Further noticeable features are its ease of use, no need of chemical reagents and the possibility of conducting spatial distribution analysis (Anabitarte, Cobo, & Lopez-Higuera, 2012; Pathak et al., 2012). Moreover, it must be noted that this technique can be applied to any material regardless of its state (solid, liquid or gas) (T. Kim & Li, 2012).

Due to its advantages, LIBS has been drawing more and more attention in the field of food analysis and the number of publications has grown in recent years. Figure 2.3 shows a bar chart including the number of publications found in

the Web of Science database (Clarivate Analytics, 2019) for the period 2013–2018, searching the keywords "laser induced breakdown spectroscopy" and "food". With this search of keywords, it was observed that the first study using LIBS in food analysis was published in 1999. However, it was not until the early 2010s that the number of studies started to grow, incrementing year by year, reaching a maximum number of publications in 2018 with 44 publications.

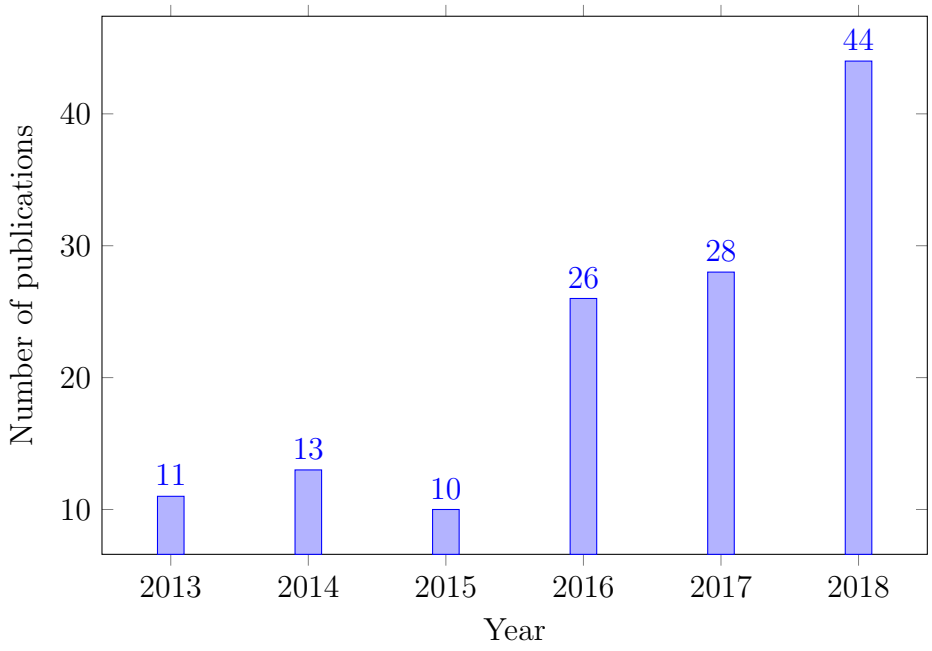

Figure 2.3: Number of publications per year (2013–2018) found in the Web of Science (Clarivate Analytics, 2019) database for the search entry: "laser induced breakdown spectroscopy" AND "food". Note that the option "All Databases" on the search menu of the Web of Science was selected for elaborating this bar chart.

2.3.1 Fundamentals of LIBS

Based on optical emission spectroscopy, LIBS employs laser pulses to vaporise small amounts (typically a few micrograms) of the sample's material and excite its elements (Andersen, Frydenvang, Henckel, & Rinnan, 2016). As a consequence of this laser-material interaction, high temperature plasma, which contains all the

excited species ablated from the target, is generated arising from the sample's surface. At the later stages of the plasma lifetime, as its temperature drops down, the excited species may emit characteristic light which can be subsequently analysed by spectrometers to infer the elemental composition of the sample (Anabitarte et al., 2012).

Plasma

Plasmas are the result of matter excitation through impacts of electrons on the particles ablated from the sample's surface, and consist of an overall electrically neutral assembly of atoms, ions, molecules and free electrons, in which the charged species often act collectively (Cremers & Radziemski, 2013; Jantzi et al., 2016). In LIBS, the goal is to generate a plasma whose elemental composition is the same as that of the sample. For that to happen, the plasma has to be optically thin and in local thermodynamic equilibrium (LTE), which means that the temperature is constant for all the species in the plasma (Hahn & Omenetto, 2010).

Plasmas are characterised by a variety of parameters such as degree of ionization, temperature, and electron density. The degree of ionization refers to the number of electrons that have been detached from their nucleus, and is measured as the ratio of electrons to other species (atoms, ions). Weakly ionised plasmas are those with low electron to atom/ion ratios, while at the other extreme, highly ionised plasmas are the ones with high electron to atom/ion ratios. Typically, LIBS plasmas have low electron to atom/ion ratios and fall in the category of weakly ionised plasmas (Cremers & Radziemski, 2013).

The first stage of the plasma lifetime is the ignition process, which takes place immediately after the laser pulse has been triggered onto the sample's surface (Figure 2.4a). At this point, the temperature of the plasma increases

rapidly, the sample material vaporises, and a crater is formed on the surface (Figure 2.4b) (Anabitarte et al., 2012). The early times are characterised by bond breaking, high ionization, and its associated emission spectrum is dominated by a strong background continuum. This continuum is mainly due to the processes of bremsstrahlung (free-free transitions) and recombination (free-bound transitions). Bremsstrahlung refers to the emission of photons by free electrons accelerated or decelerated in collision, while recombination occurs when a free electron is captured into an ionic or atomic level and a photon is released. For LIBS measurements, a delay time is needed to avoid such background continuum radiation (Cremers & Radziemski, 2013; Rakovský, Čermák, Musset, & Veis, 2014).

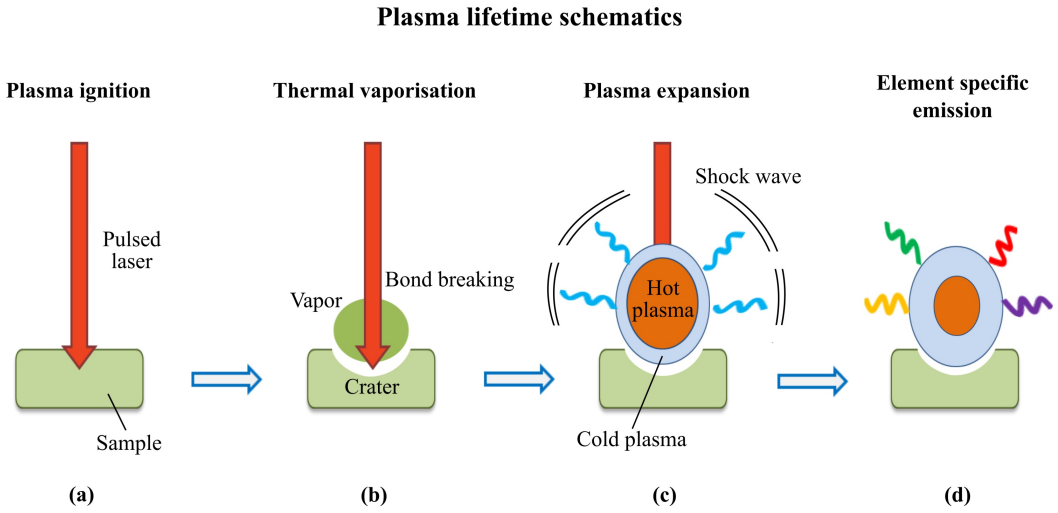

Figure 2.4: Schematic representation of the plasma lifetime.

After the vaporisation of the sample's material, the plasma expands compressing the surrounding medium and generating shock waves, while at the same time the temperature starts to drop, especially in the outer part of the plasma (Figure 2.4c). The plasma at this stage is a mixture of atoms and ions from both vaporised material and ambient gas (Anabitarte et al., 2012). Then, as the temperature of the plasma keeps decreasing (Figure 2.4d), the excited atoms and ions

within the plasma may return to the ground state and emit characteristic light in the process (Cremers & Radziemski, 2013).

Signal and spectra of LIBS

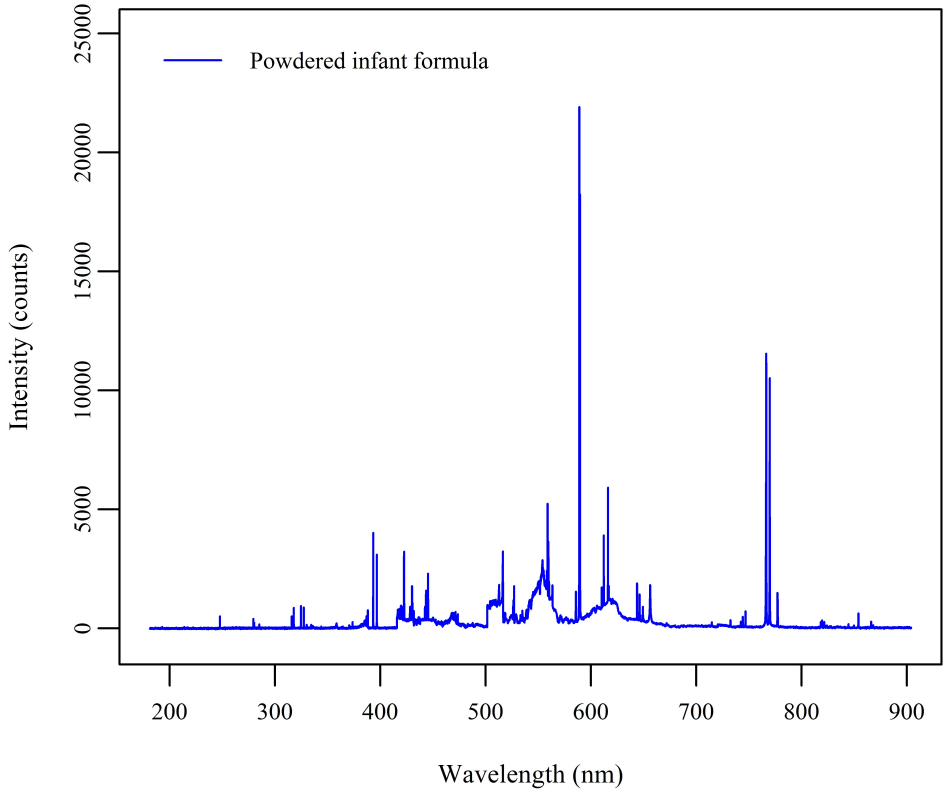

Figure 2.5: LIBS spectrum of powdered infant formula collected with a delay time of 1.27 μs and an integration time of 1.1 ms.

When conducting analysis with LIBS, the final goal is to obtain an emission spectrum by which the elemental composition of the sample can be inferred. Spectra consist of the intensity (number of photons reaching the detector) measured at each wavelength within the range of the spectrometer. An example spectrum of powdered infant formula is shown in Figure 2.5.

The intensity measured at a given wavelength is due to various phenomena. The analyte signal is the radiation emitted by the analyte element or characteris-

tic light related to a specific atomic or ionic transition at a given wavelength, e.g. emission of characteristic light due to atomic potassium (K I) at 766.49 nm. As previously seen, the plasma also emits radiation known as the background continuum. The overall intensity at a given wavelength is, therefore, the sum of the signals of both the analyte and the background continuum, plus a small contribution of the background introduced by the detector. Also, the signal is accompanied by noise, which is defined as the deviation from the average signal (Tognoni & Cristoforetti, 2016).

Figure 2.6 shows a schematic overview of the temporal history of a LIBS plasma. The signal increases rapidly and steadily at the early stages of the plasma, immediately after the laser pulse (strong background continuum). Shortly after the laser pulse incident, the signal starts decreasing gradually until the plasma emission is completely extinguished. Typical LIBS setups trigger the spectrometers with a delay time in the range of 1–10 μs approximately to avoid the background continuum radiation, and a gate window or integration time which may vary depending on the spectrometers used. The gate window refers to the exposure duration of the detector (Anabitarte et al., 2012; Rakovský et al., 2014).

LIBS spectra are also strongly dependent on the energy, pulse duration and spot size of the laser used, which affect plasma characteristics such as ablated mass and degree of ionization (Rakovský et al., 2014). Typically, in the area of food analysis, laser energies used are in the range of 30–100 mJ with pulse durations of 3–10 ns . Some other parameters related to laser-material interaction are fluence, which is a measure of energy per unit area (J cm^{-2}), and irradiance, which refers to energy per unit area and time (W cm^{-2}). Typical fluence values range from 25 to 50 J/cm^{-2} (Anabitarte et al., 2012; Markiewicz-Keszycka et al., 2017).

The number of laser pulses or shots performed on the sample's surface may

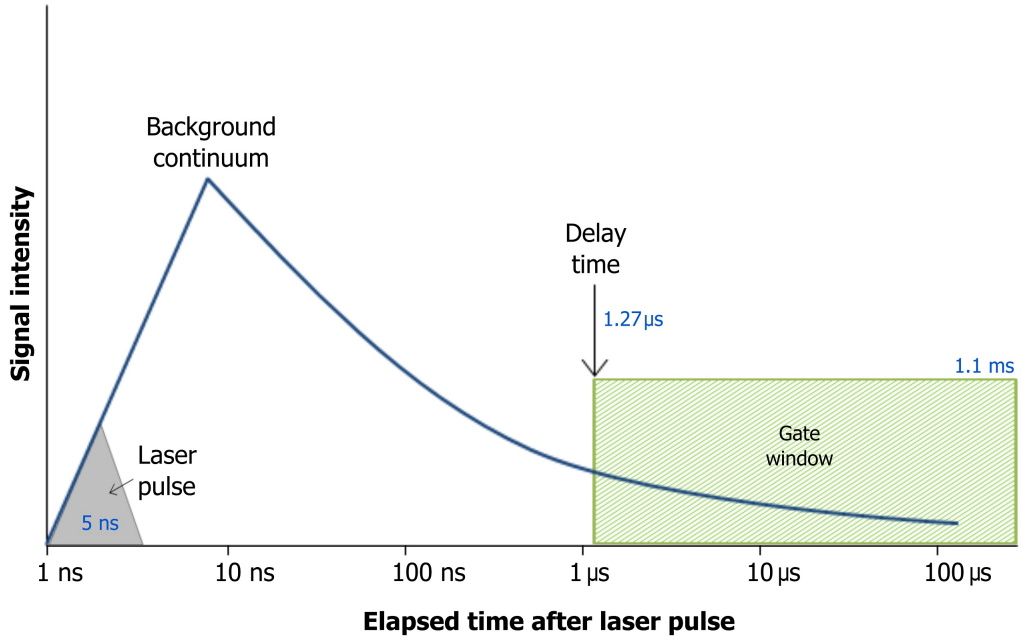

Figure 2.6: Schematic overview of the temporal history of a LIBS plasma. Time units in blue correspond to the particular values used in the experiments carried out in this thesis. Source: adapted from Cremers and Radziemski (2013)

.

vary depending on the sample material properties and experimental design. While for homogeneous samples a low number of shots may suffice, for complex and heterogeneous matrices such as food a higher number of shots at different locations within the sample are usually required in order to obtain a representative measurement. Also, spectra can be recorded on a shot-to-shot basis or after accumulation of the signal obtained from multiple shots (Tognoni & Cristoforetti, 2016).

2.3.2 State of the art

LIBS has been exploited for elemental analysis in a wide variety of fields (El Haddad et al., 2014; Jantzi et al., 2016), however, within food research it is still in its early days (Andersen et al., 2016). The method has been explored for

the determination of calcium in breakfast cereals (Ferreira et al., 2010), minor element concentrations in potatoes (Beldjilali et al., 2010), moisture content in cheese (Liu, Gigant, Baudelet, & Richardson, 2012), as well as for the classification of vegetable oils (Mbesse Kongbonga, Ghalila, Onana, & Ben Lakhdar, 2014) and the identification of meat species (Bilge, Velioglu, Sezer, Eseller, & Boyaci, 2016) among other applications.

Concerning dairy products, LIBS has been used previously for the analysis of milk and IF powders (Abdel-Salam, Al Sharnoubi, & Harith, 2013; Lei et al., 2011). Abdel-Salam et al. (2013) used LIBS for the qualitative assessment of spectral lines of nutritionally important minerals in breast milk and infant formulas, as well as the evaluation of proteins using the molecular bands of CN and C_2. In another publication, Lei et al. (2011) conducted a quantitative study in milk powders and IF. The authors employed LIBS for the determination of calcium content and other minerals by two different approaches: using calibration curves, which were obtained by mixing a reference sample with cellulose, and utilizing a calibration-free procedure which aided in overcoming matrix effects.

The potential of LIBS as at-line tool for industry has been evaluated in a recent publication (Andersen et al., 2016). The authors investigate the ability of LIBS in combination with chemometrics for the measurement of calcium content in mechanically separated poultry meat, as well as the feasibility of the method to be applied as a monitoring tool in a production setting for the detection of bone particles in deboned poultry meat.

Table 2.3 provides an overview of the recent applications of LIBS in the area of food analysis. The table includes a description of the study, type of product analysed, sample preparation procedures, data analysis, and emission lines used.

Table 2.3: Overview of LIBS applications in the field of food analysis.

Product	**Study**	**Sample preparation**	**Calibration method**[a] *pre-processing*	**Spectral lines** (I, atomic; II, ionic)	**Ref.**
Breakfast cereals	Quantification of calcium in breakfast cereals.	Samples were homogenised and pressed to make pellets.	Simple linear regression	Ca II 393.3 nm	Ferreira et al. (2010)
Potatoes	Determination of minor element mass fractions in potato skin and flesh.	Fresh potatoes were cut into cuboids of 10mm^2 surface and 5 mm height.	CF-LIBS	Mg I 383.83, 518.36; K I 769.90; Na I 588.99, 589.59; Ca I 431.86; Al I 394.40, 396.15; Li I 670.77; Si I 251.43, 251.61 nm	Beldjilali et al. (2010)
Skimmed milk powder and infant formula	Quantification of minerals in milk powders.	Milk powders were pelletised.	Simple linear regression and CF-LIBS	Ca II 317.9; K I 404.7; Mg I 517.2 nm	Lei et al. (2011)
Cheese	Moisture content determination in cheese samples.	2x1 cm pieces of Yellow American Cheese placed on microscope glass slides.	Simple linear regression *baseline correction, internal standardization*	Oxygen triplet at 777 nm	Liu et al. (2012)
Spinach leaves and rice	Quantitative analysis of minerals and detection of contaminants in spinach and rice.	Samples were washed, dried, ground, filtrated through mesh screens and pressed into pellets.	Simple linear regression and partial least squares-discriminant analysis *internal standardization*	Mg II 279.6; K I 766.5; Ca I 643.9 (spinach) 422.7 (rice); Na I 819.5 (spinach) 588.9 (rice) nm	G. Kim et al. (2012)
Wheat flour	Quantification of minerals and trace elements in wheat flour.	Samples were blended with binding agents and pressed into pellets.	Least squares regression (peak area)	P I 213.6; K I 404.4; Ca II 315.8; Mg I 285.2; Fe II 259.9; Cu I 324.7; Mn I 257.6; Zn II 202.5 nm	Peruchi et al. (2014)
Red Fuji apples	Detection of pesticide residues on apple surfaces.	Apples treated with different concentrations of pesticide were cut into pieces of 30 mm in diameter.	PCA *baseline correction*	P I 213.62, 214.91; S II 393.33; S IV 396.89; Cl I 837.50 nm	Ma and Dong (2014)

continued

Table 2.3: *(cont.)*

Product	**Study**	**Sample preparation**	**Calibration method**[a] *pre-processing*	**Spectral lines** (I; atomic, II; ionic)	**Ref.**
Orange fruits	Determination of copper content in orange peels.	Oranges were placed into vessels with different Cu solutions.	Simple linear regression	Cu I 324.754, 327.396 nm	Hu et al. (2015)
Bakery products	Determination of sodium and salt contents in bakery products.	Bread samples were dried and ground. Powdered bread samples were pressed into pellets.	Simple linear regression	Na I 589 nm	Bilge, Boyac, Eseller, Tamer, and Çakr (2015)
Milk powder and whey	Determination of whey adulteration rate in milk powder.	Milk powder and whey samples were obtained from cow's milk. Samples were freeze-dried, ground into powder, and subsequently pelletised.	PCA and PLS *SNV, second derivative, mean center*	PLS was applied to the spectra in the wavelength range of 575–756 nm.	Bilge, Sezer, et al. (2016)
Beef, pork and chicken	Identification of meat species and determination of meat adulteration rate.	Beef meat samples were adulterated with pork and chicken. Dried and defatted meat samples were ground, sieved and pressed into pellets.	PCA and PLS *second derivative, Poisson scaling, detrend, baseline, SNV, orthogonal signal correction*	PLS was applied to the whole spectra (approx.: 350–890 nm).	Bilge, Velioglu, et al. (2016)
Poultry meat	Calcium content determination in mechanically separated poultry meat.	Samples were thawed at 5 °C, stirred to mix the meat juice back into the sample and put into quadratic weighing dishes.	PLS	PLS was applied to: Ca II 392.10–394.60, 395.41–398.2; Ca I 421.11–424.29; Na I 587.71–590.78; K I 764.81–768.2, 768.5–771.28 nm	Andersen et al. (2016)
Dates	Identification and determination of elements (Ca, Mg, Cr) in date fruits under LTE conditions.	Date samples were deseeded, dried, ground and pelletised.	Simple linear regression	Mg I 277.9; Ca II 317.9; Cr I 520.4 nm	Mehder, Habibullah, Gondal, and Baig (2016)

continued

Table 2.3: *(cont.)*

Product	**Study**	**Sample preparation**	**Calibration method**[a] *pre-processing*	**Spectral lines** (I; atomic, II; ionic)	**Ref.**
Red wine	Classification of red wine samples based on their protected designation of origin (PDO).	Red wines with different PDO were mixed with collagen in order to form gel samples. Gels were then dried in square petri dishes.	Artificial neural networks	Spectral data was collected over the ranges: Mg 271–291; Ca 311–340, 390–429, 513–524; Na 581–598; H 640–675; K 760–783 nm	Moncayo, Rosales, Izquierdo-Hornillos, Anzano, and Caceres (2016)
Pumpkin, ash gourd, watermelon and musk melon seeds	Qualitative and quantitative study of minerals in cucurbit seeds.	Fruit seeds were ground, sieved, and defatted by soxhlet extraction. Samples were then pressed into pellets.	PCA and simple linear regression	Ca II 393.3; Mg II 279.5; Na I 588.9; K I 766.4 nm	Singh, Kumar, Awasthi, Singh, and Rai (2017)
Beef (lean beef, liver)	Copper content determination in beef as an indicator of offal adulteration.	Lean beef and liver were minced, dried and ground into powder. Powdered beef samples with varying content of liver were then pelletised.	PLS *SNV*	PLS was applied to spectra in the wavelength range 316.5–343.2 nm, which includes: Cu I 324.7, 327.4 nm.	Casado-Gavalda et al. (2017)
Beef (lean beef, liver)	Quantification of rubidium in beef.	Lean beef and liver were minced, dried, ground and sieved. Rubidium concentration in beef was spiked with liver. Samples were pelletised.	PLS *SNV*	PLS was applied to spectra in the wavelength range 774.53–784.82 nm, which includes: Rb I 780.01 nm.	Dixit, Casado-Gavalda, Cama-Moncunill, Markiewicz-Keszycka, et al. (2017)

[a] CF-LIBS, calibration-free LIBS; PCA, principal component analysis; PLS, partial least squares; SNV, standard normal variate.

2.3.3 Challenges

As previously seen, LIBS, in the area of food analysis, is still in its infancy. LIBS ability to perform qualitative analysis has been demonstrated in various publications (Abdel-Salam et al., 2013; Moncayo et al., 2016; Singh et al., 2017). However, quantitative analysis of food products often remains challenging. This may be due to the complexity and heterogeneous nature of food samples which can cause undesired matrix effects (Beldjilali et al., 2010). The matrix in which the analyte is embedded is known to considerably influence the emission responses of elements. Variability in the chemical and physical properties of the sample matrices can, therefore, affect notably the precision, accuracy and reproducibility of quantitative analysis in LIBS (Cremers & Radziemski, 2013; Tognoni, Cristoforetti, Legnaioli, & Palleschi, 2010).

In the literature, many publications can be found reporting the occurrence of matrix effects (Bilge, Velioglu, et al., 2016; Ferreira et al., 2010; Lei et al., 2011), as well as review articles providing an overview of the different approaches used to help overcome this limitation (El Haddad et al., 2014; Tognoni et al., 2010). Some of the strategies that have been employed to minimise matrix effects involve the development of regression models via matrix-matched reference standards, the use of multivariate data analysis/chemometrics, the internal standardization of spectral lines by using a reference element of known concentration, as well as the use of calibration-free LIBS (CF-LIBS) approaches (Anabitarte et al., 2012; El Haddad et al., 2014).

Another challenge of the LIBS technique is its complete application without any kind of sample preparation. Although LIBS can be used directly on food products (Beldjilali et al., 2010; Gondal, Habibullah, Baig, & Oloore, 2016; Hu et

al., 2015), as we can see in Table 2.3, it is a common practise to pelletise powdered samples (e.g. milk and infant formula powders), or even grind solid samples into fine powder to subsequently press it to make pellets. The reasons for this may be that LIBS analysis are influenced by particle size and smaller particles yield better results, and also, the analysis of hard, uniform surfaces generally improves quantitative analysis (Lal, St-Onge, Yueh, & Singh, 2007).

The studies presented in this thesis were aimed at addressing some of the challenges regarding quantitative analysis. Efforts focused on the assessment of different spectral pre-processing techniques, calibration model development, sampling method and sample preparation. Experiments regarding the determination of two essential minerals for infant growth and development (calcium and sodium) of powdered and ready-to-feed IF samples were conducted. Repeatability of experiments was ensured by preparing independent batches attempting to build robust calibration models which could predict mineral content accounting for physical and chemical variation in the IF products. Also, the selected calcium and sodium contents, over which calibrations were developed, were selected to be in agreement with international regulations on IF. This way, mineral contents analysed in the experiments were relevant for IF manufacture. LIBS potential of analysing macro and micro minerals comprises more elements than calcium and sodium. However, finding the optimal strategies for the determination of minerals may not be straightforward. In this regard, this thesis prioritised calcium and sodium as two of the most abundant minerals in IF and the study of optimal strategies for the development of LIBS as a rapid at-line tool for IF mineral analysis.

2.4 Chemometrics

Chemometrics involves the use of multivariate statistical techniques for the qualitative and quantitative assessment of analytical data. It offers advantages such as simultaneous analysis of multiple variables, data dimensionality reduction and extraction of relevant information (Kumar, Bansal, Sarma, & Rawal, 2014). Because of the complexity of LIBS spectra and the large sets of data which are often obtained, several chemometric techniques have been employed in LIBS analyses of food products both for qualitative and quantitative studies.

2.4.1 Pre-processing of collected data

Pre-processing techniques are applied to spectroscopic data in order to improve subsequent qualitative or quantitative analysis by removing undesired extraneous signal induced by the atmosphere or the instrument (Sobron, Wang, & Sobron, 2012). In LIBS analyses, techniques such as standard normal variate (SNV) transformation, multiple scatter correction (MSC), Savitzky-Golay filtering, normalisation by an internal standard, Euclidean norm, derivatives and Poisson scaling have been employed for the normalisation of spectra, correction of baseline shifts, or reduction of shot-to-shot fluctuations.

One of the methods found in various publications in the framework of LIBS is SNV. SNV belongs to a group of pre-processing techniques known as scatter-corrective methods (which also includes MSC). These techniques are designed to reduce the variability between samples due to scatter, as well as adjusting for baseline shifts between samples (Rinnan, van den Berg, & Engelsen, 2009). The computation of these techniques can be performed using the following equation (Equation 2.1).

$$x_{corr} = \frac{x_{org} - a_0}{a_1} \tag{2.1}$$

where x_{corr} is the corrected spectrum and x_{org} the original spectrum. The factors a_0 and a_1 can have different definitions depending on the technique used. For SNV, a_0 is the average value of the spectrum to be corrected and a_1 the standard deviation of the spectrum. Hence, for a given spectrum, SNV can be calculated as (Equation 2.2):

$$x_{SNV_i} = \frac{x_{org_i} - \overline{x}}{\sqrt{\frac{\sum_{i=1}^{N}(x_{org_i} - \overline{x})^2}{N-1}}} \tag{2.2}$$

where x_{SNV_i} and x_{org_i} are the SNV-transformed spectrum and original spectrum, respectively, at wavelength i; and $\overline{x}$ the average spectrum of the N number of wavelengths.

2.4.2 Qualitative analysis

Principal component analysis (PCA) is a technique mainly employed for data dimensionality reduction and pattern recognition (Cremers & Radziemski, 2013). PCA is an unsupervised technique as it does not require prior information with regard to object classes to develop the model. The aim of PCA is to simplify the analysis of data consisting of numerous variables while retaining the variation occurring in the dataset. To this end, new variables known as principal components (PCs) are calculated from linear combinations of the original variables on the basis of maximum variance (Miller & Miller, 2010). This way, the first set of PCs describes most of the variation in the dataset; the second set of PCs the next largest variation and so on. Normally, the first few PCs (generally accounting for

most of the variation) are then displayed as points on maps allowing the identification of similarity patterns between the samples (Abdi, 2010). PCA has been applied to LIBS data of food products in some studies (Bilge, Sezer, et al., 2016; Bilge, Velioglu, et al., 2016).

Partial least squares discriminant analysis (PLS-DA) is a partial least squares (PLS)-based technique used for classification. (G. Kim et al., 2012) demonstrated the possibility of using LIBS in combination with PLS-DA as a rapid discrimination tool for pesticide contaminated rice and spinach samples.

2.4.3 Quantitative analysis

PLS, also known as partial least squares regression (PLSR), is a multivariate statistical technique used to predict a dependent variable(s) or a response(s) (e.g. calcium content) from a set of independent variables or predictors (Lopes, Costa, Alves, & Menezes, 2004). PLS is particularly useful when the number of independent variables is considerably high, as such is often the case for spectroscopic data. This technique is based on the calculation of new variables known as latent variables or factors. These factors are linear combinations extracted from the predictors with the highest predictive ability and correlation with the responses (Miller & Miller, 2010). PLS simultaneously decomposes the original blocks of data X (predictors matrix) and Y (responses matrix) into smaller orthogonal matrices in such a way that the factors explain as much as possible of the covariance between X and Y. Ultimately, a linear regression model is developed by using that set of factors exhibiting better performance to estimate the responses (Abdi, 2010).

When establishing the calibration model, it is important to ensure that the model is not either under- or over-fitted. To this end, a commonly used technique

for identifying the optimum number of PLS factors is cross-validation (CV). Furthermore, PLS is generally followed by a validation step which is employed to assess the robustness and predictive accuracy of the model.

PLS has been used previously for the analysis of food with LIBS. Andersen et al. (2016) utilised PLS to develop a calibration model to predict calcium content in mechanically separated poultry meat. In another study, LIBS was also used in combination with PLS to determine the adulteration percentage of sweet/acid whey powders in milk powders (Bilge, Sezer, et al., 2016). Similarly, Bilge, Velioglu, et al. (2016) employed PLS to LIBS data to predict adulteration rates of pork and chicken in beef.

Artificial neural networks (ANN) are a computation method which can be used for both qualitative and quantitative analyses. ANN emulates the performance of neurons in the brain and their high degree of interconnection, hence this method consists of linked layers of artificial neurons by which a set of given inputs and outputs are associated. Prior to prediction of the outputs, ANN needs to be trained. To this end, a training set is used to infer the relationship between inputs and outputs so that it can be utilised to predict unknown input data (Yueh, Zheng, Singh, & Burgess, 2009). The network constantly adjusts and corrects itself until a certain degree of accuracy is reached, which is evaluated by a test set (Miller & Miller, 2010). Moncayo et al. (2016) used LIBS in combination with ANN as a screening tool for red wine origin discrimination.

2.5 Figures of merit and statistical parameters

A frequently reported figure of merit in LIBS papers is the limit of detection (LOD) (Bilge et al., 2015; Ferreira et al., 2010; Mehder et al., 2016; Peruchi et

al., 2014). The LOD is the lowest concentration of the measurand that can be detected at a specified level of confidence. For LIBS emission, a common definition of LOD refers to the LIBS signal significantly different from a blank concentration or background noise given by the following equation (Equation 2.3) (El Haddad et al., 2014; Peruchi et al., 2014):

$$LOD = \frac{k\sigma}{b} \tag{2.3}$$

where k is a coverage factor, σ is the standard deviation of the background noise or the blank concentration and b the slope of the calibration curve. It must be noted that k is normally given the values 2 (Bilge, Velioglu, et al., 2016; Gondal et al., 2016) or 3 (Hahn & Omenetto, 2012), where $k = 2$ roughly equals a 95 % confidence interval and $k = 3$ approximately 99 % (International Organization for Standardization, 2008).

Alternatively, the LOD can also be calculated using the equation below (Equation 2.4), which holds the advantage of being calculated entirely from the calibration curve (Hibbert & Gooding, 2006):

$$LOD = \frac{k\sigma_{y/x}}{b} \tag{2.4}$$

where k is a coverage factor as seen in Equation 2.3, $\sigma_{y/x}$ is the standard error of the regression and b the slope of the calibration curve. The standard error of the regression can be computed as:

$$\sigma_{y/x} = \sqrt{\frac{\sum_{i=1}^{N} (y_i - \hat{y}_i)^2}{N - 2}} \tag{2.5}$$

where y_i are the reference values, $\hat{y}_i$ the predicted values, and N the total number of samples.

However, for estimating the LOD value of multivariate regression models (such as PLS models), the above definition (Equation 2.3) is not entirely clear. For instance, in a multivariate model, the instrumental signals are not specific for a particular analyte (Allegrini & Olivieri, 2014).

In some publications (Cama-Moncunill et al., 2017; Casado-Gavalda et al., 2017), the limit of detection was computed according to the pseudounivariate approach ($\mathrm{LOD_{pu}}$) for PLS models in accordance with IUPAC official recommendations. $\mathrm{LOD_{pu}}$ calculation can be performed as shown in Equation 2.6 (Allegrini & Olivieri, 2014).

$$LOD_{pu} = \frac{3.3}{S_{pu}} \left[\left(1 + h_{0\ min} + \frac{1}{I} \right) var_{pu} \right]^{\frac{1}{2}} \tag{2.6}$$

where S_{pu} is the slope of the pseudounivariate line, $h_{0\ min}$ the minimum leverage when the analyte concentration is zero, I the number of samples employed for calibration and var_{pu} the variance of the regression residuals.

From the LOD value another figure of merit, the limit of quantification (LOQ), can be easily calculated (Equation 2.7). The LOQ refers to the minimum concentration of a measurand which can be reliably measured by an analytical procedure. Alternatively, it can be calculated by Equation 2.8.

$$LOQ = 3.3 \times LOD \tag{2.7}$$

$$LOQ = \frac{10\sigma}{b} \tag{2.8}$$

where, as for the calculation of the LOD, σ is the standard deviation of the background noise and b the slope of the calibration curve. The LOQ value, however, is rarely presented in LIBS works (El Haddad et al., 2014).

The precision of LIBS measurements, which can be defined as the closeness of the agreement between the results of successive measurements, is given by the standard deviation (SD) or the relative standard deviation (RSD) (El Haddad et al., 2014; Tognoni & Cristoforetti, 2016). The SD and RSD definitions can be found in Equation 2.9 and Equation 2.10, respectively.

$$SD = \sqrt{\frac{\sum_{i=1}^{N}(y_i - \overline{y})^2}{N-1}} \tag{2.9}$$

$$RSD\ (\%) = \frac{SD}{\overline{y}} \times 100 \tag{2.10}$$

where $\overline{y}$ and SD represent the mean value and standard deviation of the y_i predicted concentrations of the N samples.

When reporting a calibration model, a commonly presented figure of merit is the root-mean-square error (RMSE) (Andersen et al., 2016; Bilge, Velioglu, et al., 2016; Peruchi et al., 2014). The RMSE (Equation 2.11) is a measure of the closeness between the model-predicted concentration values and the reference values. RMSE values for calibration, cross-validation and prediction were calculated for all the calibration models developed in the experimental chapters to establish and compare the performance of the regressions.

$$RMSE = \sqrt{\frac{\sum_{i=1}^{N} (y_i - \hat{y}_i)^2}{N}} \tag{2.11}$$

where y_i are the reference values, $\hat{y}_i$ the predicted values, and N the total number of samples.

Chapter 3

Material and methods

3.1 Sample preparation

To explore the feasibility of LIBS for elemental analysis in IF, two main types of IF samples were prepared: solid (powdered) and liquid IF mixtures.

3.1.1 Powder mixtures

For solid sample preparation, PIF and powdered follow-on formula (PFOF) were acquired from a local store in Dublin, Ireland. Lactose (α-lactose monohydrate, $\geq$ 99 %), calcium carbonate ($CaCO_3$, $\geq$ 99 %) and sodium chloride (NaCl, $\geq$ 99 %) were purchased from Sigma Aldrich (Sigma Aldrich Ireland Ltd., Arklow, Ireland) to prepare mixtures with different contents of calcium and sodium.

Calcium

Five samples of PIF with varying content of calcium (Ca) were prepared for calibration (approx.: 1.1, 2.3, 3.7, 4.9, 6.1 mg Ca g^{-1}; roughly equivalent to 6.0,

12.0, 18.1, 24.1, 30.2 mg Ca 100 kJ^{-1}). One of the samples (Ca content of 3.7 mg g^{-1}) consisted only of PIF. The other four samples were obtained by mixing PIF with lactose or calcium carbonate in order to reduce or increase respectively the calcium content. To do so, proportional weights of lactose or calcium carbonate were added to IF to make a final weight of 225 g. Calculations were made on the basis of calcium contents in PIF provided by the manufacturer. Calcium contents for lactose and calcium carbonate were approximated to 0 % and 40 % (w/w) respectively. Blending of the samples was carried out using a laboratory V-mixer (FTLMV-1L&, Filtra Vibración S.L., Badalona, Spain) shown in Section 3.2 (Figure 3.1). These five calibration samples were intended to cover a range of calcium in accordance with the regulatory levels provided by the Codex Alimentarius Commission for PIF manufacturing. (Codex, 2007).

Sample preparation was repeated three times providing three independent sample sets (batches). To ensure the three batches were independent, each batch was obtained from a different PIF package (packages from the same PIF brand). Additionally, a batch contained 2 extra samples with calcium contents of approximately 3.0 mg g^{-1} and 5.5 mg g^{-1} for validation purposes. Thus, a total number of 17 samples was obtained (5 samples $\times$ 3 batches + 2 validation samples).

For LIBS analysis, pellets were prepared by pressing approx. 400 mg from each IF sample at 10 tons with a single die manual hydraulic press (Specac Ltd., Orpington, UK) for 3 minutes. Three replicate pellets were prepared per sample, hence, a total of 51 pellets were made (17 samples $\times$ 3 replicates).

Sodium

Samples with varying content of sodium (Na) were prepared by blending PIF with sodium chloride or lactose, with the goal to increase or decrease the sodium

content in the mix. A total of 7 samples were prepared, including one sample which consisted only of PIF. The selected range of sodium was approx. from 0.5 to 4 mg g^{-1} (concentrations corresponding to the lowest and highest Na content samples, respectively). In terms of energy, this range is approximately equivalent to 2.7–19.8 mg Na 100 kJ^{-1}. This range was intended to cover the regulatory sodium levels provided by the Codex Alimentarius Commission (Codex, 2007). Constituents of the mixtures (PIF, NaCl and lactose) and PFOF were ground and pre-mixed for 2 minutes using a laboratory blender (8011G, Waring Laboratory Science, Stamford, CT, USA) equipped with rotatory stainless-steel blades. This pre-mixing step was conducted to ensure that there were no aggregates occurring in the powders, hence improving subsequent blending efficiency performance. Dry mixing was then carried out using a laboratory V-mixer (FTLMV-1L&) for 20 minutes. In order to ensure reproducibility, two independent batches were prepared (batch 1 and batch 2). Each batch was composed of the aforementioned 7 samples divided into: 5 calibration samples (referred to as C1–C5), employed for PLS modelling, and 2 validation samples (V1 and V2) to test the robustness of the models. In addition to these validation samples, 2 different PFOF samples (V3 and V4) were used to assess the ability of the calibrations for predicting mineral content in infant products with different formulations. In total, 16 samples were obtained (7 samples $\times$ 2 batches + 2 PFOF samples).

Prior to LIBS analysis, powdered samples were pelletised by pressing approx. 400 mg of each sample using a manual hydraulic press fitted with a 13 mm pellet die (Specac Ltd.) at 10 tons for 3 minutes. Pellets were prepared in triplicates, giving a total number of 48 pellets (16 samples $\times$ 3 replicates). The two batches of samples were measured on different days.

3.1.2 Ready-to-feed infant formula mixtures

For liquid experimentation, RTF-IF (ready-to-feed infant formula) was purchased from a local store in Dublin, Ireland. In this case, calcium content in the mixtures was increased using calcium chloride (anhydrous, 97 %, Lancaster Synthesis, Morecambe, UK) or diluted with distilled water. Also, ready-to-feed follow-on formula (RTF-FOF, formulas intended for children over 6 months of age) was acquired from a local store in Dublin.

A total of three sample batches were prepared for calibration, each batch consisting of five samples (C1–C5) with varying content of calcium in the range of approx. 10–90 mg 100 mL^{-1}. Range of calcium roughly equivalent to 3.6–32.7 mg 100 kJ^{-1} . To prepare the different samples, RTF-IF was mixed with calcium chloride (anhydrous, 97 %, Lancaster Synthesis, Morecambe, UK) or distilled water to increase or decrease the calcium content in the mixtures, except for sample C3 which only consisted of the unmodified RTF-IF. Calculations required for sample preparation were made on the basis of the calcium contents provided by the manufacturers. To ensure reproducibility, each of the three batches was obtained from different RTF-IF bottles and prepared on different days. The calcium contents of the samples were selected intending to cover, approximately, the regulatory calcium range of the Codex Alimentarius Commission (Codex, 2007).

Aiming to test the predictive ability of the calibration models, two validation samples were prepared with calcium contents differing to those of the calibration samples (V1, approx. 20 mg 100 mL^{-1}; V2, approx. 60 mg 100 mL^{-1}). Additionally, RTF-FOF was used as an extra validation sample (V3, approx. 70 mg 100 mL^{-1}) to assess the ability of the models for predicting calcium content in formulas with different composition. In total, 18 samples (5 calibration samples

× 3 batches + 3 validation samples) were obtained. All samples were prepared in triplicates, thus, giving a final number of 54 sample solutions (18 samples × 3 replicates).

3.2 Equipment

Homogenization of powder mixtures was carried out using a laboratory V-mixer (Figure 3.1).

Figure 3.1: Laboratory V-mixer FTLMV-1L& (Filtra Vibración S.L.).

3.2.1 Atomic absorption spectroscopy

Atomic absorption spectroscopy (AAS) was selected as the reference method for mineral analysis in IF. AAS requires sample preparation procedures of solid samples prior to their analysis, including digestion of organic matter and dilution with acid to bring the analyte concentration within the optimum range of the instrument.

Assessment of calcium and sodium contents of both powdered and ready-to-feed IF samples were conducted with AAS as the reference method. The AAS instrument used in the experiments was a Varian 55B AA spectrometer (Varian Inc., Palo Alto, CA, USA), shown in Figure 3.2.

Figure 3.2: Varian 55B AA spectrometer (Varian Inc.) located in the facilities of TU Dublin.

3.2.2 LIBS instrumentation

Solid sample chamber

For LIBS analysis of powder mixtures, emission spectra were recorded using a LIBSCAN-150 system (Applied Photonics Ltd., Skipton, UK). This system was equipped with: a 150 mJ passively Q-switched Nd:YAG laser (Ultra, Quantel laser, Bozeman, MT, USA), operating at 1064 nm with a pulse duration of 5 ns; six

fibre-optic spectrophotometers (AvaSpec, Avantes BV, Apeldoorn, Netherlands), covering the wavelength range of 181–904 nm; and a solid sample chamber fitted with a motorised three-axis translation stage (Applied Photonics Ltd.), which allowed the acquisition of LIBS data at multiple locations. Furthermore, the laser head of the LIBSCAN-150 also consisted of a CCD camera which enabled the size and shape of the craters generated by laser ablation to be observed. An image of the LIBS system used in the experiments is shown in Figure 3.3.

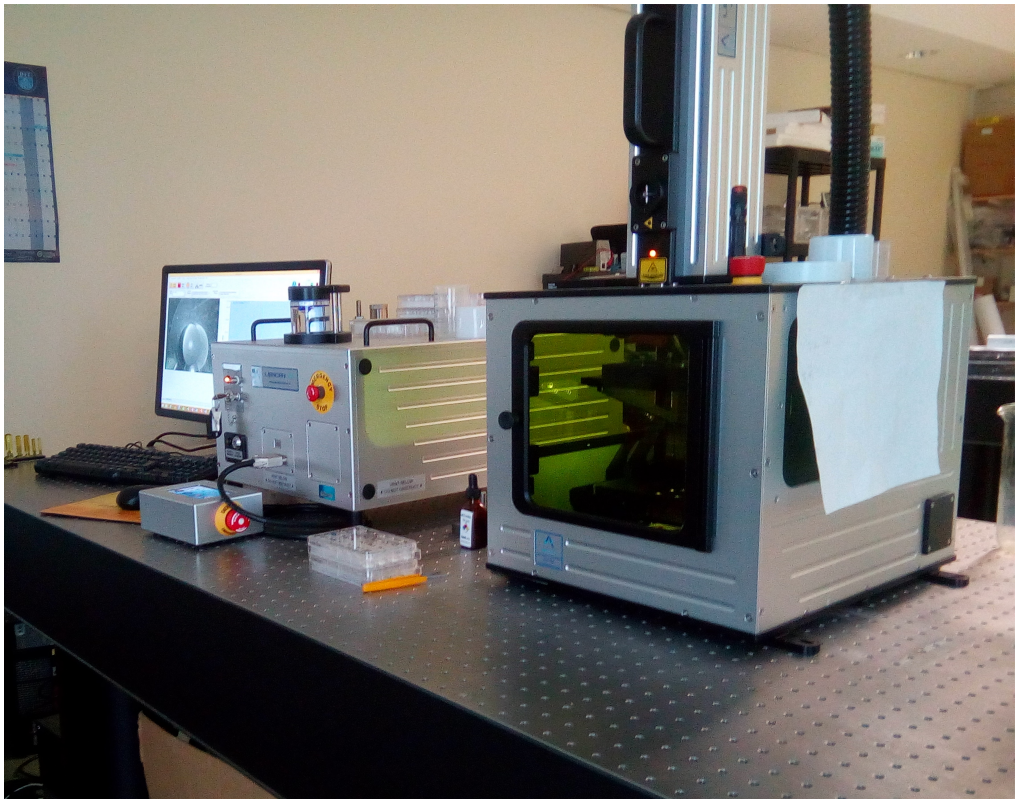

Figure 3.3: Photograph of the LIBSCAN-150 system (Applied Photonics) setup. The spectrometer unit can be seen on the middle of the image; attached to a solid sample chamber, on the right side; and connected to a computer, which enables the LIBS measurements to be monitored on the screen (left side).

Liquid sample chamber and variable energy laser

For the analysis of RTF-IF mixtures, spectra were recorded using a LIBS-6 system (Applied Photonics Ltd.) which comprised a 150 mJ Q-switched Nd:YAG laser (Nano SG 150-10, Litron lasers Ltd., Rugby, UK) with a pulse duration of 5 ns, and six spectrometers (AvaSpec, Avantes BV) covering the wavelength range of 181–904 nm. The system was also fitted with a liquid chamber (SC-LQ2, Applied Photonics Ltd.) consisting of a rotatory nickel-plated stainless-steel wheel and a liquid reservoir. An image of the liquid sample chamber is shown in Figure 3.4.

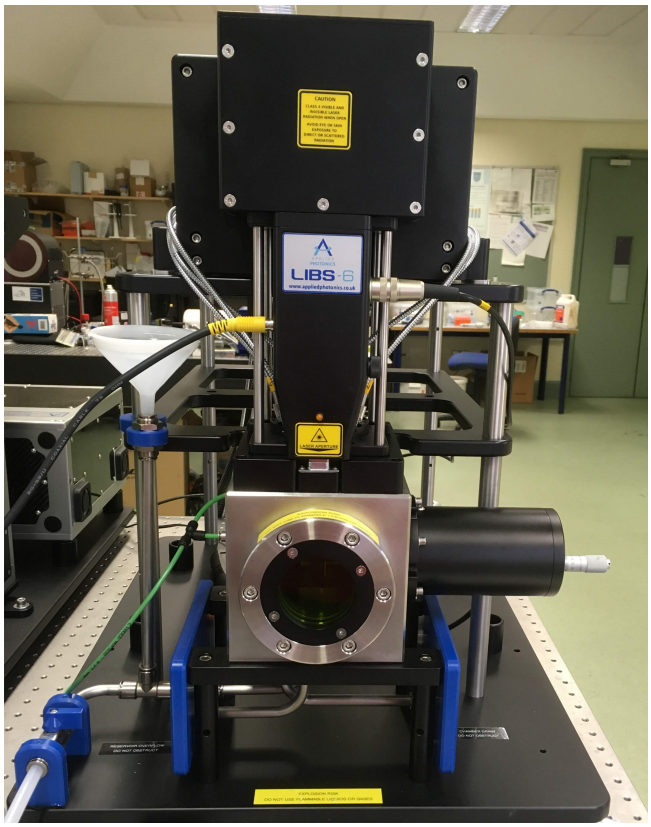

Figure 3.4: Photograph of the liquid sample chamber (SC-LQ2, Applied Photonics Ltd.) used in the assessment of RTF-IF mixtures.

To present liquids to the laser, the rotating wheel is partially submerged in the liquid, forming a thin film on the exposed region as it emerges from the liquid reservoir. This way, the film is constantly replenished at the lower part

of the wheel, and presented to the laser beam on the upper part where the laser is brought to focus. To improve the repeatability of experiments, the thickness and uniformity of the liquid film can be stabilised with the use of a gas purge jet directed at the wheel surface, beneath the focal plane of the laser. In the experiment, the sample chamber was coupled to a commercial air pump (AP4, Interpet, Dorking, UK) generating an incoming flow of air stabilising the liquid films.

Another feature of the system is variable laser energy output which can be remotely controlled by changing the flashlamp Q-switched delay on the LIBS software interface (LIBSoft V16.4.1, Applied Photonics Ltd.). With this particular LIBS setup and laser, the LIBsoft software allowed to vary the laser energy output in the range of 0–150 mJ.

3.3 Methodologies

3.3.1 AAS

Reference calcium and sodium contents of powder samples were determined by AAS following the standard method 985.35 for mineral determination in IF of the AOAC International (association of official analytical chemists) with slight modifications (AOAC, 2000). Prior to mineral determination, approx. 1.5 g of each sample was transferred into crucibles in triplicates (3 replicates per sample) and dried overnight in an oven at 102 °C. The loss of weight due to moisture evaporation was recorded for final calculations of Ca and Na contents. Samples were then heated on a hot plate as a pre-digestion step until smoking ceased. Organic matter was subsequently decomposed by dry ashing in a muffle furnace

at 525 °C for 4 h. Ashes were dissolved in 50 mL 1 M nitric acid. A further dilution step into 25 mL flasks was required to bring concentrations within the linear range of the instrument (Ca: 0–3 ppm; Na: 0–1 ppm).

For the assessment of RTF-IF mixtures, sample digestion was carried out using a microwave system (MARS 6, CEM Corporation, Matthews, NC, USA). Approx. 1 g of each sample was weighed directly into a microwave vessel (MARSXpress, CEM Corporation), and filled with 10 mL nitric acid (HNO_3 69 %, Sigma Aldrich Ireland Ltd.). Vessels were gently swirled and left open for 15 minutes to allow sample pre-digestion. The microwave heating program consisted of 2 steps: ramping from ambient temperature to 200 °C over 15 minutes (power set at 900 W), and holding that temperature for 15 additional minutes. After cooling, the digested solutions were transferred to 50 mL volumetric flasks and subsequently diluted with distilled water. A further dilution step using 25 mL flasks was carried out to bring Ca concentrations within the linear range of the instrument (Ca: 0–3 ppm).

Calibration curves for AAS experimentation were established by using aqueous standard solutions. These solutions were prepared from commercial calcium and sodium standards for AAS (1,000 mg L^{-1}, Sigma Aldrich Ireland Ltd.), with the inclusion of a blank solution prepared as detailed in the standard method 985.35 (AOAC, 2000). All AAS analysis were carried out in triplicates. Calcium absorbance was measured at 422.7 nm with a slit width of 0.5 nm; whereas sodium was measured at 589 nm (slit width 0.5 nm). Results were calculated as milligrams of calcium/sodium per gram of dried sample for powders, and milligrams per 100 millilitres for ready-to-feed samples. For all experiments, each of the independent batches was assessed separately on a different day.

3.3.2 LIBS measurements

Solid sample chamber

As previously mentioned, LIBS spectra of PIF samples were recorded using a LIBSCAN-150 system (Applied Photonics Ltd.), which covered the spectral range of 181–904 nm. The parameters set for plasma emission analysis were: a 1.27 μs delay time, to avoid the strong background continuum which characterises the early stages of the plasma lifetime (Rakovský et al., 2014); and an integration time of 1.1 μs.

Measurements were carried out by placing pellets individually into the solid sample chamber. The motorised three-axis translation stage (Applied Photonics Ltd.) allowed the acquisition of LIBS data at multiple locations. For the experiments corresponding to sample preparation for varying calcium content PIF mixtures (Chapter 4), single laser shots were recorded at 100 different spatial positions for each pellet. The 100 shots were obtained by following a 10 $\times$ 10 grid pattern of approximately 0.7 mm distance between each measurement (Figure 4.2). The measurements were conducted operating the laser in a continuous mode with a repetition rate of 1 Hz, giving an approximate measurement time of 1 minute and 40 seconds per pellet (100 laser shots).

For the experiments related to varying sodium content PIF mixtures (Chapter 5), since one of the aims of this work was to study the effect of penetrating deeper into the sample, a different spectral acquisition was carried out. In this experiment, spectra were acquired by recording 5 consecutive laser shots (depth measurements) at each of the 100 locations, giving a total number of 500 measurements per pellet. Data resulting from these consecutive laser shots can be considered as spectra corresponding to 5 different layers of the pellets, i.e. the

repetitive firing of the laser at the same location causes the ablation of the outer material thus allowing measurements deeper into the sample (Cremers & Radziemski, 2013).

Both for calcium and sodium PIF experiments, the independent batches were analysed separately on different days in order to evaluate the reproducibility of the method.

Liquid sample chamber

Spectra of liquid samples were recorded using a LIBS-6 system (Applied Photonics Ltd.) coupled to the SC-LQ2 liquid chamber, which consists of a rotatory nickel-plated stainless-steel wheel and a liquid reservoir. Plasma emission was analysed with a delay time of 1.27 μs and an integration time of 1.1 ms.

LIBS measurements were carried out analysing samples individually by pouring approx. 40 mL into the liquid reservoir. Both the reservoir and the wheel were thoroughly rinsed with distilled water before the analysis of each sample. Three different energy measurements with an output of 50, 100, and 150 mJ were performed and their resulting spectra recorded.

Preliminary testing was conducted to determine the optimum values for the following parameters: number of laser shots, repetition rate, rotational speed of the wheel, and film position relative to the focal plane of the laser beam. It was observed that accumulating a high number of laser shots produced better spectra in terms of signal-to-noise ratio. Thus, spectral acquisition was carried out by recording 200 consecutive laser shots (accumulations) for each energy measurement, giving a total number of 600 shots per sample. The laser was operated at a repetition rate of 2 Hz, and the rotatory wheel was set to revolve at an approx-

imate speed of 1.26 rad s^{-1} (12 rpm). The position of the liquid film relative to the focal plane was adjusted using a manual micrometre control located at the sample chamber side. The final position was established based on a low wheel signal contribution, namely Ni I emission due to ablation of the wheel's surface material.

Also, as seen for the PIF mixtures, each of the independent batches was measured with LIBS individually on different days.

3.4 Data analysis

Pre-processing and data analysis of the acquired spectra were performed with R statistical software (R Core Team, 2014). The R package "pls" (Mevik, Wehrens, & Liland, 2015) was employed to conduct PLSR (partial least squares regression) to develop calibration models from the spectral data, and to calculate the figures of merit used to evaluate the performance of the PLS models. Generally, LIBS data was firstly averaged over the multiple measured locations and different replicates, and then divided into two groups: a calibration dataset, for building the model; and a validation dataset, for testing the robustness and accuracy of the calibration.

Pre-processing techniques are applied to spectra in order to reduce the contribution of undesired extraneous signals (i.e. signals introduced by the atmosphere and the instrument), as well as to facilitate the extraction of relevant chemical information from the samples (Rinnan et al., 2009). For each experiment, different combinations of pre-processing techniques were applied to the acquired spectra. The optimum combination of pre-processing techniques was then selected based on the performance exhibited by the calibrations models when multivariate data analysis was performed. The combinations applied to spectra involved the

use of the following pre-processing techniques: SNV (standard normal variate), baseline correction, Savitzky-Golay filtering, normalisation by internal standards, Euclidean norm and/or derivatives.

Following the pre-processing of spectra, data were subsequently assessed by means of multivariate analytical techniques. PCA (principal component analysis) was used to perform preliminary qualitative tests (i.e. identification of similarity patterns among the samples). For quantitative analysis, PLSR was employed to build regression models for the prediction of calcium/sodium content in the samples. PLS models were developed using the cross-validation leave-one-out (LOO) method in order to evaluate the fit of the calibrations. Also, simple linear regression (SLR), or univariate analysis, was performed to provide a comparison with PLSR, as well as to calculate figures of merit such as the relative standard deviation (RSD) or the limit of detection (LOD).

The performances of the obtained PLS models were evaluated by the coefficients of determination and the values of root-mean-square error for calibration (R_c^2, RMSEC) and cross-validation (R_{cv}^2, RMSECV); as well as for prediction (R_p^2, RMSEP) when validation datasets were used. The PLSR commands used for the calculations of these figures of merit are included in the "pls" package for R.

3.5 Chemical prediction maps

One of the advantages of LIBS compared to the conventional methods for mineral content analysis (e.g. AAS) is that it can provide not only chemical (i.e. emission spectra), but also spatial information from the sample surface. The objective of generating chemical maps was to test the ability of LIBS as a method for exploring the homogeneity of sample surfaces, which could be beneficial for industries to

verify spatial mineral distribution. Specifically, in the experiments, chemical maps were conducted to ensure the PIF sample pellets were homogeneous, as well as to show the potential of LIBS for chemical mapping.

Provided that the LIBS system can perform measurements at multiple locations, chemical maps, or images, can be generated by displaying the chemical information for each location as pixels in an image. This way, chemical maps can be regarded as 2D representations of the sample surface. In the experiments involving PIF mixtures, and thus a pellet surface, chemical maps of calcium/sodium distribution were generated. Following PLS regression, the calibration models were used to predict the calcium/sodium contents of all measurements carried out on the surface of PIF pellets. LIBS measurements were performed at 100 locations per sample in a 10 $\times$ 10 grid pattern, hence, the chemical prediction maps can be considered as images made of 10 $\times$ 10 pixels, where each pixel in the maps shows the calcium content predicted for a specific location on the sample surface. Therefore, allowing the visualization of elemental distribution within the samples.

Furthermore, for the sodium experiments in Chapter 5, not only were chemical maps generated for the 100 locations on the surface, but also for all the layers or depth measurements assessed. In this case, a chemical map was obtained for each depth layer, giving a total 5 chemical maps per sample. This allowed the study of measurements deeper into the sample; thus, obtaining spatial information not only restricted to the outermost layer.

Chapter 4

LIBS as an at-line validation tool for calcium determination in IF

Calcium is an essential nutrient and one of the most important minerals for human health. It is mostly found in the form of salts in the human body, the functions of which are primarily related to maintenance of bones and growth (Lima et al., 2016). Furthermore, in its ionised form, calcium plays a key role in many vital processes such as nerve conduction, hormone secretion and blood coagulation (FAO/WHO, 2004; Guo, 2014b).

Milk and dairy products provide a high amount of calcium in the human diet (Vavrusova & Skibsted, 2014), particularly with regard to infants. Infant formula (IF) is a milk-like product intended to supplement or act as a substitute for breast milk (Sola-Larrañaga & Navarro-Blasco, 2006). Thus, IF may be the infant's only source of calcium. IF is primarily derived from cow's milk (Murgia et al., 2016). However, the composition of this milk differs significantly from breast milk and it must be modified to be suitable for infant consumption. In this

regard, after overall mineral content adjustment, calcium needs to be increased to meet the optimal levels for the infant's requirements. Calcium carbonate, among other commercial calcium salts, is a common additive used to enhance the calcium content of various foods (Smith, Gordon, & Holroyd, 2013), including IF (Guo & Ahmad, 2014a). According to the Codex Alimentarius Commission, which aims at providing global food standards to protect consumers and promote fair trade (FAO/WHO, 2019), IF should not contain less than 12 mg of calcium per 100 kJ (Codex, 2007). Although a maximum level for calcium is not provided, it is recommended not to exceed (guided upper level) 35 mg per 100 kJ. These guidelines provide a range of calcium over which any novel technology for IF quality assessment should be reliable.

Laser-induced breakdown spectroscopy (LIBS) is a promising emission spectroscopic technique for elemental analysis. It is described as a real-time method with little to no sample preparation (Anabitarte et al., 2012; Mehder et al., 2016) which also holds the possibility of spatial distribution analysis (Pathak et al., 2012). LIBS has been exploited for elemental analysis in a wide variety of fields (El Haddad et al., 2014; Jantzi et al., 2016). Nonetheless, within food research it is still in its early days (Andersen et al., 2016). LIBS has been used previously for the analysis of milk and IF powders in other studies (Abdel-Salam et al., 2013; Lei et al., 2011). Abdel-Salam et al. (2013) used LIBS for the qualitative assessment of spectral lines of nutritionally important minerals in breast milk and infant formulas, as well as the evaluation of proteins using the molecular bands of CN and C_2. In another publication, Lei et al. (2011) conducted a quantitative study in milk powders and IF. The authors employed LIBS for the determination of calcium content and other minerals by two different approaches: using calibration curves, which were obtained by mixing a reference sample with cellulose, and utilizing a calibration-free procedure which aided in overcoming matrix effects. Matrix ef-

fects are caused by differences among chemical and physical properties of samples and standards which can result in undesired deviations among the emission line intensities of elements. In LIBS analysis, samples are analysed integrally with no previous digestion of the sample; consequently, the matrix can influence the atomic or ionic emission phenomena of the analyte (Babos et al., 2019).

In the present study, a 150 mJ LIBS system was assessed to predict the calcium content in PIF (powdered infant formula) samples in combination with chemometric techniques (partial least squares regression). A different approach as reported in the literature is proposed here aiming to demonstrate the feasibility of LIBS to become an at-line validation tool for the IF manufacturing industry. To this end, the studied range of calcium was selected to be in conformity with the Codex Alimentarius. Moreover, the calcium contents of the samples were adjusted by adding lactose or calcium carbonate to PIF. Both of these compounds occur naturally in PIF and are permitted to vary within a certain range. Furthermore, the ability of LIBS as a method for exploring sample homogeneity via chemical prediction maps is also illustrated in this work.

4.1 Sample preparation

A description of the sample preparation procedure can be found in Section 3.1.1. In this study, a total of three independent batches were prepared for developing a calibration model. Each of the three batches consisted of five PIF samples with different contents of calcium (approx.: 1.1, 2.3, 3.7, 4.9, 6.1 mg g^{-1}). Additionally, a batch contained 2 extra samples with a calcium content of approximately 3.0 mg g^{-1} and 5.5 mg g^{-1} for validation purposes (validation of the calibration model). Thus, giving a total number of 17 samples. For LIBS analysis, samples were

pelletised in triplicates (three replicate pellets per sample), giving a total of 51 pellets (17 samples × 3 replicates).

4.2 LIBS measurements and instrumentation

LIBS spectra of the 51 pellets were recorded using a LIBSCAN-150 system (Applied Photonics Ltd.). A schematic representation of the LIBS system setup is shown in Figure 4.1. The system was composed of a spectrometer unit (six fibre-optic spectrometers), a 150 mJ Nd:YAG laser and a solid sample chamber equipped with a three-axis translation stage. As seen in this figure, the laser head was fitted with six lenses (one for each spectrometer) arranged in a circular shape around the laser aperture (the three different colors indicate which type of radiation the lenses could detect, e.g. ultaviolet, visible and near-infrared). Additionally, the laser head was also equipped with a CCD camera, which enabled the measurements to be monitored on the computer screen.

A detailed description of the measurements carried out with LIBS can be found in Section 3.3.2. Briefly, pellets were placed individually into the sample chamber equipped with a motorised three-axis translation stage, which allowed the acquisition of LIBS data at multiple locations. For each pellet, single laser shots were recorded at 100 different spatial positions, following a 10 × 10 grid pattern of approximately 0.7 mm distance between each measurement (Figure 4.2). Such measurements were conducted operating the laser in a continuous mode with a repetition rate of 1 Hz, giving an approximate measurement time of 1 minute and 40 seconds per pellet (100 laser shots).

The three independent batches were analysed separately on different days in order to evaluate the reproducibility of the method.

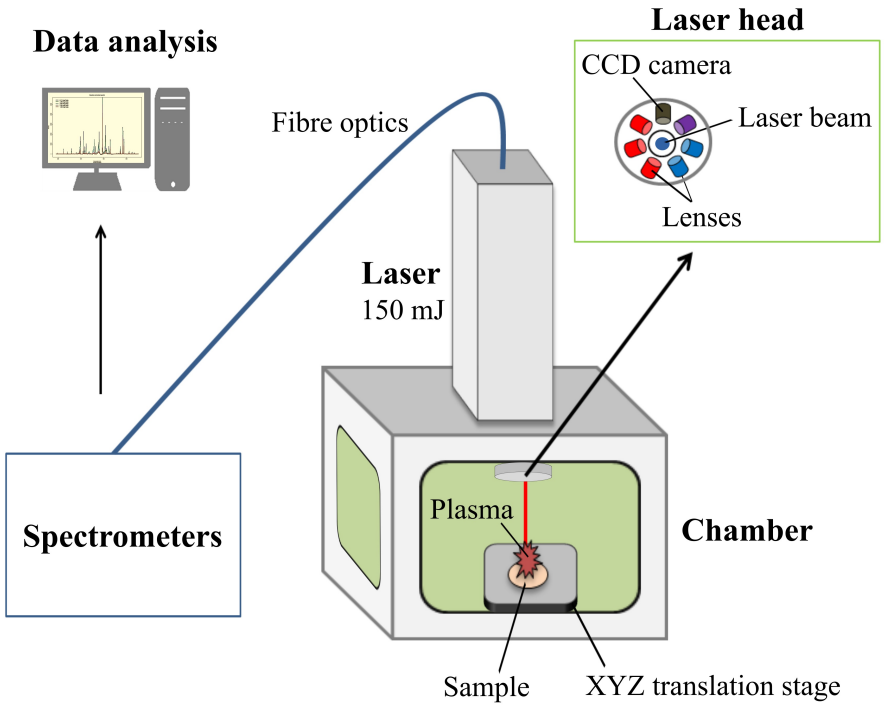

Figure 4.1: LIBS system schematic setup.

4.3 Data analysis

Data analysis was performed with R (R Core Team, 2014). The LIBS data was first averaged to obtain a single spectrum per analysed pellet. That is, the average of the 100 laser shots. Combinations of pre-processing techniques were applied to the spectra as part of the model building process. The standard normal variate (SNV) transformation was then selected based on model performance.

The package pls (Mevik et al., 2015) was used for conducting multivariate analysis with partial least squares regression (PLSR). PLSR was employed to relate the LIBS spectral data to the variation of calcium content. The pre-processed data was divided into a training set (N = 30), which was used to obtain the calibration model, and a validation set (N = 21) by which model robustness was assessed as

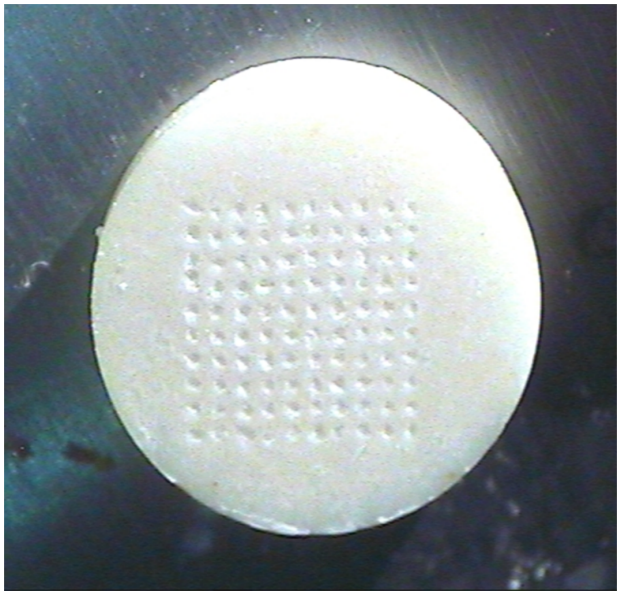

Figure 4.2: Image of a PIF and lactose pellet (sample 1 batch 1) showing the craters formed on its surface by the 100 laser pulses in a 10 × 10 grid pattern.

external validation. Furthermore, the model was built using the cross-validation leave-one-out method as internal validation.

The model performance was evaluated by the coefficients of determination and the values of root-mean-square error for calibration (R_c^2, RMSEC) and cross-validation (R_{cv}^2, RMSECV); as well as for prediction (R_p^2, RMSEP) when the validation dataset was used. The PLSR commands used for the calculations of these figures of merit are included in the pls package for R. The bias between predicted and reference values was also investigated as further evaluation of the calibration model.

To provide comparison with PLSR, univariate analysis was conducted. Simple linear regression (SLR) models were developed by correlating the intensities of several calcium (Ca) emission lines to the calcium contents determined by AAS. Similarly as for PLSR, the training dataset (N = 30) was used to build the calibration curves, while the validation set (N = 21) was employed to assess the

predictive ability of the univariate approach. Figures of merit such as the relative standard deviation (RSD), the limit of detection (LOD) and the RMSEP (root-mean-square error of prediction) were estimated for the best calibration curve.

4.4 Atomic absorption spectroscopy

AAS was conducted as the reference method for calcium determination in IF. Calcium contents of the PIF mixtures, along with pure lactose and pure calcium carbonate samples, were determined with a Varian 55B AA (Varian Inc.). AAS requires a sample digestion step prior to mineral analysis. Sample digestion and determination of calcium content were performed according to the standard method 985.35 of the AOAC International (AOAC, 2000). A full description of the followed procedure can be found in Section 3.3.1.

Calcium concentrations in the PIF mixtures of the three batches are presented in Table 4.1. The calibration curves established by aqueous standards exhibited an excellent linearity with high coefficients of determination ($R^2 \geq 0.998$). The results obtained for the low calcium content samples (lactose blends) showed consistency over the analysed replicates with standard deviations (SD) in the range of 0.01–0.08 mg Ca g^{-1} and little variation was observed between different batches. Similar results were found for the pure PIF samples (SD $\leq$ 0.09) with slightly higher variation occurring between batches. The high calcium content samples (calcium carbonate blends) presented standard deviations over replicates in the range of 0.03–0.31 mg g^{-1} and a noticeable variation between the batches, especially with regard to the highest level.

Calcium contents corresponding to pure lactose and calcium carbonate samples were also determined by AAS. As expected, lactose showed a considerably low

Table 4.1: Calcium contents in milligrams per gram of dried sample in the PIF mixtures and the pure lactose and $CaCO_3$ samples determined by AAS.

No. sample (additive)	**Batch 1** Ca cont. (mg g^{-1})[a]	**Batch 2** Ca cont. (mg g^{-1})[a]	**Batch 3** Ca cont. (mg g^{-1})[a]
1 (lactose)	1.49 ± 0.04	1.52 ± 0.03	1.40 ± 0.05
2 (lactose)	3.06 ± 0.01	3.06 ± 0.02	3.05 ± 0.08
3 (pure PIF)	4.86 ± 0.09	4.74 ± 0.09	4.23 ± 0.03
4 ($CaCO_3$)	5.17 ± 0.18	5.66 ± 0.12	5.14 ± 0.03
5 ($CaCO_3$)	7.01 ± 0.31	7.41 ± 0.18	6.56 ± 0.16
6 (lactose)	—	—	3.51 ± 0.09
7 ($CaCO_3$)	—	—	6.54 ± 0.07
8 (pure lactose)	0.07 ± 0.01	—	—
9 (pure $CaCO_3$)	433.93 ± 8.78	—	—

[a] Mean ± standard deviation (N = 3).

concentration of calcium: 0.07 mg g^{-1}, whereas a high calcium content of 433.93 mg g^{-1} was found for calcium carbonate.

4.5 LIBS spectral features

The averaged LIBS spectra obtained for three different samples are presented in Figure 4.3. For clarity, only the samples corresponding to the lowest calcium concentration of the second batch (PIF and lactose blend at 1.52 mg Ca g^{-1}), the highest (PIF and calcium carbonate blend at 7.41 mg Ca g^{-1}) and pure PIF (4.74 mg Ca g^{-1}) were included.

The graph revealed the main emission spectral lines occurring in the LIBS spectra of the PIF mixtures. Such spectral lines were associated with the most probable elements emitting at the observed wavelengths (Table 4.2), using the spectral lines provided by the NIST database as a reference (Kramida et al., 2016). Good agreement was found with identified spectral lines reported in other

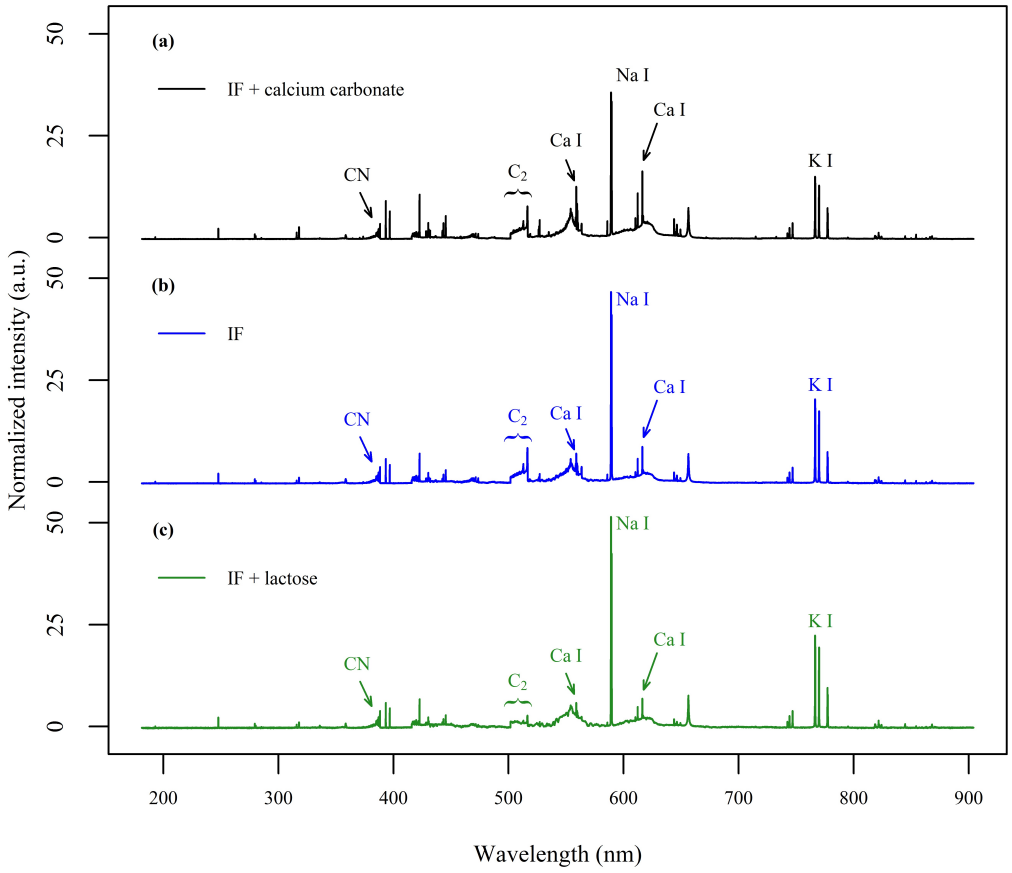

Figure 4.3: Averaged LIBS spectra of samples: **(a)** PIF and calcium carbonate blend (sample 5, batch 2) at 7.41 mg Ca g^{-1}, **(b)** pure PIF (sample 3, batch 2) at 4.74 mg Ca g^{-1} and **(c)** PIF and lactose blend (sample 1, batch 2) at 1.52 mg Ca g^{-1}. Spectra are vertically offset for clarity.

studies (Bilge, Sezer, et al., 2016; Bilge, Velioglu, et al., 2016); as well as for the molecular emission of the C_2 and CN bands (Abdel-Salam et al., 2013).

Some differences between the samples can be observed in Figure 4.3. For instance, the PIF and calcium carbonate mixture exhibited higher intensity at the calcium emission line at 616.28 nm, whereas lower intensity was found for the lactose mixture. The same result was found for several calcium emission lines. For other minerals such as sodium, a decrease in intensity was found in the calcium carbonate mixture at 589.05 nm (Na I).

Table 4.2: Observed spectral lines occurring in the LIBS spectra and their possible associated elements. These associations were made using the NIST database as a reference (Kramida et al., 2016).

Observed wavelength (nm)	Element/molecular emission
247.87	C I
279.56	Mg II
385.03–388.31	CN
393.34	Ca II
396.86	Ca II
422.70	Ca I
445.50	Ca I
512.87–516.47	C_2
558.90	Ca I
589.05	Na I
612.25	Ca I
616.28	Ca I
643.93	Ca I
656.35	H I
746.91	N I
766.46	K I
769.93	K I
777.43	O I

For the emission of molecular species identified in the spectra, no appreciable difference between the different samples was observed for the CN bands occurring in the range of 385.03–388.31 nm. However, the emission of C_2 bands at 512.87–516.47 nm for lactose mixtures exhibited lower intensities when compared to pure PIF or the calcium carbonate blend.

4.6 Calibration model

The calibration model was built by applying PLSR to the training dataset. The concentrations determined by AAS were used as the reference values for PLSR, thus correlating the assessed calcium contents to the pre-processed LIBS spectral data.

The first 3 main PLS factors of the model explained approximately 85 % of the total variance. The PLS loading plot for the first factor of the calcium model is shown in Figure 4.4, which explained 60 % of the total variance. Several calcium (Ca I) emission lines were found to contribute to the loading values of the first factor. The most prominent lines occur approximately at 422.65 nm, 558.90 nm, 612.25 nm and 616.80 nm. This result, along with the presence of singly ionised calcium lines (Ca II), demonstrated that most of the variation occurring in the samples was related to the calcium content. However, other spectral lines with a noticeable contribution were that of the sodium (Na I) line at 589.05 nm and potassium (K I) at 766.45 nm. Both of these emission lines showed negative loading values indicating that for an increasing content of sodium and potassium, a decreasing content of calcium was expected in the predicted values. The presence of sodium and potassium lines in the loading values was an expected outcome as when varying the composition of PIF by adding lactose or calcium carbonate, the levels of these minerals are also modified.

The performance of the calibration model obtained for calcium prediction is summarised in Table 4.3, which contains the coefficients of determination and the root-mean-square errors for calibration (R_c^2, RMSEC), cross-validation (R_{cv}^2, RMSECV) and prediction by an independent dataset (R_p^2, RMSEP). The model showed good linearity, with calibration coefficients of determination (R_c^2) of 0.95

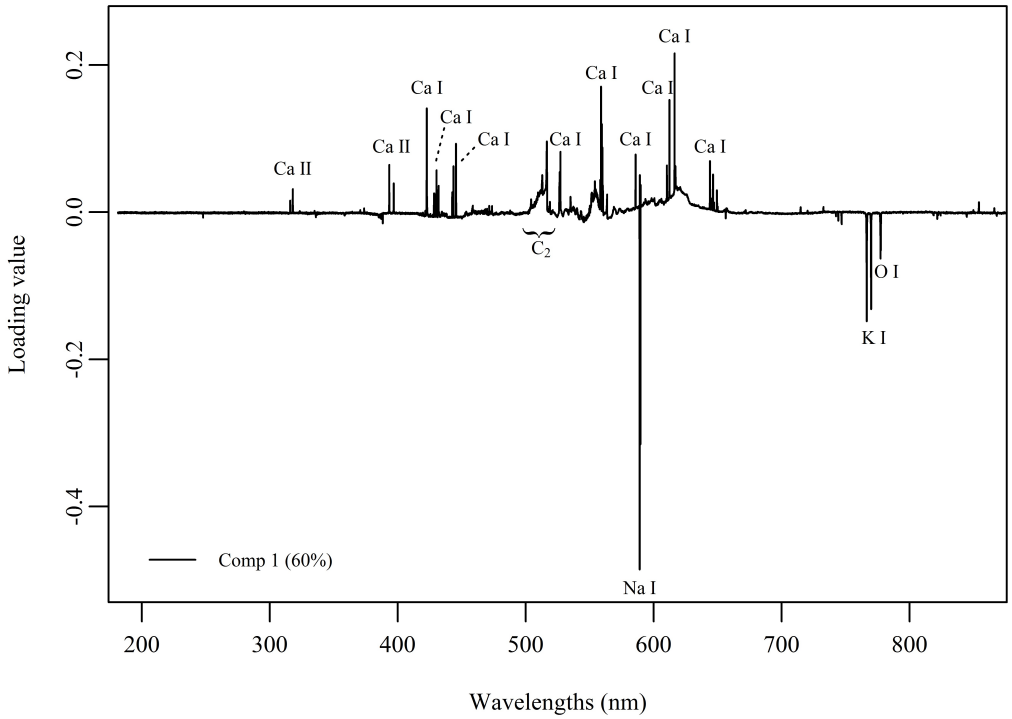

Figure 4.4: Loading plot showing the contribution of each wavelength to the first PLS factor.

and 0.96, for 3 and 4 PLS factors respectively. When interrogated by cross-validation, the model was found to fit reasonably well with an R^2_{cv} value of 0.90 for 3 PLS factors. Although the coefficient of determination R^2_c was higher using 4 components, the value for cross-validation R^2_{cv} together with the minimum value found for RMSECV, indicated that the model would perform better for estimating calcium content when 3 PLS factors were used.

4.6.1 Validation of the calibration model

Validation was performed in order to evaluate the robustness of the calibration model. In this regard, the 3 PLS factors model was used to predict the calcium contents of the validation dataset.

Table 4.3: PLS regression model performance evaluated by cross-validation (LOO) and external validation (using the validation dataset).

No. PLS factors	Calibration (N = 30)				Validation (N = 21)		
	R_c^2	RMSEC[a]	R_{cv}^2	RMSECV[a]	R_p^2	RMSEP[a]	Bias[a]
2	0.93	0.53	0.89	0.66	0.46	1.28	1.17
3	0.95	0.44	0.90	0.62	0.85	0.68	0.56
4	0.96	0.38	0.89	0.64	0.82	0.75	0.66

[a] Expressed in milligrams per gram of calcium.

The predicted calcium values for the PIF samples are shown in Figure 4.5. The RMSEP value obtained was similar to the RMSECV value: 0.68 mg g^{-1} and 0.62 mg g^{-1} respectively. This result indicated that the model was not overfitted. It can be observed in Figure 4.5 that the predictions established for the highest levels of calcium (calcium carbonate blends) were more accurate than the predictions for the lowest levels (lactose blends). This may be due to the fact that a considerably lower amount of calcium carbonate was required to bring concentrations to the desired levels, compared to the amounts of lactose needed to decrease the calcium content in the mixtures. Thus, the addition of lactose could possibly lead to a major change in the matrix embedding the calcium, i.e. the physical and chemical composition of some calibration samples is considerably different than the others where lactose was not added to the mixtures. The matrix is known to have notable effects on the emission intensities of LIBS measurements (Ferreira et al., 2010; Lei et al., 2011; Tognoni et al., 2010).

Figure 4.5 also displays the values of the coefficients of determination of calibration and external validation (prediction). As previously stated, the model showed good linearity with an R_c^2 of 0.95. Regarding the predictions, the R_p^2 value was 0.85. This result indicated reasonable model performance for an independent

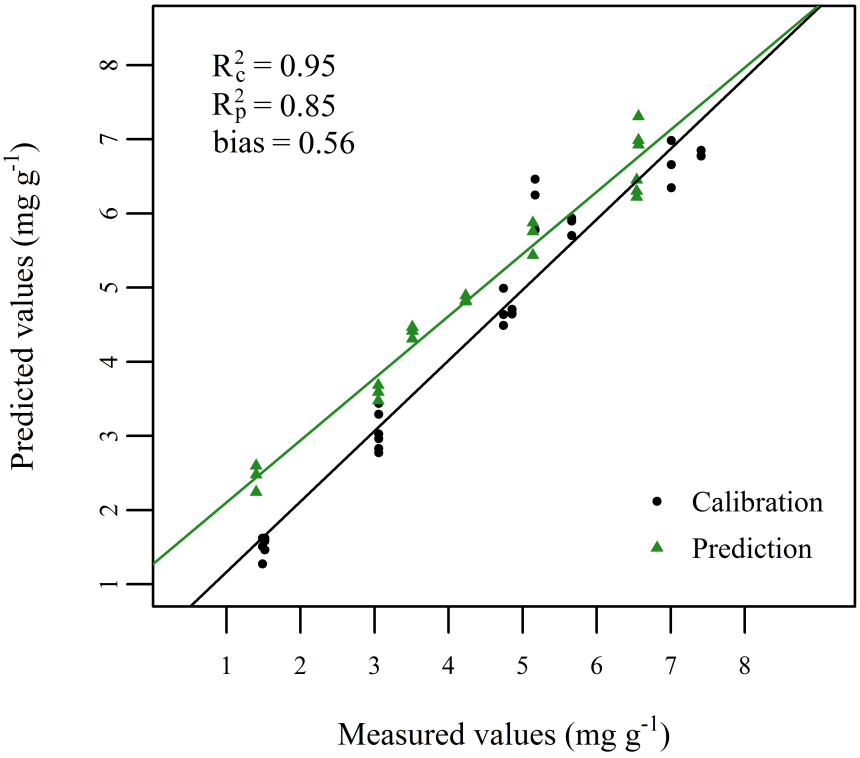

Figure 4.5: PLSR calibration curve with reference values and calcium predicted contents for the validation dataset. The bias value is expressed in mg g^{-1}.

batch which has not been used for developing the calibrations. The bias value, found between the reference values and the predictions, was 0.56 mg g^{-1} indicating that in terms of predictive accuracy the method still needs further enhancement to be fully developed as a validation tool for industry. It should be noted, however, that the lowest calcium content sample, which contains a large amount of lactose, had a negative contribution to both the R_p^2 and the bias, whereas the predictions for the other levels were considerably more accurate.

As previously mentioned, other studies have reported the use of LIBS for the analysis of milk and IF powders, qualitatively (Abdel-Salam et al., 2013) and quantitatively (Lei et al., 2011). Lei et al. (2011) used two methods to quantify calcium, potassium and magnesium in milk powders and IF: using calibration

curves, by mixing a reference sample with cellulose, and a CF-LIBS (calibration-free LIBS) approach. The authors encountered a loss of repeatability due to the high sensitivity of the LIBS signal to experimental fluctuations and matrix effects using calibration curves with reference samples. As a solution, the authors demonstrated the potential of CF-LIBS for overcoming strong matrix effects. In the study conducted in this thesis, a different approach was proposed to obtain robust calibrations by obtaining different concentrations of calcium mixing IF with naturally occurring constituents such as lactose and calcium carbonate, together with the application of multivariate analysis with PLS.

4.6.2 Comparison to univariate analysis

For completeness, univariate analysis was conducted to provide calibration models for each of the calcium emission lines reported in Table 4.2. Overall, a low calibration performance was observed for all the assessed spectral lines. The model using the Ca I emission line at 616.28 nm yielded the highest R^2 with a value of 0.73 and a RSD of 13.66 %. The calibration curve of this model is shown in Figure 4.6 **(a)**. As in PLS, the model was employed to predict the calcium content of the validation sample set. Predicted versus measured values are displayed in Figure 4.6 **(b)**.

The values of bias and RMSEP were then investigated in order to compare the univariate prediction ability with that of the PLS regression. The bias value was found to be 0.80 mg g^{-1} of calcium and the RMSEP value was 1.09 mg g^{-1}. Both values were considerably higher than those obtained with PLS (bias: 0.56 mg g^{-1} and RMSEP: 0.68 mg g^{-1}) substantiating that better accuracy and precision can be obtained with PLS regression. These results indicated that PLS may help overcome the matrix effect as reported elsewhere (El Haddad et al.,

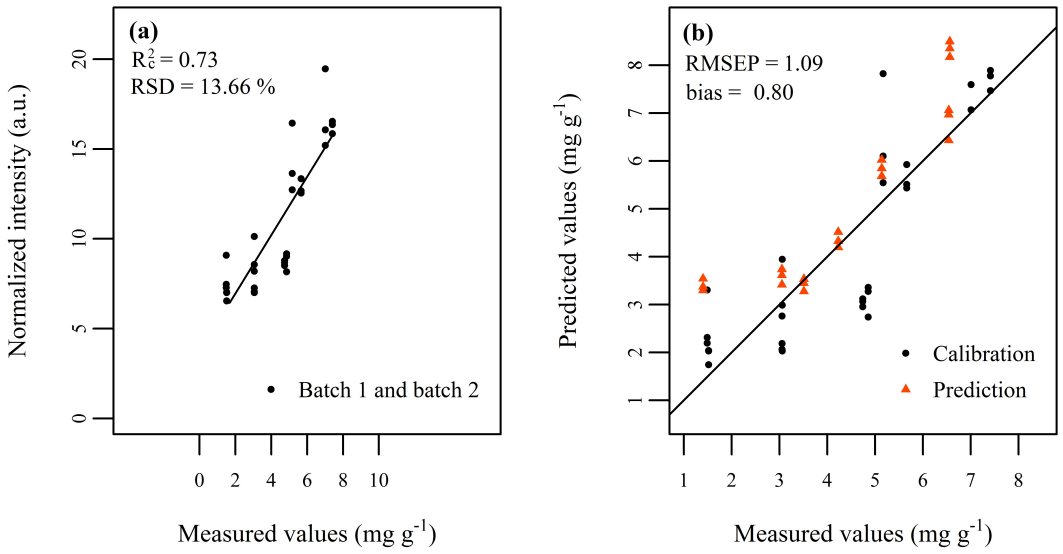

Figure 4.6: **(a)** Univariate calibration curve obtained by using the calcium emission line at 616.28 nm and the AAS reference values. **(b)** Calcium predicted contents versus reference values for the calibration and validation datasets. The RMSEP and bias values are expressed in mg g^{-1}.

2014). Additionally, the LOD (limit of detection) serves as an indicator of the detectable concentration limits. Due to a lack of a blank PIF sample with zero calcium concentration and the possibility to estimate its standard deviation, it was preferred to compute the LOD value as shown in (Equation 2.4 section 2.5), which is calculated as 3 times the standard error of the regression divided by the slope of the calibration curve. The LOD value for the calibration curve using the 616.28 nm Ca line was 3.69 mg g^{-1}. Lower limits of detection for LIBS analysis of calcium in food products have been reported in other studies (Sezer et al., 2017), indicating that potentially LIBS can detect concentrations lower that the LOD reported above. However, this LOD value was provided mainly as an estimate using the univariate analysis method which did not provide a calibration as robust as PLSR.

4.7 Chemical maps of calcium

Most analytical techniques need a certain degree of sample preparation before the sample can be presented to the instrumentation. For instance, AAS requires wet digestion or dry-ashing procedures of solid samples so that it consists of a homogeneous acid solution with a given analyte concentration within the optimum rage of the instrument (AOAC, 2000). As previously seen, LIBS is a technique which offers advantages over conventional methods for mineral analysis, and one of these advantages is little to no sample preparation. However, while generally regarded as an advantage, it may also be the case that the sample has not been mixed and homogenised thoroughly prior to its analysis, hence leading to errors when determining analyte contents from a given number of measurements on the sample surface (T. Kim & Li, 2012). Nonetheless, another feature of LIBS is the possibility of conducting spatial distribution analysis.

In order to generate chemical maps showing calcium distribution within the samples, the PLS calibration model previously built was used to predict the calcium content of each measurement carried out on the sample surface. As previously mentioned, measurements were performed at 100 locations per pellet in a 10×10 grid pattern. Therefore, the chemical prediction maps can be considered as images made of 10×10 pixels. Each pixel displays the calcium content predicted for a specific location or crater formed on the sample surface. The craters were estimated to measure an average distance of 0.5 mm in diameter. Pixels in the chemical maps, however, display the spectral information collected of measurements spatially separated by 0.7 mm, as such distance was kept to avoid overlapping of the craters.

In this study, chemical maps of the pellets corresponding to the two validation

samples were generated. Additionally, 200 mg of PIF with a calcium content of approx. 1.1 mg g^{-1} and 200 mg of PIF with a calcium content of approx. 6.1 mg g^{-1} were placed side by side in the die at the hydraulic press and a single pellet was obtained. A chemical map for this pellet was also generated with the aim of allowing a better understanding of homogeneity.

Chemical predicted maps obtained for the three different pellets (replicates) of the two additional validation samples at 3.51 mg g^{-1} and 6.54 mg g^{-1} are displayed in Figure 4.7 **(a–f)**. Colour scale in the figure indicates calcium content in mg g^{-1}. From highest to lowest, a red colour corresponds to a high concentration of calcium (around 8 mg g^{-1}), the colour then transitions to yellow (6 mg g^{-1}), cyan (4 mg g^{-1}) and lastly blue (2 mg g^{-1}). It can be observed that a few pixels in the chemical maps are higher or lower in Ca content than the neighbouring pixels, however, none of the predicted values were found to be extreme. Although some variability was found, the evaluation of the results suggested that, overall; the pellets were homogeneous with no clumps or aggregates occurring. In order to show a case of non-homogeneity, Figure 4.7 **(g)** includes a chemical map of a single pellet consisting of two different concentrations of calcium arranged side by side. In this chemical map, a high variation can be observed between two areas of the pellet. This result contrasts the homogeneity observed for the other predicted PIF samples.

4.8 Conclusions

In the present work, a LIBS system in combination with chemometric techniques was successfully employed to predict the calcium content of PIF samples over a relevant range (approx. 1.4–7.0 mg g^{-1}) for IF manufacturing, as it was selected

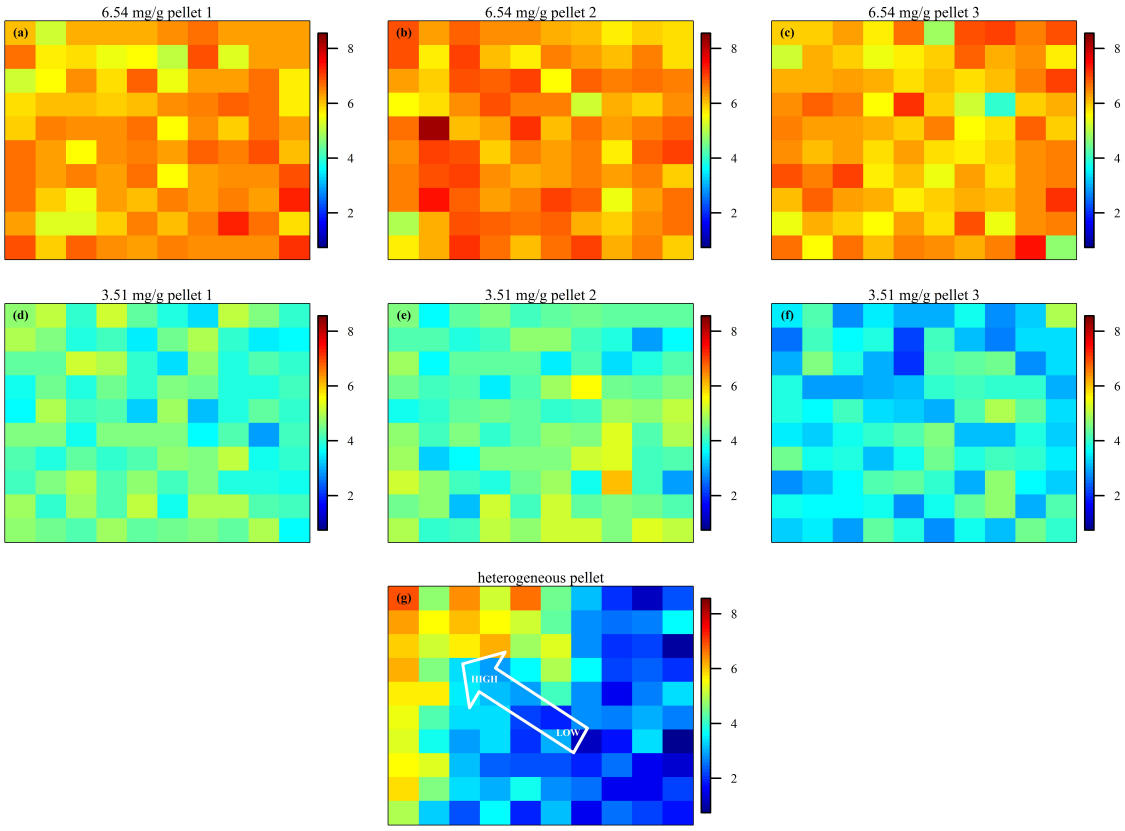

Figure 4.7: **(a–c)** Chemical predicted maps obtained for the three pellets of the validation sample at 6.54 mg Ca g^{-1} (batch 3: sample 6), and **(d–f)** chemical maps of the three pellets made for the validation sample at 3.51 mg Ca g^{-1} (batch 3: sample 7). **(g)** Shows the distribution of a single pellet consisting of two different concentrations of calcium arranged side by side (low: 1.52 mg g^{-1}, high: 7.41 mg g^{-1}), included for illustration purposes only.

to be in agreement with the guidelines provided by the Codex Alimentarius. The most remarkable advantages of the LIBS system compared to conventional methods for calcium content determination are its speed, ease of operation and minimal sample preparation.

PLS regression was applied to the LIBS spectral data to build a calibration model for calcium content prediction. The data consisted of three independent sample sets in order to evaluate the reproducibility of the method. When examined by cross-validation and external validation, the model exhibited high values of

R^2_{cv} and R^2_p, corroborating a good fit over the selected range. The predictive accuracy was considered acceptable. Although these results need further enhancement in terms of predictive accuracy, the study presented here illustrates the potential of LIBS to be applied as an at-line validation method for the quantification of calcium in the IF manufacturing industry.

Furthermore, the chemical mapping conducted in this experiment allows a better understanding of the calcium distribution within the samples. Moreover it demonstrates the possibility of LIBS to extract not only chemical, but also spatial information from the sample surface, even within the selected relevant range for IF manufacturing.

Chapter 5

Sampling effects on the quantification of sodium in IF

Sodium is an essential mineral; it is the main cation in extracellular fluid playing a vital role in the regulation of osmolarity, acid-base equilibrium, active transport across cells and membrane potential (Guo, 2014b). Although a minimum intake is indispensable for healthy functioning, excessive consumption of sodium in the human diet is related to higher blood pressure and an increased risk of developing cardiovascular diseases (Masotti et al., 2012; Tamm et al., 2016). With regard to infancy, studies have also associated an excessive sodium intake with increased blood pressure in the later stages of life, indicating that blood pressure may track with age (Campbell et al., 2014; John et al., 2016).

Conventional well-established methods for mineral analysis in infant formula include atomic absorption spectroscopy (AAS), inductively coupled plasma optical emission spectroscopy (ICP-OES) and inductively coupled plasma mass spectroscopy (ICP-MS) (Poitevin, 2016). These methods, despite their high sensitivity

and accuracy, generally require time-consuming and laborious sampling procedures and the use of chemical reagents such as acids and gases, as well as an associated high cost of consumables (e.g. argon) (G. Kim et al., 2012).

Laser-induced breakdown spectroscopy (LIBS) is an analytical technique based on optical emission in which laser pulses are employed as the excitation source to vaporise a small part of the sample material. LIBS, while relatively new to food analysis, has gained remarkable popularity in the last few years with an increase in the number of publications and extensive reviews concerning food samples (Markiewicz-Keszycka et al., 2017; Sezer et al., 2017). Advantages that LIBS offers compared to conventional methods are its speed, a relatively low cost, little to no sample preparation and elemental surface mapping capabilities (Casado-Gavalda et al., 2017; Dixit, Casado-Gavalda, Cama-Moncunill, Cama-Moncunill, et al., 2017). Further attractive features include: remote sensing, as it constitutes an entirely optical technique, and suitability for on-/at-line applications, allowing the technology to be considered a potential process analytical technology (PAT) for qualitative and quantitative chemical analysis (Cullen et al., 2017). Nonetheless, LIBS also has limitations or drawbacks, especially concerning quantitative analyses. Some of these limitations include signal fluctuations on a shot-to-shot basis (Tognoni & Cristoforetti, 2016) and difficulties in establishing suitable calibration curves due to strong matrix effects (Ferreira et al., 2010; Lei et al., 2011).

In this study, LIBS and multivariate data analysis with partial least squares regression (PLSR) was employed to predict the sodium content of IF samples. In order to provide for reference sodium contents, atomic absorption spectroscopy (AAS) was used. The aim of this study was to demonstrate the ability of LIBS as a rapid screening tool for quantifying sodium over a range relevant to IF manufacturing, offering a means for industries to rapidly verify target mineral contents.

Furthermore, strategies concerning the acquisition and pre-processing of LIBS data were explored: spectra were acquired at different measuring depths (repetition of laser shots), which allowed investigating the benefits of measuring inner layers of the sample, and several pre-processing techniques were applied and compared to one another in terms of sodium estimation. Additionally, the spectra from various measuring depths were summated in order to determine whether accumulated spectra from multiple layers improved the accuracy of sodium predictions.

5.1 Sample preparation

Sample preparation was carried out as described in Section 3.1.1. Samples with varying content of sodium were prepared by blending PIF with sodium chloride or lactose, giving a total of 7 different sodium content samples in the range of 0.5–4 mg g^{-1}. In order to ensure reproducibility, two independent batches were prepared (batch 1 and batch 2). Each batch was composed of the aforementioned 7 samples divided into: 5 calibration samples (referred to as C1–C5), employed for PLS modelling; and 2 validation samples (V1, V2), used for testing the robustness of the models.

Additionally, 2 different follow-on formula samples were included in the experiment as extra validation samples (V3, V4). These samples were intended to further assess the robustness of the models by predicting sodium content in infant products with different formulations. Considering these two samples, in total, 16 samples were obtained (7 samples $\times$ 2 batches + 2 PFOF samples). For LIBS analysis, samples were pelletised in triplicates, giving a total number of 48 pellets (16 samples $\times$ 3 replicates).

5.2 LIBS measurements and instrumentation

LIBS analysis of the 48 pellets were performed using a LIBSCAN-150 system (Applied Photonics Ltd.). A detailed explanation regarding the system's characteristics can be found in Section 3.2.2. In brief, the LIBS system consisted of: a 150 mJ Nd:YAG laser operating at 1064 nm; six spectrometers, which covered the wavelength range of 181–904 nm; and a solid sample chamber, equipped with a motorised three-axis translation stage.

As seen in Section 3.3.2, pellets were measured individually by firing consecutive laser shots at 100 locations in a 10 × 10 grid pattern. Specifically, spectral acquisition was carried out by recording 5 laser shots (depth measurements) at each of the 100 locations, giving a total number of 500 measurements per pellet. Data resulting from these consecutive laser shots can be considered as spectra corresponding to 5 different layers of the pellets, i.e. the repetitive firing of the laser at the same location causes the ablation of the outer material penetrating and allowing to measure deeper into the sample (Cremers & Radziemski, 2013).

Spectral data collected from the 5 laser shots were stored separately in order to assess the best layer from which to build the sodium quantification model, and allow subsequent comparison between accumulated and non-accumulated laser shots.

The two independent batches were analysed with LIBS on separate days to assess the reproducibility of the method.

5.3 Data analysis

Data analysis was performed with R (R Core Team, 2014) using the R package pls (Mevik et al., 2015) for conducting PLSR (partial least squares regression), as well as other in-house functions.

Firstly, the average of the LIBS spectra collected at multiple locations was calculated for each layer, resulting in 5 spectra per pellet. Data was then divided into a training dataset (N = 30), a test set (N = 12), and additionally the follow-on formula extra validation samples (N = 6). Prior to PLS modelling, combinations of different pre-processing techniques and normalisation methods were applied to the spectra with the aim of reducing the signal fluctuations due to extraneous sources of variability and to minimise matrix effects (Sobron et al., 2012). Specifically, the techniques explored were: baseline correction (R package baseline) (Liland, Mevik, & Canteri, 2015), second derivative and standard normal variate (SNV). Spectral normalisation by an internal standard and the Euclidean norm were also explored.

PLS calibration models using the different pre-processing techniques were developed for each of the 5 layers of the pellets. The LOO (leave-one-out) method was employed for cross-validation. The performance of each model was evaluated by the root-mean-square error of cross-validation (RMSECV), as well as the root-mean-square error of prediction (RMSEP). The wavelength range used for modelling was limited to 560–825 nm since this region encompassed the main sodium (Na) emission lines, while decreasing the total number of variables that do not contain useful peaks (Moncayo, Manzoor, Rosales, Anzano, & Caceres, 2017).

To provide for a comparison between the accumulated and non-accumulated

shots, spectra corresponding to the different layers were summated so that 2, 3, 4 and 5 accumulations were obtained. PLS modelling of the accumulated spectra was then carried out, and their resulting performances were compared to those of the single-layer-spectra models.

The limit of detection was computed according to the pseudounivariate approach (LOD_{pu}) for PLS models as proposed in a publication elsewhere (Allegrini & Olivieri, 2014) in conformity with IUPAC official recommendations. LOD_{pu} calculation was performed as illustrated in Section 2.5 (Equation 2.6).

5.4 Atomic absorption spectroscopy

AAS was selected as the reference method for sodium quantification in PIF. Na contents were established using a Varian 55B AA spectrometer (Varian Inc.) following the standard method 985.35 for mineral determination in IF of the AOAC International (see Section 3.3.1). All replicates and batches were measured on different days.

In AAS, the accuracy of the results relies heavily upon the calibration curve established from reference standard solutions of the desired element. Calibration curves were established using aqueous standards prepared from a commercial sodium stock solution (Sodium standard for AAS – 1,000 mg L^{-1}, Sigma Aldrich Ireland Ltd.). Linear calibration curves were obtained rendering values for the coefficient of determination (R^2) ≥ 0.99.

Sodium contents of the PIF samples determined with AAS, expressed in mg g^{-1}, are shown in Table 5.1. The Na contents obtained for all samples showed consistency over the analysed replicates (N = 3) with low values of standard

deviation (SD). Furthermore, little variation between the contents of the two batches was observed.

Table 5.1: Sodium contents in milligrams per gram of samples corresponding to calibration (C1–C5) and validation (V1–V4) determined by AAS.

Sample	Constituents	Batch 1 [Na] (mg g^{-1})[a]	Batch 2 [Na] (mg g^{-1})[a]	Extra validation [Na] (mg g^{-1})[a]
C1	PIF + lactose	0.48 ± 0.05	0.54 ± 0.03	—
C2	PIF	1.40 ± 0.21	1.34 ± 0.07	—
C3	PIF + NaCl	2.11 ± 0.11	2.07 ± 0.02	—
C4	PIF + NaCl	2.78 ± 0.16	2.72 ± 0.07	—
C5	PIF + NaCl	3.69 ± 0.54	3.74 ± 0.18	—
V1	PIF + lactose	0.93 ± 0.06	0.98 ± 0.06	—
V2	PIF + NaCl	2.22 ± 0.04	2.48 ± 0.21	—
V3	PFOF	—	—	1.18 ± 0.04
V4	PFOF	—	—	2.38 ± 0.36

[a] Mean ± standard deviation (N = 3).

5.5 LIBS spectral features

An initial exploratory analysis of the LIBS spectra was conducted in order to determine the main differences among the samples studied. For comparison purposes, the averaged spectra of pellets corresponding to the lactose-PIF mixture (C1, approx. 0.5 mg Na g^{-1}), pure PIF (C2, approx. 1.3 mg Na g^{-1}) and the sodium chloride-IF mixture (C5, approx. 3.7 mg Na g^{-1}) are shown in Figure 5.1. In this figure, several of the most important spectral lines of elements occurring in the spectra can be seen. The main element emission lines in the spectra were identified using the NIST database (Kramida et al., 2016). These emission lines included: C I 247.86 nm, Ca II 393.37; 396.85 nm, Ca I 422.67; 558.88; 612.22; 616.22 nm, H I 656.29 nm, N I 744.23; 746.83 nm, K I 766.49; 769.90 nm, O I 777.19 nm and Na I 589.05; 589.59 nm. Moreover, three Na I lines were iden-

tified at 568.26, 568.82 and 819.48 nm. Other possible Na lines in the spectra were discarded and not considered for quantitative analysis since the intensities at these wavelengths were marginal, which is consistent with the NIST guidelines for sodium.

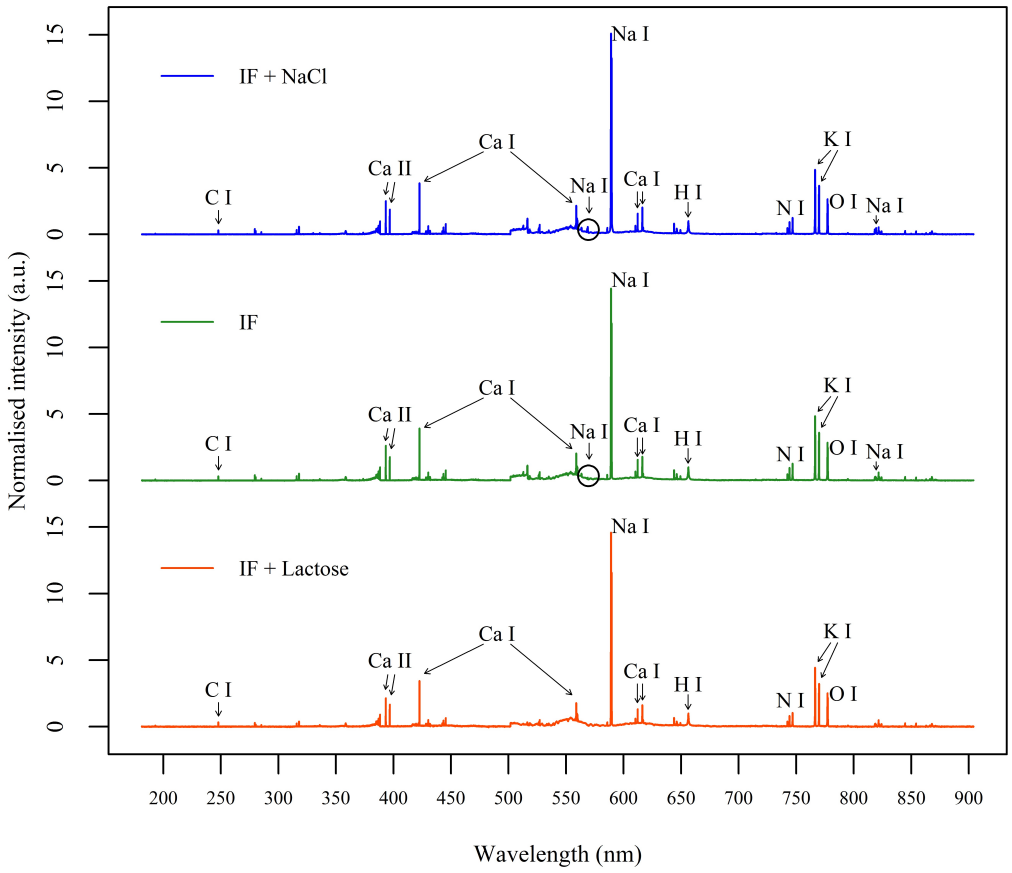

Figure 5.1: Averaged normalised spectra corresponding to, from top to bottom, the sodium chloride-PIF mixture at approx. 3.7 mg Na g^{-1}, the pure PIF sample at approx. 1.3 mg Na g^{-1} and the sodium lactose-PIF mixture at approx. 0.5 mg Na g^{-1}. Spectra are vertically offset for illustration purposes.

5.6 Multivariate analysis with PLS

PLS is a method for predicting a quantitative response, stored in a matrix Y, from numerous predictor variables (i.e. spectral data), stored in a matrix X. To do so, it

decomposes simultaneously the two matrices into new variables, known as factors or latent variables (LV), in such a way that they explain as much as possible of the covariance between X and Y. A multivariate linear model is then fitted using the latent variables to predict the quantitative response (Abdi, 2010). PLS modelling has been demonstrated to successfully develop quantitative calibration models from LIBS spectral data of food samples in previous publications (Andersen et al., 2016; Markiewicz-Keszycka et al., 2018; Sezer et al., 2018). In the present study, PLS was employed to build the calibration models for the determination of sodium content by correlating the pre-processed LIBS spectra in the wavelength range of 560–825 nm to the reference Na contents obtained from AAS analysis.

5.6.1 PLS modelling: performance of sampling methods and spectral pre-processing

As previously mentioned, different pre-processing techniques and sampling strategies (measuring depths and accumulations) were explored. To this end, various calibrations were developed using the approaches detailed in Section 5.3. A summary of PLS performances for these calibrations can be found in Table 5.2 (for briefness, this table only includes some of the most relevant models). The criterion followed for establishing an optimum number of LVs for each model considered a low value of RMSECV (root-mean-square error of cross-validation) with a low number of LVs to avoid overfitting. In order to determine the best calibration for quantifying sodium content in IF samples, both RMSECV and RMSEP (root-mean-square error of prediction) were used.

Table 5.2: Summary of performances for the PLS models developed using different sampling methods and pre-processing techniques.

Experiment	**Depth**[a]	**Pre-processing**	**Calibration**			**Cross-validation**		**Validation**	
			LVs	R^2	RMSEC	R^2_{cv}	RMSECV	R^2_p	RMSEP
Single layer	3	None	3	0.85	0.43	0.77	0.53	0.91	0.22
Single layer	1	H I 656.3	3	0.90	0.35	0.82	0.47	0.61	0.44
Single layer	2	H I 656.3	3	0.86	0.42	0.78	0.52	0.50	0.50
Single layer	**3**	**H I 656.3**	**3**	**0.93**	**0.29**	**0.89**	**0.37**	**0.97**	**0.13**
Single layer	4	H I 656.3	3	0.88	0.38	0.79	0.51	0.92	0.21
Single layer	5	H I 656.3	3	0.82	0.46	0.67	0.64	0.91	0.21
Accumulations	4 (0/4)	H I 656.3	3	0.93	0.29	0.88	0.38	0.91	0.21
Accumulations	5 (0/5)	H I 656.3	3	0.92	0.32	0.86	0.42	0.94	0.18
Accumulations	4 (1/3)	H I 656.3	3	0.92	0.29	0.87	0.37	0.94	0.21
Single layer	3	Ca I 422.6	3	0.94	0.28	0.89	0.36	0.97	0.13
Single layer	3	C I 247.9	3	0.92	0.31	0.88	0.39	0.89	0.23
Single layer	3	K I 766.4	3	0.94	0.27	0.91	0.33	0.91	0.21
Single layer	3	SNV	3	0.94	0.28	0.89	0.37	0.95	0.16

continued

Table 5.2: *(cont.)*

Experiment	**Depth**[a]	**Pre-processing**	**Calibration**			**Cross-validation**		**Validation**	
			LVs	R^2	RMSEC	R^2_{cv}	RMSECV	R^2_p	RMSEP
Single layer	4	SNV	3	0.92	0.32	0.85	0.43	0.87	0.26
Single layer	5	SNV	2	0.87	0.41	0.82	0.47	0.91	0.21
Accumulations	4 (0/4)	SNV	2	0.88	0.38	0.84	0.44	0.85	0.27
Accumulations	5 (0/5	SNV	2	0.88	0.38	0.84	0.44	0.90	0.23
Accumulations	4 (1/3)	SNV	2	0.88	0.39	0.83	0.45	0.89	0.31
Single layer	3	Euclidean	3	0.94	0.27	0.89	0.37	0.95	0.16
Single layer	4	Euclidean	2	0.87	0.40	0.82	0.46	0.89	0.23
Single layer	5	Euclidean	2	0.87	0.41	0.82	0.47	0.91	0.21
Accumulations	4 (0/4)	Euclidean	2	0.88	0.38	0.84	0.44	0.81	0.31
Accumulations	5 (0/5)	Euclidean	2	0.88	0.38	0.84	0.44	0.87	0.25

[a] The best performing model is shown in bold. Values in parentheses in the Depth column are number of conditioning shots/number of accumulated spectra.

With regard to pre-processing techniques, the best performances were obtained for normalised spectra with SNV, Euclidean norm and normalisation using the H I at 656.29 nm and Ca I at 422.67 nm emission lines as internal standards. All the methods above yielded similar results for calibration (Table 5.2): e.g. the third-layer-spectra models (measurement depth: 3) using these pre-processing techniques rendered values of almost 0.94 for the coefficient of determination (R^2). These models also provided similar results for root-mean-square errors of cross-validation and prediction: third-layer-spectra models yielded values of approx. 0.37 mg g^{-1} for RMSECV and values in the range of approx. 0.13–0.16 mg g^{-1} for RMSEP. Other techniques such as baseline correction or normalisation with other internal standards (C I at 247.86 nm and K I at 766.49 nm) provided good calibrations and reasonable validation performances. However, the RMSEP values were slightly higher than those obtained with SNV, Euclidean, H I 656.29 nm or Ca I 422.67 nm. Second derivative pre-processing was found not to be effective for calibration, with low values of R^2 and R^2_{cv} (coefficient of determination for cross-validation), as well as high values of root-mean-square errors (RMSE, RMSECV).

During the modelling of layers or depth measurements, it was observed that the third-layer spectra exhibited the best results regardless of the pre-processing technique used. The first and second layers, while providing a good calibration, showed performances considerably lower for cross-validation and validation. The fourth and fifth layers exhibited an overall good performance, but with lower R^2 values and higher RMSECV and RMSEP as compared to the third layer. The effect of measuring deeper in the sample on spectral quality, and as a mechanism to avoid surface contamination has been previously investigated (Cama-Moncunill et al., 2017). Similarly, in this publication PLS models were developed for different layers of the samples with the aim of quantifying copper and iron contents in infant formula premixes (blends designed to contain specified nutrients). These authors

observed that PLS performances, especially with regard to validation, improved as measuring depth increased. In the present study, this trend was also observed, however, finding an optimum at the third measurement depth. It is worth noting that depending on the laser energy and sample type, the optimum number of shots on the same location may change substantially since these parameters affect the laser-material interaction, for instance the size of the crater formed or the amount of ablated mass (Tognoni & Cristoforetti, 2016).

Table 5.2 also shows the performances for some of the PLS models developed with the accumulated spectra. In this regard, the modelling of accumulated spectra only proved to yield notably better performances for the first two laser shots as compared to applying PLS separately on these layers. A larger number of accumulations did not provide better models than just using the third-layer-spectra alone. In other publications, authors chose to accumulate spectra as a means to mitigate signal fluctuations (Markiewicz-Keszycka et al., 2017). The fact that, in this work, accumulating spectra did not considerably improve the results may be due to an already high sampling number (average of 100 locations) along with an optimum of 3 laser shots, the first two of which ablate away the surface which may have been contaminated.

Considering both pre-processing and sampling method, the best performing PLS model to predict sodium content was the third-layer spectra which had been normalised using the H I emission line at 656.29 nm.

5.6.2 Validation of the selected calibration model

The hydrogen-normalised third-layer-spectra model was used as the calibration to perform sodium content predictions. Figure 5.2 shows the values of RMSECV

for each LV of this model. A total of 3 LVs was selected as further factors did not result in a notable improvement in terms of RMSECV while, at the same time, the quality of the predictions for the validation set decreased, indicating that a higher number of LVs could result in overfitting of the model. The first 3 main LVs explained approximately 95.7 % of the total spectral variance.

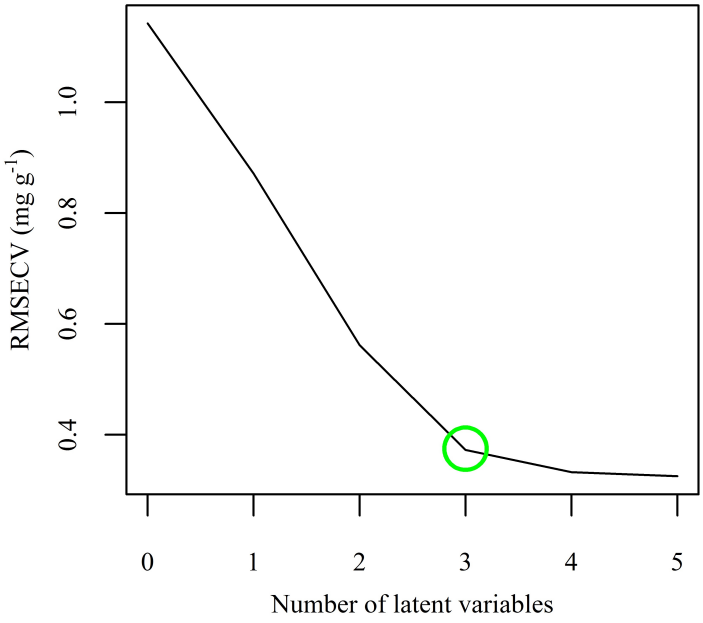

Figure 5.2: RMSECV (root-mean-square error of cross-validation) for each number of PLS factors or latent variables.

Figure 5.3 shows the loading values for the first three factors of the PLS model in the wavelength range assessed. One main sodium (Na I) emission line at 589.59 nm contributed to the loading values. Other Na I spectral lines were the doublet at 568.26 and 568.82 nm, and the emission line at 819.48 nm. These spectral lines had a relatively small contribution as compared to the sodium doublet at around 589 nm. Negative loading values were only observed for nitrogen (N I 744.23 and 746.83 nm) and oxygen (O I 777.19 nm), both elements showing minor values.

The PLS model exhibited an R^2 of 0.93 for the calibration. With regard

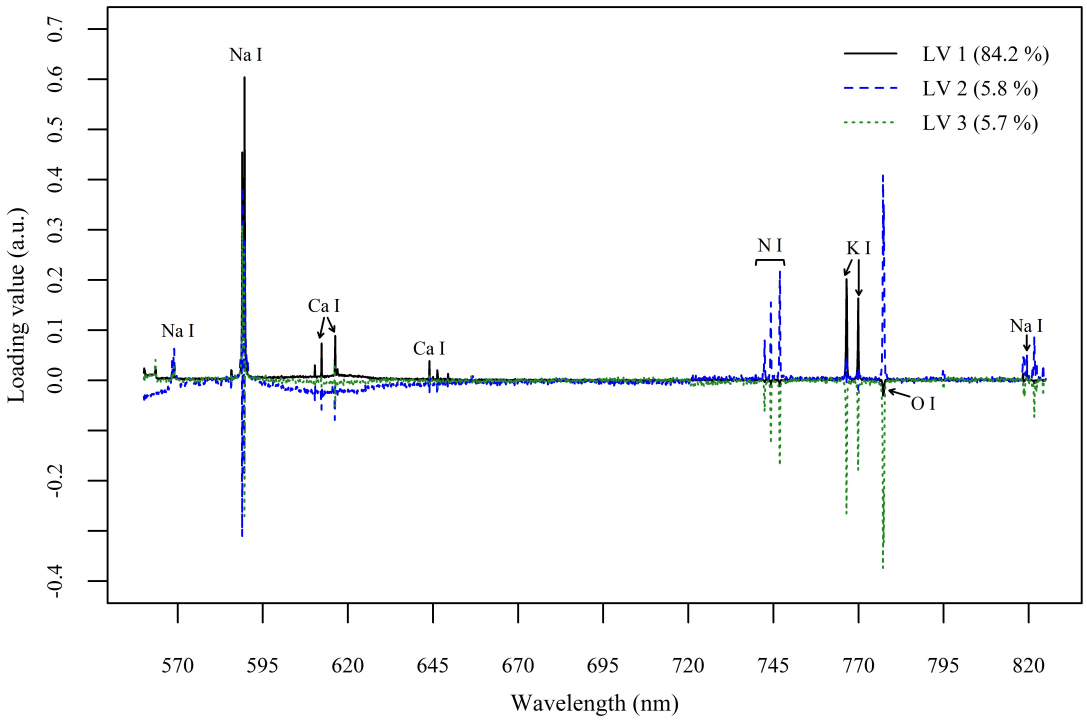

Figure 5.3: Loading value of each wavelength for the three LVs included in the development of the PLS model. Percentages in brackets show variance explained by each LV.

to cross-validation, an R^2_{cv} value of 0.89 and an RMSECV of 0.37 mg g^{-1} were obtained, indicating a reasonable fit and accuracy of the calibration. Validation of the PLS model was carried out by predicting the Na contents of 2 samples not included in the training set with the aim of evaluating the robustness of the model. The model exhibited a good prediction accuracy as indicated by a high R^2_p (coefficient of determination for the validation set) of 0.97 and an RMSEP value of 0.13 mg Na g^{-1}. Figure 5.4 shows the PLS calibration curve with the predicted values for the validation set. To further evaluate the closeness of the predictions to the actual concentration values, the relative error (RE) was calculated as reported elsewhere (Câmara et al., 2017). The RE value of the validation set was 7.22 %.

Additionally, Na contents for 2 follow-on formulas were also predicted in order

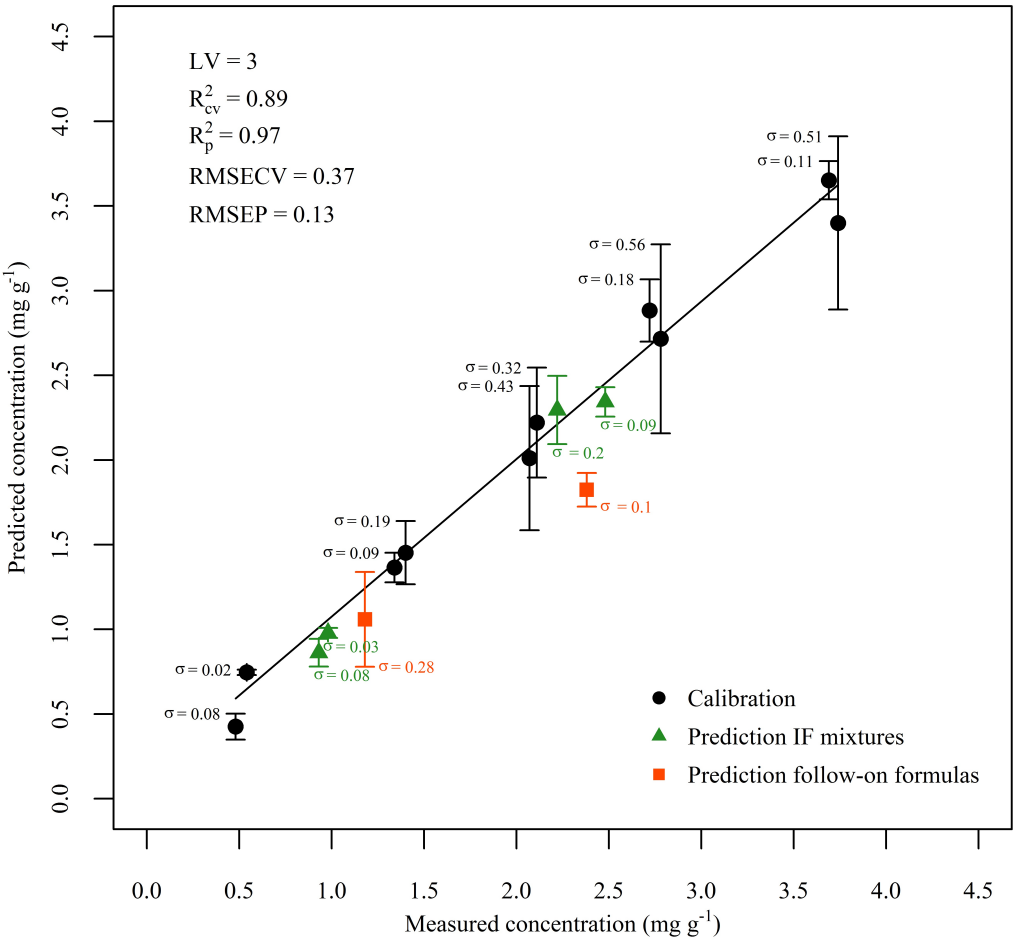

Figure 5.4: PLS calibration model developed using the third-layer spectra and normalised by the H I 656.29 emission line showing predicted Na contents for the validation set and follow-on formulas. Standard deviation values (σ) are expressed in mg g^{-1}.

to explore the model's response to different formulations of infant products. In this case, the predictions were not as accurate as the validation set, giving a RE value of 23.32 %. This loss in accuracy was expected as LIBS measurements are highly dependent on the matrix. However, this result indicated that the model can provide reasonable predictions even with a certain degree of variability in the raw materials. The limit of detection of the model was estimated by following the pseudounivariate approach as described in Section 2.5 (Equation 2.6). This

approach was carried out to provide a LOD value calculated from a multivariate calibration. In Chapter 4, a LOD estimate was given using the calibration curve obtained via univariate analysis which resulted in a high value of LOD. For this reason, in this experiment, the LOD was computed from the PLSR calibration. The LOD value corresponding to the PLSR calibration model for sodium content prediction was 1.11 mg g^{-1}.

5.7 Chemical maps of sodium

As mentioned before, the best performance was given by spectra collected after 3 laser shots. To further investigate why the third layer provided better results, the sodium content was predicted, in this case, for each location in the 10 × 10 measuring grid. In order to do so, the raw spectral data acquired from sample V2, chosen as a point close to the centre of the calibration curve, were normalised by the hydrogen emission line without averaging the data of multiple locations. Na contents were subsequently predicted employing the coefficients extracted from the PLS model. Figure 5.5 shows a schematic representation of the V2 pellet displaying sodium content in each spatial position for the first 3 measurement depths. The same intensity scale for the three measurements was implemented to allow comparison. It can be observed that the predictions for the third layer, Figure 5.5 **(c)**, provided a more homogeneously distributed sodium within the analysed area.

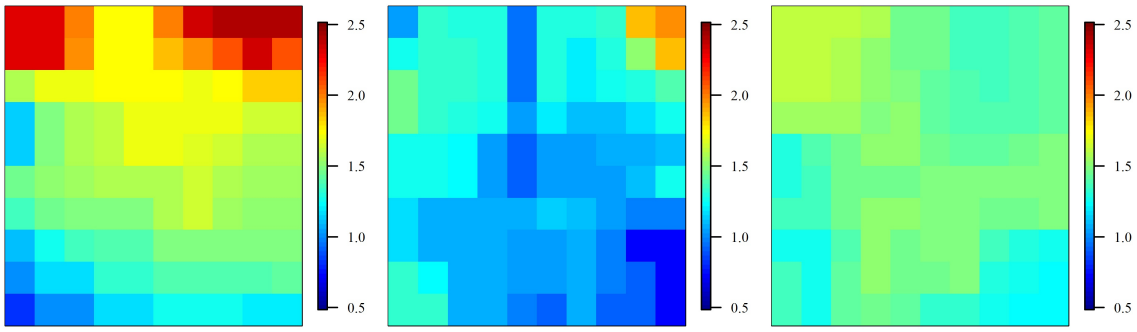

Figure 5.5: Predicted sodium maps for the validation sample (V2) at 2.48 mg Na g^{-1} for the first three measuring depths: **(a)** first layer, **(b)** second layer, and **(c)** third layer. The same intensity scale was implemented for the three measurements to facilitate comparison.

5.8 Conclusions

LIBS was successfully applied for quantifying sodium over a range in conformity with the product's regulatory guidelines, hence, demonstrating the feasibility of the technique as a potential screening tool for IF manufacturing. Multivariate analysis with PLSR was applied to spectral data processed by a range of different pre-processing techniques, measuring depths and accumulations. The resulting calibration models were compared in terms of PLS performance: coefficients of determination and root-mean-square errors; for calibration (R^2, RMSEC), leave-one-out cross-validation (R^2_{cv}, RMSECV) and validation (R^2_p, RMSEP). The best PLS calibration was obtained using the third-layer spectra normalised by the H I emission line at 656.29 nm, yielding a R^2 of 0.93 and a R^2_{cv} of 0.89. When performing validation of this model, the resulting R^2_p and RMSEP values were 0.97 and 0.13 mg Na g^{-1} respectively, proving its ability to accurately predict samples not included in the calibration set.

In this study, accumulation of the spectra on the same spot did not notably

improve the performances of the PLS models as compared to using the third layer alone. Furthermore, chemical mapping with PLS of the analysed area (100 measurements in a 10 × 10 grid pattern) showed that sodium was more homogeneously distributed than for the first two layers. These results suggested that conditioning the surface of the pelletised sample, while keeping a low number of shots on the same spot, can provide a good predictive accuracy without the need of large sampling numbers.

In addition to the application of multivariate and pre-processing techniques aiming at improving LIBS capabilities for quantitative analysis of IF, future experimentation involving variable laser shot energy may allow for better quantification.

Chapter 6

Direct analysis of calcium in liquid IF

Infancy is a crucial phase of growth and development which requires appropriate nutrition. Breast milk is considered the ideal food for infants (WHO, 2018); it provides the adequate amounts of nutrients for growth, as well as other substances with added health benefits. However, for numerous reasons breastfeeding is either supplemented or replaced with breast milk substitutes. Infant formula (IF) is an industrially produced food designed to fulfil the nutritional requirements of infants during the first six months of life (Silva, Brandao, Matos, & Ferreira, 2015). To ensure the nutritional safety and adequacy of infant products, the amounts of all these components must be in conformity with national regulatory bodies such as the European Commission in the European Union, the Food and Drug Administration (FDA) in the United States, or the Codex Alimentarius Commission at an international level (Montagne et al., 2009). Therefore, minimum and maximum contents of nutrients in IFs are clearly specified according to accepted scientific evidence (Codex, 2007; European Commission, 2006).

Typically, IFs are commercially available in powder form. Liquid formulas, including ready-to-feed infant formula (RTF-IF) and liquid concentrates, are increasingly found in the market. Although liquid formulas account for a small volume of the global IF sales, mainly due to a higher retail price, the ready-to-feed format may be preferred in certain situations (Happe & Gambelli, 2015). It represents a convenient and hygienic option as it does not require preparation before consumption. Moreover, sterile RTF-IF are the predominant choice for feeding pre-term, low-birth-weight or immunocompromised infants (Happe & Gambelli, 2015; Marino et al., 2013).

Despite the high sensitivity and accuracy of the conventional methods for mineral analysis in IF (e.g. AAS, ICP-OES, ICP-MS), industries may benefit from the application of on-line/at-line technologies with real-time monitoring capabilities due to their speed, ease of operation and high sampling rates.

Laser-induced breakdown spectroscopy (LIBS) has been defined as a versatile real-time technique which allows in-situ analysis of any sort of material regardless of its physical state (Lazic & Jovićević, 2014). In the area of food analysis, LIBS has been gaining attention and the number of publications found in the literature has grown remarkably in the last few years. To date, publications employing the technique for both qualitative and quantitative analysis of elements in various solid food samples can be found throughout the literature (Markiewicz-Keszycka et al., 2017). However, less attention has been paid to liquid food samples, especially with regard to direct analysis.

LIBS configurations for the analysis of liquids have been reported, e.g. liquid jets for chromium (Cr) determination in industrial wastewater (N. K. Rai & Rai, 2008), double-pulse LIBS in bulk water (De Giacomo, Dell'Aglio, Colao, Fantoni, & Lazic, 2005), and liquid surface analysis of formulations containing sodium

chloride (St-Onge, Kwong, Sabsabi, & Vadas, 2004); nevertheless it has also been discussed that the direct analysis of liquids may be problematic. The reason for this is due to undesired effects such as shorter plasma durations, splashing, and formation of shockwaves on the liquid surface, which consequently lower the sensibility and repeatability of LIBS measurements (V. N. Rai, Yueh, & Singh, 2007; Sezer et al., 2017; St-Onge et al., 2004). In the area of food analysis, the transformation of liquids into solid-matrix samples has been proposed. To do so, authors have employed the use of lyophilisation techniques to remove the water content from milk samples (Moncayo et al., 2017), the formation of solid gel matrices by adding a binding agent such as collagen to milk (Sezer et al., 2018) and wine (Moncayo et al., 2016) samples, or the deposition of maternal milk and IF preparations (reconstituted powder) onto ashless filter papers (Abdel-Salam et al., 2013). Alternatively, the formation of aerosols using sprayers for the quantification of calcium in milk has also been reported (Bilge, Sezer, Boyaci, Eseller, & Berberoglu, 2018). These techniques although obtaining improved results, required additional long sample preparation steps, which impeded real-time analysis.

In this study, the calcium content in RTF-IF samples was determined using a LIBS system equipped with a sample chamber designed for the direct analysis of liquids. Multivariate analysis with partial least squares regression (PLSR) was employed to develop a calibration model to reliably predict calcium content. LIBS measurements with different laser energy outputs were also performed and evaluated. The aim of this study was to assess the ability of LIBS for calcium content determination in RTF-IF, as well as illustrating its potential for the direct analysis of liquid foods.

6.1 Sample preparation

A detailed description of the sample preparation procedure carried out for this study can be found in Section 3.3.2. A total of three sample batches were prepared for calibration, each batch consisting of five RTF-IF samples (C1–C5) with equally distributed varying content of calcium in the range of approx. 10–90 mg 100 mL^{-1}. To ensure reproducibility, each of the three batches was obtained from different RTF-IF bottles and prepared on different days.

For validation of the models, two other samples were prepared with calcium contents differing to those of the calibration samples (V1, approx. 20 mg 100 mL^{-1}; V2, approx. 60 mg 100 mL^{-1}). Additionally, RTF-FOF (ready-to-feed follow-on formula) was used as an extra validation sample (V3, approx. 70 mg 100 mL^{-1}) to assess the ability of the models for predicting calcium content in formulas with different compositions. In total, 18 samples were prepared (5 calibration samples $\times$ 3 batches + 2 validation samples + 1 extra validation).

All samples were prepared in triplicates, giving a total number of 54 liquid samples (18 samples $\times$ 3 replicates).

6.2 LIBS measurements and instrumentation

Spectra of the 54 liquid samples were recorded using a LIBS-6 system (Applied Photonics Ltd.). A schematic representation of the LIBS system attached to a liquid sample chamber is presented in Figure 6.1. This system comprised a 150 mJ Q-switched Nd:YAG laser operating at 1064 nm, which was connected to a power supply unit; and a spectrometer unit containing six spectrometers, which covered the wavelength range of 181–904 nm. Moreover, the system was coupled

to a liquid sample chamber (SC-LQ2, Applied Photonics Ltd.) consisting of a rotatory nickel-plated stainless-steel wheel and a liquid reservoir of approximately 40 ml capacity.

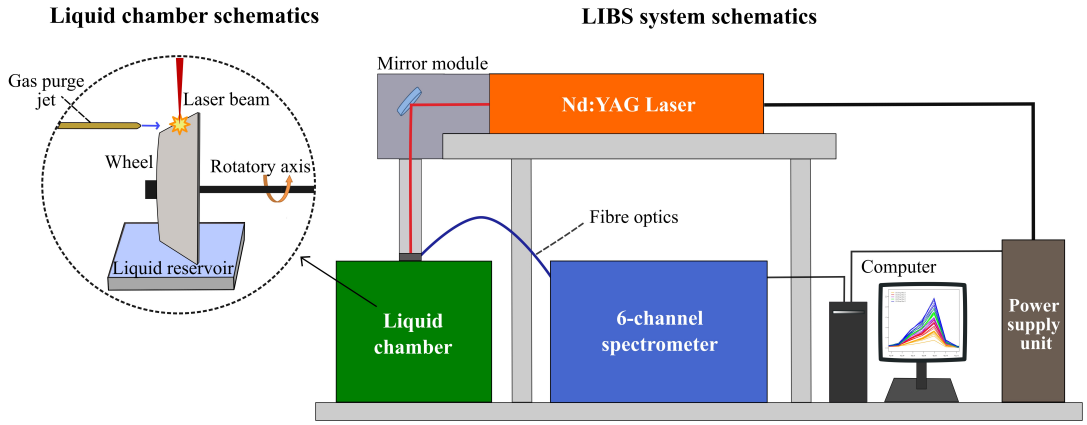

Figure 6.1: Schematic representation of the LIBS system and liquid chamber used in the experiments.

Section 3.3.2 contains a full description of the measurements carried out by LIBS. Briefly, samples were measured individually by pouring approx. 40 mL into the liquid reservoir. Both the reservoir and the wheel were thoroughly rinsed with distilled water before the analysis of each sample. Three different energy measurements with an output of 50, 100, and 150 mJ were performed and their resulting spectra recorded. Each of the three calibration batches was measured with LIBS individually on different days (validation samples were measured together with the first batch).

6.3 Data analysis

Univariate and multivariate data analysis were performed with R (R Core Team, 2014), along with the R package pls (Mevik et al., 2015) for PLSR (partial least

square regression) modelling.

Univariate analysis was conducted by means of SLR (simple linear regression) at 422.67 nm (Ca I); correlating LIBS signal intensities to the AAS measured Ca content of all 3 batches intended for calibration (N = 45).

Prior to PLSR, several pre-processing techniques were applied to the spectra with the aim of reducing undesired sources of signal fluctuations. Among the pre-processing techniques assessed, spectral normalisation against the H I spectral line at 656.29 nm was selected based on PLS-model performance. This normalisation approach was found to provide suitable calibration curves in a previous study (see Section 5.6.1). Firstly, data were divided into a calibration set (N = 45) used to develop the calibration curve, and a validation set (N = 6) to assess the robustness of the calibration. RTF-FOF (N = 3) was employed separately to assess the feasibility of the model for predicting calcium content in products with different compositions (extra validation set).

The fit and robustness of the PLS model were evaluated by the coefficients of determination and root-mean-square errors for calibration (R_c^2, RMSEC), cross-validation (R_{cv}^2, RMSECV) and prediction (R_p^2, RMSEP). RMSE values were calculated as defined in Section 2.5 (Equation 2.11).

6.4 Atomic absorption spectroscopy

Reference Ca contents for all 54 samples were established with a Varian 55B AA spectrometer (Varian Inc.) as detailed in Section 3.3.1. The three calibration batches were measured individually on different days (validation samples were measured along with the first batch).

Calibration of the AA instrument was performed prior to the analysis of each batch. Calibration curves were obtained by using five standard solutions prepared from a commercial calcium standard for AAS (1,000 mg L^{-1}, Sigma Aldrich Ireland Ltd.) together with a blank solution, covering the range of 0–3 ppm. Good linearity was observed for the calibration curves rendering coefficient of determination values of ≥ 0.99. Detailed concentrations of calcium in the RTF-IF mixtures established with AAS are shown in Table 6.1.

Table 6.1: Calcium contents in the RTF-IF samples for calibration and validation batches determined with AAS.

Sample	**Batch 1** Ca cont. (mg 100 mL^{-1})[a]	**Batch 2** Ca cont. (mg 100 mL^{-1})[a]	**Batch 3** Ca cont. (mg 100 mL^{-1})[a]	**Batch 4** Ca cont. (mg 100 mL^{-1})[a]
C1	5.70 ± 0.10	5.54 ± 0.08	6.40 ± 0.25	–
C2	15.64 ± 0.98	19.58 ± 1.11	24.96 ± 0.58	–
C3	31.88 ± 0.68	38.32 ± 2.29	35.67 ± 0.68	–
C4	49.65 ± 1.52	67.80 ± 7.36	58.69 ± 0.60	–
C5	84.63 ± 2.79	102.57 ± 3.88	93.44 ± 0.53	–
V1	–	–	–	22.32 ± 0.83
V2	–	–	–	66.53 ± 1.30
V3	–	–	–	68.61 ± 0.79

[a] Contents expressed as mean ± standard deviation of three replicates.

Results showed concentrations between batches slightly different as some variability would be expected; this in turn helps building a robust calibration where variability is taken into account.

6.5 Laser energy and spectral features

An initial evaluation of the collected spectra was carried out to establish the principal differences between the three energy levels used, as well as to identify

the main elemental emission lines in the spectra.

Figure 6.2 shows the LIBS spectra acquired from the pure RTF-IF (sample C3, batch 1) using the three laser-shot energies 50, 100, and 150 mJ. Several of the most important spectral lines of elements occurring in the spectra can be seen. The main element emission lines in the spectra were identified using the NIST database (Kramida et al., 2016). These emission lines included: Ca II 393.37, 396.85 nm; Ca I 422.67 nm; H I 656.29 nm; N I 744.23, 746.83, 821.63 nm; K I 766.49, 769.90 nm; O I 777.19 nm; and Na I 589.05, 589.59 nm. The presence of several emission lines, namely Ni I, in the wavelength range from approx. 300 to 370 nm was attributed to ablation of wheel surface material (nickel plating). Ni I emission lines were identified at 300.25, 301.20, 305.08 310.16, 341.48, 345.85, 349.30, 352.46, 356.64, and 361.94 nm.

It can be seen in Figure 6.2 that the signal intensity increased with increasing laser energy, thus the spectra recorded with 150 mJ exhibited the highest overall intensity. The same pattern was observed for spectra collected from all other samples (not included in this figure for clarity purposes). Several emission lines occurring in the 100 and 150 mJ spectra had marginal intensities in the 50 mJ measurement, including the Ca II lines within the wavelength range 393–397 nm and the Ca I line at 422.67 nm. With these experimental conditions, a pulse energy of 50 mJ may not be high enough to ablate and vaporise a sufficient amount of material to produce a strong emission signal of calcium lines.

A comparison between relative standard deviations of the intensities of samples at 422.67 nm using the three energy levels is presented in Figure 6.3. The energy level of 150 mJ provided better results for quantification as relative standard deviations were lower than those obtained for 50 and 100 mJ. Taking into account the results presented in Figure 6.2 and Figure 6.3, the energy level of 150 mJ was

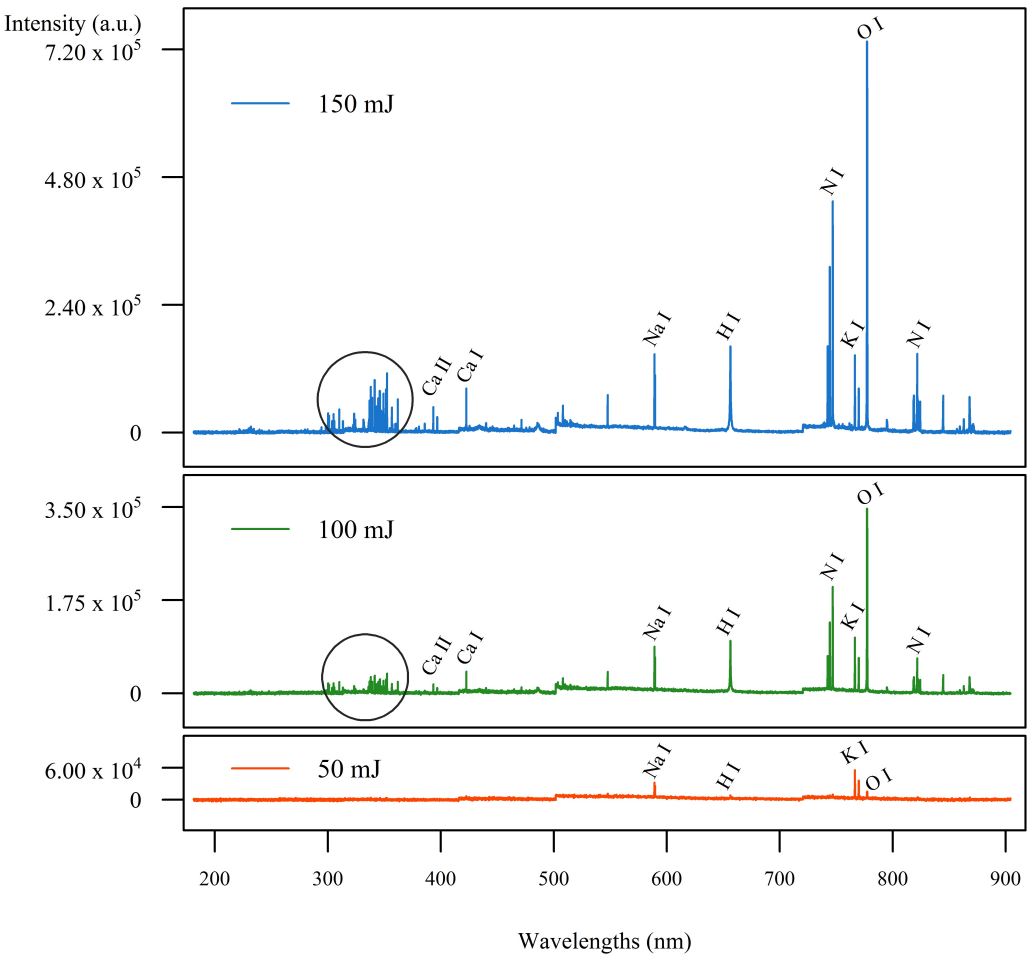

Figure 6.2: LIBS spectra of RTF-IF (sample C3, 31.88 mg Ca 100 mL^{-1}) acquired with different laser energy outputs: from bottom to top, 50 mJ, 100 mJ and 150 mJ. Circles indicate areas of probable wheel contribution.

established as the optimum level for best results and therefore the univariate and multivariate analysis were applied on the data obtained at 150 mJ laser energy.

6.6 Univariate analysis

An examination of the calcium emission lines indicated that spectra at 422.67 nm (Ca I) were correctly arranged according to their calcium content. Therefore,

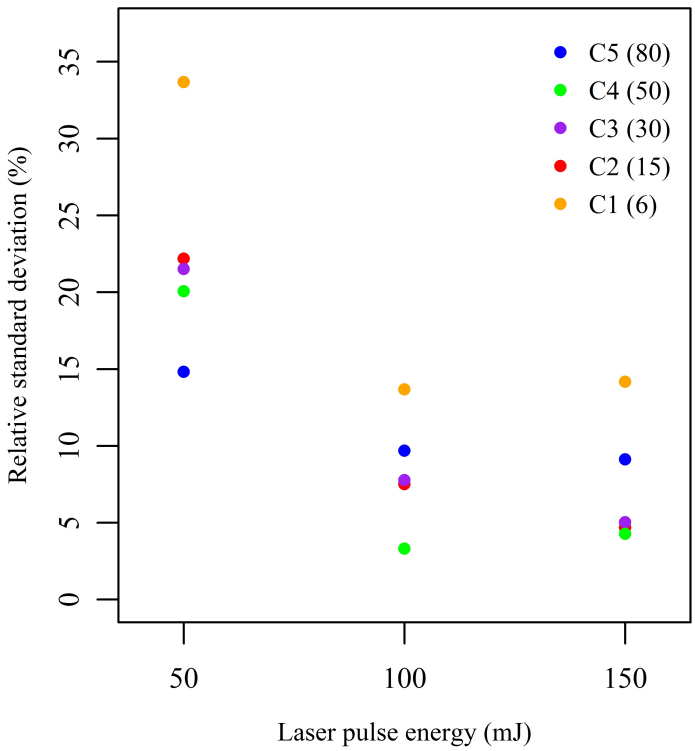

Figure 6.3: Relative standard deviations for each sample at 422.67 nm corresponding to the three energy measurements: 50, 100, and 150 mJ. Numbers between parentheses indicate approx. calcium content in mg 100 mL^{-1}.

SLR (simple linear regression) at 422.67 nm was conducted, correlating signal intensities to the AAS-measured calcium contents.

Reasonable linearity was observed for SLR comprising the three calibration batches (N = 45), exhibiting a coefficient of determination for calibration (R_c^2) of 0.87. A calibration curve showing predicted versus measured Ca contents for all batches is presented in Figure 6.4. The RMSEC (root-mean-square error of calibration) value obtained for this calibration curve was 12.56 mg 100 mL^{-1}. The regression coefficients of the calibration curve were also employed to predict Ca content in validation (V1, V2) and extra validation (V3) samples. Validation datasets were observed to fit relatively close to the calibration curve with a RMSEP value of 10.04 mg 100 mL^{-1}.

Additionally, calibration curves fitting batches individually (N = 15) were also developed, which provided better linearity with R^2 values in the range of 0.92–0.93 depending on the batch used. This result suggested that variability from batch to batch limited the performance of the regression.

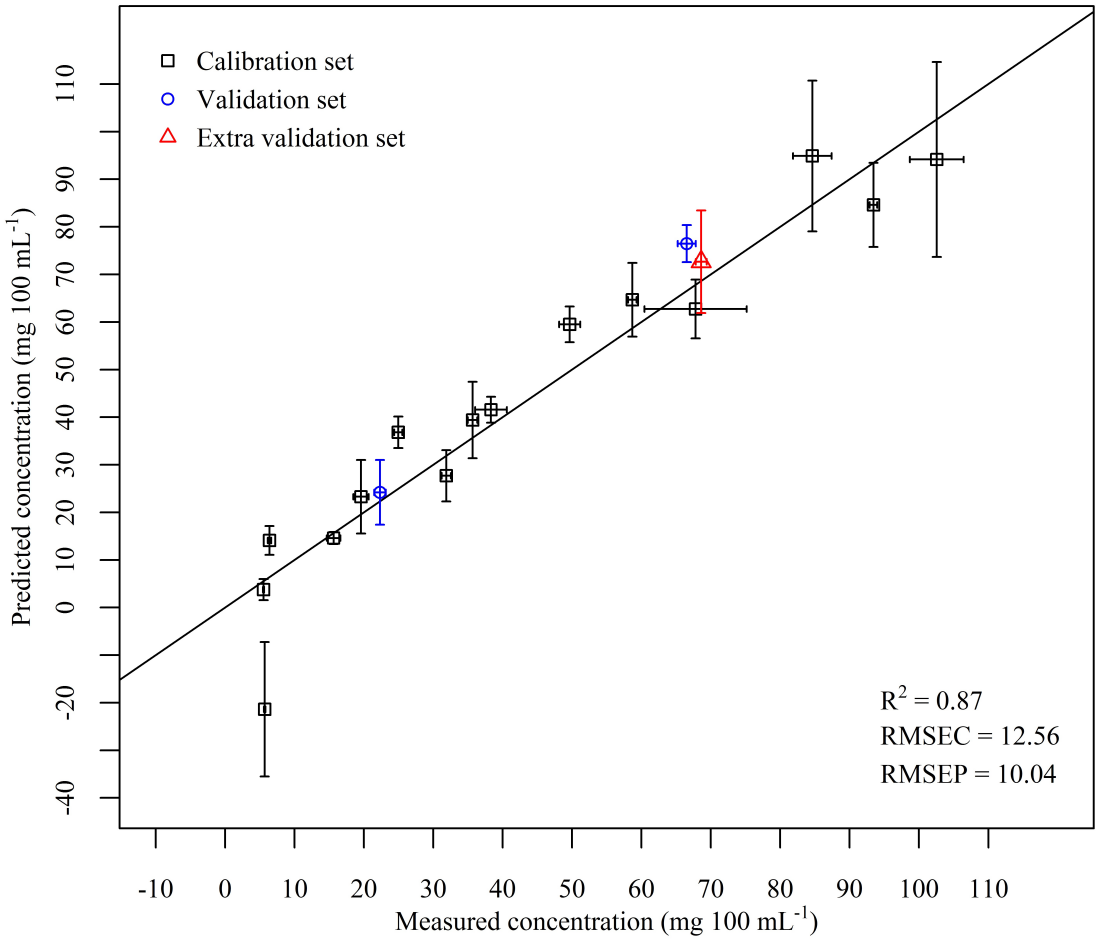

Figure 6.4: Predicted versus measured Ca contents for the calibration (N = 45), validation (N = 6) and extra validation (N = 3) datasets obtained via simple linear regression at 422.67 nm. RMSE values are expressed in mg 100 mL^{-1}.

With the goal of improving the fit and accuracy of the regression, multivariate analysis with PLSR and spectral pre-processing were explored.

6.7 PLS modelling

6.7.1 Model development and cross-validation

In order to develop a suitable calibration curve, spectra were normalised using the H I spectral line at 656.29 nm as internal standard and multivariate analysis was carried out. PLSR together with leave-one-out (LOO) cross-validation were applied to data corresponding to the three calibration batches. The wavelength area showing the probable wheel contribution (300–370 nm) was not included for PLSR. Although removing these wavelengths did not considerably impact the model performance, it slightly improved the results of R^2 and RMSE, especially concerning cross-validation.

LOO cross-validation was carried out to evaluate the performance of the models and determine the optimum number of latent variables (LV) (Cremers & Radziemski, 2013). The number of LVs to include for calibration was established based on the RMSECV (root-mean square error of cross-validation). The PLS model included 4 LVs since the RMSECV resulted in a minimum value of 10.23 mg 100 mL^{-1} (Table 6.2). This number of LVs explained approx. 95 % of the total variance of the model.

The calibration model exhibited suitable linearity shown by an R_c^2 of 0.96, which considerably improved the result obtained for univariate analysis (R_c^2 of 0.87 using three batches for calibration). When assessed by cross-validation an R_{cv}^2 value of 0.89 was obtained, indicating a good fit for the PLS model.

Table 6.2: PLS-model performance in terms of R^2 (coefficients of determination) and RMSE (root-mean-square error) values for calibration (N = 45), LOO cross-validation, and external validation using the validation dataset (N = 6).

No. LVs	Calibration		Cross-validation		Validation	
	R^2_c	RMSEC[a]	R^2_{cv}	RMSECV[a]	R^2_p	RMSEP[a]
2	0.66	18.36	0.59	20.16	0.14	20.48
3	0.86	11.89	0.80	13.98	0.89	7.43
4	0.96	6.56	0.89	10.23	0.91	6.45
5	0.99	3.20	0.88	10.69	0.92	6.23

[a] Expressed in milligrams per 100 millilitres.

6.7.2 Validation of the calibration model

As previously mentioned, validation was carried out to test the ability of the model to predict the Ca content of samples not included in the calibrations. Specifically, normalised spectral data of samples V1 and V2, with Ca contents of 22.32 and 66.53 mg 100 mL^{-1} respectively, were used for validation. Additionally, an extra validation sample V3, with Ca content of 68.61 mg 100 mL^{-1} was predicted to assess the ability of the models for predicting calcium content in different composition formulas.

The PLSR calibration curve as well as the predicted concentrations of the validation set and extra validation with sample V3 are presented in Figure 6.5. The y-axis shows the PLSR predicted concentrations, and the x-axis the reference Ca contents established by AAS. Ca contents and standard deviation values are in milligrams per 100 millilitres. In this figure, it can be observed that the highest and lowest Ca content samples (C1 and C5) presented higher standard deviations compared to that of the other samples. Lower accuracy for C1 and C5 measurements was also detected in the RSD values at 422.67 nm as shown in Figure 6.3.

Although this indicated that the concentration of these samples may be out of the optimum working range, the Ca content of sample C1 is below the minimum permitted level provided by the Codex Alimentarius Commission and C5 over the maximum.

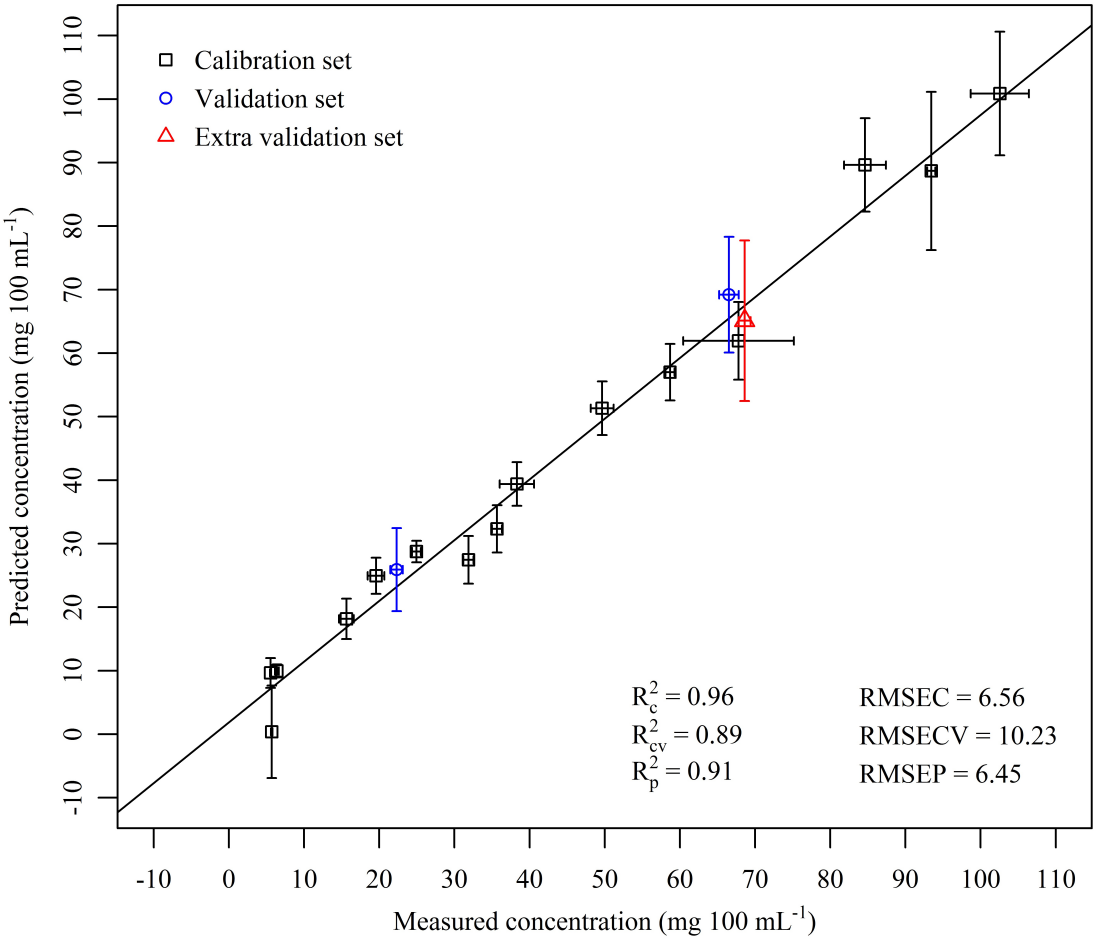

Figure 6.5: PLS model built with the spectral data normalised by the H I 656.29 nm emission line corresponding to the calibration set (N = 45). The graph also shows the predicted Ca contents for the validation (V1 and V2) and extra validation (V3) sets. RMSE values are expressed in mg 100 mL^{-1}.

When predicting the calcium contents of the validation set, the model exhibited a good predictive accuracy as corroborated by an R^2_p of 0.91 and a RMSEP (root-mean square error of prediction) value of 6.45 mg 100 mL^{-1}.

Regarding the extra validation set consisting of RTF-FOF (ready-to-feed follow-on formula); the PLS predicted calcium content was 65.10 mg 100 mL^{-1}, showing closeness to the measured value (68.61 mg 100 mL^{-1}). However, a high standard deviation of 12.64 mg 100 mL^{-1} (N = 3) was also observed for this measurement. The matrix or composition of follow-on formulas differ from that of IF, therefore, this result suggested that the model could still estimate the calcium concentration of products with a certain degree of variation.

In Chapter 4, the application of LIBS for calcium content determination in powdered IF was evaluated. Similarly, PLSR was employed to develop a quantitative model correlating LIBS spectra to reference Ca content. In that study, the PLS models rendered a similar fit in terms of the R_c^2 and R_{cv}^2. The current work therefore proves that, despite the difficulties associated with the direct analysis of liquids, LIBS combined with PLSR analysis obtained results as good as the analysis of solid samples. The direct analysis of liquids can also provide advantages such as a greater homogeneity of samples. Moreover, this method requires no sample preparation in comparison with powdered samples where a pellet is often required. This can be considerably beneficial for on-line/at-line applications in the industry, where small samples could be drawn from the process line directly to the system reservoir for analysis.

In another study reported in the literature (Bilge et al., 2018), the authors performed LIBS analysis of calcium in liquid milk using a configuration, which employed a sprayer and argon gas flow rate, that turned samples into aerosols to overcome difficulties associated with the analysis of liquids. In that publication, PLS calibration curves were reported with successful results with high coefficients of determination for calibration and validation (approx. $R^2 = 0.99$). In the work presented in this thesis, another strategy was proposed using a rotatory

wheel. The results in terms of coefficients of determination and root-mean-square errors were considered suitable for rapid analysis of RTF-IF provided that three independent batches were employed for calibration and no sample preparation was required.

6.8 Conclusions

In this work, LIBS combined with multivariate analysis was successfully employed for quantifying the calcium content of RTF-IF samples. The direct analysis of liquids can be problematic due to a number of effects such as splashing or formation of ripples on the liquid surface, which, as a result, hinder the sensitivity and repeatability of LIBS experiments. Here, the use of a sample chamber designed for the direct analysis of liquids was proposed as a method for mineral quantification in liquid food samples. This sample chamber uses a rotatory wheel to present the sample in the form of a thin film to the laser beam. Also, it offers the advantage that the sample is constantly replenished as the wheel rotates, thus the laser can be repeatedly pulsed on new spots of the liquid film.

PLSR was carried out to develop a suitable calibration model for calcium content prediction in RTF-IF samples. The PLS model obtained exhibited an R_c^2 of 0.96 and an R_{cv}^2 of 0.89, corroborating a good fit for the model. The RMSECV value was 10.23 mg 100 mL^{-1}. Validation of the calibration model was performed to test the robustness of the model obtaining an RMSEP value of 6.45 mg 100 mL^{-1}. These results illustrated the possibility of LIBS as a real-time tool for mineral analysis in liquid foods without the need for sample preparation, with added potential at-line/on-line applications.

Chapter 7

Concluding remarks and future recommendations

Infant formula faces strict regulations and must satisfy all standards of quality laid down by national and supranational authorities. For this reason, manufacturers need efficient and reliable analytical methods. Conventional methods used for the analysis of minerals in IF, although sensitive and accurate, generally involve long lasting sample preparation procedures, as well as the use of expensive consumables (e.g. argon) and highly corrosive substances (e.g. acids). Current trends in the area of food analysis aim at developing analytical methods with real-time monitoring capabilities. These methods could be used to timely measure core quality attributes providing real-time information on the physical and chemical properties of the materials; allowing to adjust for incoming sources of variability. Moreover, potentially minimising the dependence on off-line laboratory testing.

The research work developed in this thesis encompassed the use of LIBS for mineral determination in powdered and liquid IF. Particularly, this work priori-

tised minimal sample preparation with the aim of assessing the potential of LIBS for at-line measurements of IF. This way, manufacturers could utilise this technology at the production line, for instance, to verify whether the product reached the target concentration of the desired minerals.

In Chapter 4, the LIBS system, along with PLSR, was successfully employed to predict calcium contents of PIF samples over a range of calcium in conformity with the Codex Alimentarius Commission regulations; thus, a range of calcium relevant for IF manufacturing. The development and validation of the PLS calibration model were carried out using three different independent sample batches in order to ensure the reproducibility of the method. The model showed a suitable fit and robustness; allowing a reasonable predictive accuracy of calcium content.

The prediction of sodium contents in PIF mixtures was also successfully conducted in Chapter 5. As seen for calcium, LIBS analysis were performed over a range of sodium in conformity with the product's regulatory guidelines. Therefore, demonstrating the feasibility of the technique as a rapid at-line tool for sodium content determination in IF manufacturing. Multivariate analysis with PLSR was employed for modeling LIBS spectra obtained from data processed by a range of different pre-processing techniques, measuring depths and accumulations. The developed models were then compared in terms of PLS performance to establish the optimum aforementioned pre-processing, measuring depth and number of accumulations. The best performing PLS model showed a high R_p^2 and low RMSEP; proving its ability to accurately predict samples not included in the calibration dataset.

In conclusion, to this point, LIBS proved to be successful both for calcium and sodium content prediction in PIF samples. Two minerals being among the most abundant in IF, as well as indispensable for infant growth and development.

Furthermore, the chemical mapping conducted in this experiment allowed a better understanding of mineral distribution within the samples. Moreover, it demonstrated the possibility of LIBS to extract not only chemical, but also spatial information from the sample surface; even within the selected (relevant) range for IF manufacturing.

Lastly, regarding Chapter 6, calcium content determination in RTF-IF was also evaluated. The LIBS configuration used in the experiments, i.e. a LIBS system fitted with a liquid sample chamber, combined with multivariate analysis, showed a suitable performance in terms of PLSR calibration and a predictive accuracy as good as LIBS prediction of solid (powdered) IF samples. Therefore, substantiating that LIBS can also be utilised to infer mineral contents of liquid IF. Moreover, illustrating the possibility of LIBS as a real-time tool for mineral analysis in liquid foods, without the need for sample preparation; and with added potential at-line/on-line applications.

Given the relatively low cost and advantages of LIBS, IF manufacturers could benefit from the application of this technology to rapidly establish whether the contents of these minerals lie within the permitted values and modify the production process accordingly. In this regard, LIBS could be implemented at the initial stages of the manufacturing process to analyse the liquid IF preparation after the addition of minerals, or to verify the raw material premixes to be added to the preparation. As seen in Chapter 6, the analysis of liquids could be performed at-line without any sample preparation procedure. Alternatively, LIBS could be applied after spray drying and before packaging to determine if the product, in a powder form, fulfils the specifications of mineral contents. In this case, a certain degree of sample preparation (pressing powders into pellets) would be recommended to avoid loose particles being ejected as a consequence of the firing of

the laser. It is important to note that LIBS is a multielemental analysis technique as discussed below in future recommendations; thus, adding the possibility of determining the contents of multiple elements at once.

Following the concluding remarks of the thesis, a list of recommendations, which could be explored in future research, is proposed below:

- Assessment of optimal strategies for multielemental analysis of IF (or other food products). LIBS is a multielemental technique, i.e. multiple elements are assessed at a time. However, finding an optimal procedure, including sample preparation, pre-processing techniques and multivariate analysis, to obtain accurate results for all desired elements at the same time, may not be straightforward.

- Development of LIBS as a rapid food authenticity tool. For instance, studies involving the application of a high resolution LIBS system for measuring isotope ratios in food products could be carried out. In this regard, the isotope ratios of pertinent elements could be utilised to track the origin of certain food products.

- Evaluation of strategies to enhance LIBS sensitivity. For instance, with the use of nanoparticles as a means of increasing plasma ablation and photon characteristic emission (Tang, Hao, & Hu, 2019), or the removal of air in the sample chamber (or around the plasma formation area) by pumping in inert gases such as argon, nitrogen or helium. Inert gases enhance the sensitivity of LIBS by preventing the reaction of the sample plasma with air (Lin, Lin, & Guo, 2019). Although these strategies would be beneficial in terms of LIBS detection ability, it would be detrimental as to the speed of analysis, incrementing the length of sample preparation; cost and/or transportability

of the system. Therefore, these strategies would preferably be aimed at developing LIBS as a sensitive tool, in contrast with the rapid detection tool proposed in the work carried out in this thesis.

- Regarding the analysis of liquids, other possibilities could be assessed. For instance, using the same LIBS configuration as Chapter 6; however, exploring wheels made of other materials, e.g. a graphite wheel, which may simplify subsequent analysis of the spectra due to a lower interference of the wheel material on the emission at certain wavelengths; or using a binder (e.g. cellulose) to form a higher viscosity liquid/paste, so that it could potentially result in a higher adherence on the wheel surface, allowing an increased ablation of the sample material. Alternatively, other strategies not involving a liquid sample chamber could also be investigated, e.g. turning the liquid into an aerosol (Bilge et al., 2018).

List of Publications

First author

1. **Cama-Moncunill, X.**, Markiewicz-Keszycka, M., Cama-Moncunill, R., Dixit, Y., Casado-Gavalda, M. P., Cullen, P. J., & Sullivan, C. (2018). Sampling effects on the quantification of sodium content in infant formula using laser-induced breakdown spectroscopy (LIBS). *International Dairy Journal*, 85, 49–55. doi:10.1016/j.idairyj.2018.04.014

2. **Cama-Moncunill, X.**, Markiewicz-Keszycka, M., Dixit, Y., Cama-Moncunill, R., Casado-Gavalda, M. P., Cullen, P. J., & Sullivan, C. (2017). Feasibility of laser-induced breakdown spectroscopy (LIBS) as an at-line validation tool for calcium determination in infant formula. *Food Control*, 78, 304–310. doi:10.1016/j.foodcont.2017.03.005

Co-author

3. Markiewicz-Keszycka, M., Casado-Gavalda, M.P., **Cama-Moncunill, X.**, Cama-Moncunill, R., Dixit, Y., Cullen, P.J., & Sullivan, C. (2018). Laser-induced breakdown spectroscopy (LIBS) for rapid analysis of ash, potassium and magnesium in gluten free flours. *Food Chemistry*, 244, 324–330. doi:10.1016/j.foodchem.2017.10.063

4. Cama-Moncunill, R., Casado-Gavalda, M. P., **Cama-Moncunill, X.**, Markiewicz-Keszycka, M., Dixit, Y., Cullen, P. J., & Sullivan, C. (2017). Quantification of trace metals in infant formula premixes using laser-induced breakdown spectroscopy. *Spectrochimica Acta Part B: Atomic Spectroscopy*, 135, 6–14. doi:10.1016/j.sab.2017.06.014

5. Dixit, Y., Casado-Gavalda, M. P., Cama-Moncunill, R., Markiewicz-Keszycka, M., **Cama-Moncunill, X.**, Cullen, P. J., & Sullivan, C. (2017). Quantification of rubidium as a trace element in beef using laser-induced breakdown spectroscopy. *Meat Science*, 130, 47–49. doi:10.1016/j.meatsci.2017.03.013

6. Markiewicz-Keszycka, M., **Cama-Moncunill, X.**, Casado-Gavalda, M. P., Dixit, Y., Cama-Moncunill, R., Cullen, P. J., & Sullivan, C. (2017). Laser-induced breakdown spectroscopy (LIBS) for food analysis: A review. *Trends in Food Science & Technology*, 65, 80–93. doi:10.1016/j.tifs.2017.05.005

7. Casado-Gavalda, M. P., Dixit, Y., Geulen, D., Cama-Moncunill, R., **Cama-Moncunill, X.**, Markiewicz-Keszycka, M., Cullen, P. J., & Sullivan, C. (2017). Quantification of copper content with laser-induced breakdown spectroscopy as a potential indicator of offal adulteration in beef. *Talanta*, 169, 123–129. doi:10.1016/j.talanta.2017.03.071

8. Dixit, Y., Casado-Gavalda, M. P., Cama-Moncunill, R., **Cama-Moncunill, X.**, Markiewicz-Keszycka, M., Cullen, P. J., & Sullivan, C. (2017). Laser-induced breakdown spectroscopy for quantification of sodium and potassium in minced beef: a potential technique for detecting beef kidney adulteration. *Anal. Methods*, 9, 3314–3322. doi:10.1039/C7AY00757D

Conferences

- **Cama-Moncunill, X.**, Markiewicz-Keszycka, M., Dixit, Y., Cama-Moncunill, R., Casado-Gavalda, M., Cullen, P. J., & Sullivan, C. Feasibility of LIBS for prediction of minerals in powdered infant formula. (Oral presentation). *SciX*, 8–13 October 2017. Reno, Nevada, USA.

- **Cama-Moncunill, X.**, Markiewicz-Keszycka, M., Casado-Gavalda, M., Cama-Moncunill, R., Dixit, Y., Cullen, P. J., & Sullivan, C. Calcium quantification in infant formula via a novel laser-induced breakdown spectroscopy system. (Oral presentation). *Food Factor I*, 2–4 November 2016. Barcelona, Catalonia, Spain.

- Markiewicz-Keszycka, M., **Cama-Moncunill, X.**, Casado-Gavalda, M. P., Cullen, P. J., & Sullivan, C. Laser induced breakdown spectroscopy for quantification of minerals in powdered infant formula. (Oral presentation). *Innovations in Food Science and Human Nutrition*, 13–15 September 2018. Rome, Italy.

- Dixit, Y., Casado-Gavalda, M. P., Cama-Moncunill, R., **Cama-Moncunill, X.**, Markiewicz-Keszycka, M., El-Arnaout, T., Cullen, P. J., & Sullivan, C. Detecting offal adulteration in meat using LIBS. (Poster presentation). *Food Factor I*, 2–4 November 2016. Barcelona, Catalonia, Spain.

References

Abdel-Salam, Z., Al Sharnoubi, J., & Harith, M. A. (2013). Qualitative evaluation of maternal milk and commercial infant formulas via LIBS. *Talanta*, *115*, 422–426. doi:10.1016/j.talanta.2013.06.003

Abdi, H. (2010). Partial least squares regression and projection on latent structure regression (PLS Regression). *Wiley Interdisciplinary Reviews: Computational Statistics*, *2*(1), 97–106. doi:10.1002/wics.51

Allegrini, F., & Olivieri, A. C. (2014). IUPAC-Consistent Approach to the Limit of Detection in Partial Least-Squares Calibration. *Analytical Chemistry*, *86*(15), 7858–7866. doi:10.1021/ac501786u

Anabitarte, F., Cobo, A., & Lopez-Higuera, J. M. (2012). Laser-Induced Breakdown Spectroscopy: Fundamentals, Applications, and Challenges. *ISRN Spectroscopy*, *2012*, 12. doi:10.5402/2012/285240

Andersen, M.-B. S., Frydenvang, J., Henckel, P., & Rinnan, Å. (2016). The potential of laser-induced breakdown spectroscopy for industrial at-line monitoring of calcium content in comminuted poultry meat. *Food Control*, *64*, 226–233. doi:10.1016/j.foodcont.2016.01.001

AOAC. (2000). *Official methods of analysis* (17th ed.). Gaithersburg, MD, USA: AOAC international.

Babos, D. V., Barros, A. I., Nóbrega, J. A., & Pereira-Filho, E. R. (2019). Calibration strategies to overcome matrix effects in laser-induced breakdown

spectroscopy: Direct calcium and phosphorus determination in solid mineral supplements. *Spectrochimica Acta Part B: Atomic Spectroscopy*, *155*, 90–98. doi:10.1016/j.sab.2019.03.010

Beldjilali, S., Borivent, D., Mercadier, L., Mothe, E., Clair, G., & Hermann, J. (2010). Evaluation of minor element concentrations in potatoes using laser-induced breakdown spectroscopy. *Spectrochimica Acta Part B: Atomic Spectroscopy*, *65*(8), 727–733. doi:10.1016/j.sab.2010.04.015

Bilge, G., Boyac, s. H., Eseller, K. E., Tamer, U., & Çakr, S. (2015). Analysis of bakery products by laser-induced breakdown spectroscopy. *Food chemistry*, *181*, 186–90. doi:10.1016/j.foodchem.2015.02.090

Bilge, G., Sezer, B., Boyaci, I. H., Eseller, K. E., & Berberoglu, H. (2018). Performance evaluation of laser induced breakdown spectroscopy in the measurement of liquid and solid samples. *Spectrochimica Acta Part B: Atomic Spectroscopy*, *145*, 115–121. doi:10.1016/J.SAB.2018.04.016

Bilge, G., Sezer, B., Eseller, K. E., Berberoglu, H., Topcu, A., & Boyaci, I. H. (2016). Determination of whey adulteration in milk powder by using laser induced breakdown spectroscopy. *Food Chemistry*, *212*, 183–188. doi:10.1016/j.foodchem.2016.05.169

Bilge, G., Velioglu, H. M., Sezer, B., Eseller, K. E., & Boyaci, I. H. (2016). Identification of meat species by using laser-induced breakdown spectroscopy. *Meat science*, *119*, 118–122. doi:10.1016/j.meatsci.2016.04.035

Blanchard, E., Zhu, P., & Schuck, P. (2013). Infant formula powders. In B. Bhandari, N. Bansal, M. Zhang, & P. Schuck (Eds.), *Handbook of food powders* (pp. 465–483). Cambridge, UK: Woodhead Publishing. doi:10.1533/9780857098672.3.465

Cama-Moncunill, R., Casado-Gavalda, M. P., Cama-Moncunill, X., Markiewicz-Keszycka, M., Dixit, Y., Cullen, P. J., & Sullivan, C. (2017). Quantification

of trace metals in infant formula premixes using laser-induced breakdown spectroscopy. *Spectrochimica Acta Part B: Atomic Spectroscopy*, *135*, 6–14. doi:10.1016/j.sab.2017.06.014

Câmara, A. B. F., de Carvalho, L. S., de Morais, C. L. M., de Lima, L. A. S., de Araújo, H. O. M., de Oliveira, F. M., & de Lima, K. M. G. (2017). MCR-ALS and PLS coupled to NIR/MIR spectroscopies for quantification and identification of adulterant in biodiesel-diesel blends. *Fuel*, *210*, 497–506. doi:10.1016/J.FUEL.2017.08.072

Campbell, K. J., Hendrie, G., Nowson, C., Grimes, C. A., Riley, M., Lioret, S., & McNaughton, S. A. (2014). Sources and Correlates of Sodium Consumption in the First 2 Years of Life. *Journal of the Academy of Nutrition and Dietetics*, *114*(10), 1525–1532.e2. doi:10.1016/j.jand.2014.04.028

Casado-Gavalda, M. P., Dixit, Y., Geulen, D., Cama-Moncunill, R., Cama-Moncunill, X., Markiewicz-Keszycka, M., ... Sullivan, C. (2017). Quantification of copper content with laser induced breakdown spectroscopy as a potential indicator of offal adulteration in beef. *Talanta*, *169*, 123–129. doi:10.1016/j.talanta.2017.03.071

Clarivate Analytics. (2019). *Web of Science [v.5.32] – All Databases Basic Search.* Retrieved 2019-04-04, from https://apps.webofknowledge.com/UA_GeneralSearch_input.do?product=UA&SID=D3N33QKh5nIGBbw8mEM&search_mode=GeneralSearch

Codex. (2007). *Standard for infant formula and formulas for special medical purposes intended for infants, CODEX STAN 72 1981.* Rome, Italy: FAO/WHO Codex Alimentarius.

Cremers, D. A., & Radziemski, L. J. (2013). *Handbook of Laser-Induced Breakdown Spectroscopy* (2nd ed.). Chichester, UK: John Wiley & Sons Ltd.

Cullen, P., Bakalis, S., & Sullivan, C. (2017). Advances in control of food mixing

operations. *Current Opinion in Food Science*, *17*(Supplement C), 89–93. doi:10.1016/j.cofs.2017.11.002

De Giacomo, A., Dell'Aglio, M., Colao, F., Fantoni, R., & Lazic, V. (2005). Double-pulse LIBS in bulk water and on submerged bronze samples. *Applied Surface Science*, *247*(1-4), 157–162. doi:10.1016/J.APSUSC.2005.01.034

de Kruif, C. G., Huppertz, T., Urban, V. S., & Petukhovb, A. V. (2012). Casein micelles and their internal structure. *Advances in Colloid and Interface Science*, *171–172*, 36–52. doi:10.1016/J.CIS.2012.01.002

Dixit, Y., Casado-Gavalda, M. P., Cama-Moncunill, R., Cama-Moncunill, X., Markiewicz-Keszycka, M., Jacoby, F., ... Sullivan, C. (2017). Introduction to laser induced breakdown spectroscopy imaging in food: Salt diffusion in meat. *Journal of Food Engineering*. doi:10.1016/j.jfoodeng.2017.08.010

Dixit, Y., Casado-Gavalda, M. P., Cama-Moncunill, R., Markiewicz-Keszycka, M., Cama-Moncunill, X., Cullen, P. J., & Sullivan, C. (2017). Quantification of rubidium as a trace element in beef using laser induced breakdown spectroscopy. *Meat Science*, *130*, 47–49. doi:10.1016/j.meatsci.2017.03.013

dos Santos Augusto, A., Barsanelli, P. L., Pereira, F. M. V., & Pereira-Filho, E. R. (2017). Calibration strategies for the direct determination of Ca, K, and Mg in commercial samples of powdered milk and solid dietary supplements using laser-induced breakdown spectroscopy (LIBS). *Food Research International*, *94*, 72–78. doi:10.1016/j.foodres.2017.01.027

El Haddad, J., Canioni, L., & Bousquet, B. (2014). Good practices in LIBS analysis: Review and advices. *Spectrochimica Acta Part B: Atomic Spectroscopy*, *101*, 171–182. doi:10.1016/j.sab.2014.08.039

European Commission. (2006). *Commission Directive 2006/141/EC of 22 December 2006 on infant formulae and follow-on formulae and amending Directive 1999/21/EC (Text with EEA relevance)*. Official Journal of the European

Union. Retrieved from http://eur-lex.europa.eu/legal-content/EN/ALL/?uri=CELEX:32006L0141

FAO/WHO. (2004). *Vitamin and mineral requirements in human nutrition* (2nd ed.). Geneva, Switzerland: World Health Organization. Retrieved from http://www.who.int/nutrition/publications/micronutrients/9241546123/en/

FAO/WHO. (2019). *About Codex Alimentarius*. Retrieved 2019-08-12, from http://www.fao.org/fao-who-codexalimentarius/about-codex/en/

FDA. (2004). *Guidance for Industry PAT A Framework for Innovative Pharmaceutical Development, Manufacturing, and Quality Assurance*. Rockville, USA: U.S. Department of Health and Human Services.

Ferreira, E. C., Menezes, E. A., Matos, W. O., Milori, D. M. B. P., Nogueira, A. R. A., & Martin-Neto, L. (2010). Determination of Ca in breakfast cereals by laser induced breakdown spectroscopy. *Food Control*, *21*(10), 1327–1330. doi:10.1016/j.foodcont.2010.04.004

Gondal, M. A., Habibullah, Y. B., Baig, U., & Oloore, L. E. (2016). Direct spectral analysis of tea samples using 266nm UV pulsed laser-induced breakdown spectroscopy and cross validation of LIBS results with ICP-MS. *Talanta*, *152*, 341–352. doi:10.1016/j.talanta.2016.02.030

Guo, M. (2014a). 1 – Introduction: trends and issues in breastfeeding and the use of infant formula. In M. Guo (Ed.), *Human milk biochemistry and infant formula manufacturing technology* (pp. 1–16). Cambridge, UK: Woodhead Publishing. doi:10.1533/9780857099150.1

Guo, M. (2014b). 2 – Chemical composition of human milk. In M. Guo (Ed.), *Human milk biochemistry and infant formula manufacturing technology* (pp. 19–32). Cambridge, UK: Woodhead Publishing. doi:10.1533/9780857099150.1.19

Guo, M., & Ahmad, S. (2014a). 6 – Formulation guidelines for infant formula. In M. Guo (Ed.), *Human milk biochemistry and infant formula manufacturing technology* (pp. 141–171). Cambridge, UK: Woodhead Publishing. doi:10.1533/9780857099150.2.141

Guo, M., & Ahmad, S. (2014b). 7 – Ingredients selection for infant formula. In M. Guo (Ed.), *Human milk biochemistry and infant formula manufacturing technology* (pp. 172–210). Cambridge, UK: Woodhead Publishing. doi:10.1533/9780857099150.2.172

Hahn, D. W., & Omenetto, N. (2010). Laser-Induced Breakdown Spectroscopy (LIBS), Part I: Review of Basic Diagnostics and Plasma – Particle Interactions: Still-Challenging Issues within the Analytical Plasma Community. *Applied Spectroscopy*, *64*(12), 335A–336A. doi:10.1366/000370210793561691

Hahn, D. W., & Omenetto, N. (2012). Laser-Induced Breakdown Spectroscopy (LIBS), Part II: Review of Instrumental and Methodological Approaches to Material Analysis and Applications to Different Fields. *Applied Spectroscopy*, *66*(4), 347-419. doi:10.1366/11-06574

Happe, R. P., & Gambelli, L. (2015). 12 – Infant formula. In G. Talbot (Ed.), *Specialty oils and fats in food and nutrition* (pp. 285–315). Cambridge, UK: Woodhead Publishing. doi:10.1016/B978-1-78242-376-8.00012-0

Hibbert, D. B., & Gooding, J. J. (2006). *Data Analysis for Chemistry. An Introductory Guide for Students and Laboratory Scientists*. New York, USA: Oxford University Press.

Hu, H., Huang, L., Liu, M., Chen, T., Yang, P., & Yao, M. (2015). Nondestructive Determination of Cu Residue in Orange Peel by Laser Induced Breakdown Spectroscopy. *Plasma Science and Technology*, *17*(8), 711. doi:10.1088/1009-0630/17/8/17

Ikem, A., Nwankwoala, A., Odueyungbo, S., Nyavor, K., & Egiebor, N. (2002). Levels of 26 elements in infant formula from USA, UK, and Nigeria by microwave digestion and ICPOES. *Food Chemistry*, *77*(4), 439–447. doi:10.1016/S0308-8146(01)00378-8

International Organization for Standardization. (2008). *Guide 98-3. Uncertainty of measurement – Part 3: Guide to the expression of uncertainty in measurement (GUM:1995)* (1st ed.). Geneva, Switzerland: ISO/IEC.

Jantzi, S. C., Motto-Ros, V., Trichard, F., Markushin, Y., Melikechi, N., & De Giacomo, A. (2016). Sample treatment and preparation for laser-induced breakdown spectroscopy. *Spectrochimica Acta Part B: Atomic Spectroscopy*, *115*, 52–63. doi:10.1016/j.sab.2015.11.002

Jet Propulsion Laboratory (NASA). (2015). *Looking Up at Mars Rover Curiosity in 'Buckskin' Selfie.* Retrieved 2018-03-22, from https://www.jpl.nasa.gov/spaceimages/details.php?id=pia19808

Jiang, Y. J. (2014). 11 – Infant formula product regulation. In M. Guo (Ed.), *Human milk biochemistry and infant formula manufacturing technology* (pp. 273–310). Cambridge, UK: Woodhead Publishing. doi:10.1533/9780857099150.3.273

Jiang, Y. J., & Guo, M. (2014). 8 – Processing technology for infant formula. In M. Guo (Ed.), *Human milk biochemistry and infant formula manufacturing technology* (pp. 211–229). Cambridge, UK: Woodhead Publishing. doi:10.1533/9780857099150.2.211

John, K. A., Cogswell, M. E., Zhao, L., Maalouf, J., Gunn, J. P., & Merritt, R. K. (2016). US consumer attitudes toward sodium in baby and toddler foods. *Appetite*, *103*, 171–175. doi:10.1016/J.APPET.2016.04.009

Kim, G., Kwak, J., Choi, J., & Park, K. (2012). Detection of Nutrient Elements and Contamination by Pesticides in Spinach and Rice Samples Using Laser-

Induced Breakdown Spectroscopy (LIBS). *Journal of Agricultural and Food Chemistry*, *60*(3), 718–724. doi:10.1021/jf203518f

Kim, T., & Li, C.-T. (2012). Laser-Induced Breakdown Spectroscopy. In M. A. Farrukh (Ed.), *Advanced aspects of spectroscopy* (pp. 131–164). InTech. doi:10.5772/48281

Kramida, A., Ralchenko, Y., Reader, J., & NIST ASD team. (2016). *NIST Atomic Spectra Database (version 5.4)*. Retrieved 2017-12-04, from https://www.nist.gov/pml/atomic-spectra-database

Kress-Rogers, E., & Brimelow, C. J. (2001). Appendix A – Glossary: terms in instrumentation and sensors technology. In E. Kress-Rogers & C. J. Brimelow (Eds.), *Instrumentation and sensors for the food industry (second edition)* (2nd ed., pp. 779–799). Cambridge, UK: Woodhead Publishing. doi:10.1533/9781855736481.appendices

Kumar, N., Bansal, A., Sarma, G., & Rawal, R. K. (2014). Chemometrics tools used in analytical chemistry: An overview. *Talanta*, *123*, 186 - 199. doi:https://doi.org/10.1016/j.talanta.2014.02.003

Lal, B., St-Onge, L., Yueh, F.-Y., & Singh, J. P. (2007). 12 LIBS Technique for Powder Materials. In J. P. Singh & S. N. Thakur (Eds.), *Laser-induced breakdown spectroscopy* (1st ed. ed., pp. 287–311). Amsterdam, The Netherlands: Elsevier. doi:10.1016/B978-044451734-0.50015-6

Lazic, V., & Jovićević, S. (2014). Laser induced breakdown spectroscopy inside liquids: Processes and analytical aspects. *Spectrochimica Acta Part B: Atomic Spectroscopy*, *101*, 288–311. doi:10.1016/J.SAB.2014.09.006

Lei, W. Q., El Haddad, J., Motto-Ros, V., Gilon-Delepine, N., Stankova, A., Ma, Q. L., ... Yu, J. (2011). Comparative measurements of mineral elements in milk powders with laser-induced breakdown spectroscopy and inductively coupled plasma atomic emission spectroscopy. *Analytical and Bioanalytical*

Chemistry, *400*(10), 3303–3313. doi:10.1007/s00216-011-4813-x

Lesniewicz, A., Wroz, A., Wojcik, A., & Zyrnicki, W. (2010). Mineral and nutritional analysis of Polish infant formulas. *Journal of Food Composition and Analysis*, *23*(5), 424–431. doi:10.1016/j.jfca.2010.02.005

Liland, K. H., Mevik, B.-H., & Canteri, R. (2015). *baseline: Baseline Correction of Spectra*. Retrieved from https://cran.r-project.org/web/packages/baseline/index.html

Lin, J., Lin, X., & Guo, L. (2019). Enhancement effects of different elements by argon shield in laser induced breakdown spectroscopy. *Optik*, *accepted manuscript*. doi:10.1016/J.IJLEO.2018.10.146

Liu, Y., Gigant, L., Baudelet, M., & Richardson, M. (2012). Correlation between laser-induced breakdown spectroscopy signal and moisture content. *Spectrochimica Acta Part B: Atomic Spectroscopy*, *73*, 71–74. doi:10.1016/j.sab.2012.07.009

Lopes, J. A., Costa, P. F., Alves, T. P., & Menezes, J. C. (2004). Chemometrics in bioprocess engineering: process analytical technology (PAT) applications. *Chemometrics and Intelligent Laboratory Systems*, *74*(2), 269–275. doi:10.1016/j.chemolab.2004.07.006

Ma, F., & Dong, D. (2014). A Measurement Method on Pesticide Residues of Apple Surface Based on Laser-Induced Breakdown Spectroscopy. *Food Analytical Methods*, *7*(9), 1858–1865. doi:10.1007/s12161-014-9828-4

Marino, L. V., Meyer, R., & Cooke, M. L. (2013). Cost comparison between powdered versus energy dense infant formula for undernourished children in a hospital setting. *e-SPEN Journal*, *8*(4), e145–e149. doi:10.1016/J.CLNME.2013.04.002

Markiewicz-Keszycka, M., Cama-Moncunill, X., Casado-Gavalda, M. P., Dixit, Y., Cama-Moncunill, R., Cullen, P. J., & Sullivan, C. (2017). Laser-induced

breakdown spectroscopy (LIBS) for food analysis: A review. *Trends in Food Science & Technology*, *65*, 80–93. doi:10.1016/j.tifs.2017.05.005

Markiewicz-Keszycka, M., Casado-Gavalda, M. P., Cama-Moncunill, X., Cama-Moncunill, R., Dixit, Y., Cullen, P. J., & Sullivan, C. (2018). Laser-induced breakdown spectroscopy (LIBS) for rapid analysis of ash, potassium and magnesium in gluten free flours. *Food Chemistry*, *244*, 324–330. doi:10.1016/j.foodchem.2017.10.063

Masotti, F., Erba, D., De Noni, I., & Pellegrino, L. (2012). Rapid determination of sodium in milk and milk products by capillary zone electrophoresis. *Journal of Dairy Science*, *95*(6), 2872–2881. doi:10.3168/JDS.2011-5146

Mbesse Kongbonga, Y. G., Ghalila, H., Onana, M. B., & Ben Lakhdar, Z. (2014). Classification of vegetable oils based on their concentration of saturated fatty acids using laser induced breakdown spectroscopy (LIBS). *Food chemistry*, *147*, 327–31. doi:10.1016/j.foodchem.2013.09.145

Mehder, A. O., Habibullah, Y. B., Gondal, M. A., & Baig, U. (2016). Qualitative and quantitative spectro-chemical analysis of dates using UV-pulsed laser induced breakdown spectroscopy and inductively coupled plasma mass spectrometry. *Talanta*, *155*, 124–32. doi:10.1016/j.talanta.2016.04.036

Mevik, B.-H., Wehrens, R., & Liland, K. H. (2015). *Pls: Partial least squares and principal component regression*. Retrieved from `https://cran.r-project.org/web/packages/pls/index.html`

Miller, J. N., & Miller, J. C. (2010). *Statistics and chemometrics for analytical chemistry* (6th ed. ed.). Harlow, UK: Pearson Education Limited.

Misra, N. N., Sullivan, C., & Cullen, P. J. (2015). Process Analytical Technology (PAT) and Multivariate Methods for Downstream Processes. *Current Biochemical Engineering*, *2*(1), 4–16. doi:10.2174/2213385203666150219231836

Moncayo, S., Manzoor, S., Rosales, J. D., Anzano, J., & Caceres, J. O. (2017). Qualitative and quantitative analysis of milk for the detection of adulteration by Laser Induced Breakdown Spectroscopy (LIBS). *Food Chemistry*, *232*, 322–328. doi:10.1016/j.foodchem.2017.04.017

Moncayo, S., Rosales, J. D., Izquierdo-Hornillos, R., Anzano, J., & Caceres, J. O. (2016). Classification of red wine based on its protected designation of origin (PDO) using Laser-induced Breakdown Spectroscopy (LIBS). *Talanta*, *158*, 185–191. doi:10.1016/j.talanta.2016.05.059

Montagne, D. H., Van Dael, P., Skanderby, M., & Hugelshofer, W. (2009). 9 Infant Formulae Powders and Liquids. In A. Y. Tamime (Ed.), *Dairy powders and concentrated products* (pp. 294–331). Oxford, UK: Blackwell Publishing.

Murgia, A., Scano, P., Contu, M., Ibba, I., Altea, M., Bussu, M., ... Caboni, P. (2016). Characterization of donkey milk and metabolite profile comparison with human milk and formula milk. *LWT - Food Science and Technology*, *74*, 427–433. doi:10.1016/j.lwt.2016.07.070

Pandelova, M., Lopez, W. L., Michalke, B., & Schramm, K.-W. (2012). Ca, Cd, Cu, Fe, Hg, Mn, Ni, Pb, Se, and Zn contents in baby foods from the EU market: Comparison of assessed infant intakes with the present safety limits for minerals and trace elements. *Journal of Food Composition and Analysis*, *27*(2), 120–127. doi:10.1016/j.jfca.2012.04.011

Pathak, A. K., Kumar, R., Singh, V. K., Agrawal, R., Rai, S., & Rai, A. K. (2012). Assessment of LIBS for Spectrochemical Analysis: A Review. *Applied Spectroscopy Reviews*, *47*(1), 14–40. doi:10.1080/05704928.2011.622327

Pehrsson, P. R., Patterson, K. Y., & Khan, M. A. (2014). Selected vitamins, minerals and fatty acids in infant formulas in the United States. *Journal of Food Composition and Analysis*, *36*(1), 66–71. doi:10.1016/j.jfca.2014.06.004

Peruchi, L. C., Nunes, L. C., de Carvalho, G. G. A., Guerra, M. B. B., de Almeida, E., Rufini, I. A., ... Krug, F. J. (2014). Determination of inorganic nutrients in wheat flour by laser-induced breakdown spectroscopy and energy dispersive X-ray fluorescence spectrometry. *Spectrochimica Acta Part B: Atomic Spectroscopy*, *100*, 129–136. doi:10.1016/j.sab.2014.08.025

Poitevin, E. (2016). Official Methods for the Determination of Minerals and Trace Elements in Infant Formula and Milk Products: A Review. *Journal of AOAC International*, *99*(1), 42–52. doi:10.5740/jaoacint.15-0246

R Core Team. (2014). *R: A language and environment for statistical computing*. Viena, Austria. Retrieved from http://www.r-poject.org/

Rai, N. K., & Rai, A. K. (2008). LIBS – An efficient approach for the determination of Cr in industrial wastewater. *Journal of Hazardous Materials*, *150*(3), 835–838. doi:10.1016/J.JHAZMAT.2007.10.044

Rai, V. N., Yueh, F. Y., & Singh, J. P. (2007). 10 – Laser-Induced Breakdown Spectroscopy of Liquid Samples. In J. Singh & S. Thakur (Eds.), *Laser-induced breakdown spectroscopy* (pp. 223–254). Amsterdam, The Netherlands: Elsevier. doi:10.1016/B978-044451734-0.50013-2

Rakovský, J., Čermák, P., Musset, O., & Veis, P. (2014). A review of the development of portable laser induced breakdown spectroscopy and its applications. *Spectrochimica Acta Part B: Atomic Spectroscopy*, *101*, 269–287. doi:10.1016/j.sab.2014.09.015

Rathore, A. S., Chopda, V. R., & Gomes, J. (2016). Knowledge management in a waste based biorefinery in the QbD paradigm. *Bioresource Technology*, *215*, 63–75. doi:10.1016/j.biortech.2016.03.168

Rinnan, Å., van den Berg, F., & Engelsen, S. B. (2009). Review of the most common pre-processing techniques for near-infrared spectra. *TrAC Trends in Analytical Chemistry*, *28*(10), 1201–1222. doi:10.1016/j.trac.2009.07.007

Sezer, B., Bilge, G., & Boyaci, I. H. (2017). Capabilities and limitations of LIBS in food analysis. *TrAC Trends in Analytical Chemistry*, *97*(Supplement C), 345–353. doi:10.1016/j.trac.2017.10.003

Sezer, B., Durna, S., Bilge, G., Berkkan, A., Yetiemeyen, A., & Boyaci, I. H. (2018). Identification of milk fraud using laser-induced breakdown spectroscopy (LIBS). *International Dairy Journal*, *81*, 1–7. doi:10.1016/J.IDAIRYJ.2017.12.005

Silva, A. S., Brandao, G. C., Matos, G. D., & Ferreira, S. L. C. (2015). Direct determination of chromium in infant formulas employing high-resolution continuum source electrothermal atomic absorption spectrometry and solid sample analysis. *Talanta*, *144*, 39–43. doi:10.1016/J.TALANTA.2015.05.046

Singh, J., Kumar, R., Awasthi, S., Singh, V., & Rai, A. K. (2017). Laser Induced breakdown spectroscopy: A rapid tool for the identification and quantification of minerals in cucurbit seeds. *Food Chemistry*, *221*, 1778–1783. doi:10.1016/j.foodchem.2016.10.104

Smith, G. P. S., Gordon, K. C., & Holroyd, S. E. (2013). Raman spectroscopic quantification of calcium carbonate in spiked milk powder samples. *Vibrational Spectroscopy*, *67*, 87–91. (10.1016/j.vibspec.2013.04.005)

Sobron, P., Wang, A., & Sobron, F. (2012). Extraction of compositional and hydration information of sulfates from laser-induced plasma spectra recorded under Mars atmospheric conditions – Implications for ChemCam investigations on Curiosity rover. *Spectrochimica Acta Part B: Atomic Spectroscopy*, *68*, 1–16. doi:10.1016/j.sab.2012.01.002

Sola-Larrañaga, C., & Navarro-Blasco, I. (2006). Preliminary chemometric study of minerals and trace elements in Spanish infant formulae. *Analytica Chimica Acta*, *555*(2), 354–363. doi:10.1016/j.aca.2005.09.015

St-Onge, L., Kwong, E., Sabsabi, M., & Vadas, E. B. (2004). Rapid analysis of liquid formulations containing sodium chloride using laser-induced breakdown spectroscopy. *Journal of Pharmaceutical and Biomedical Analysis*, *36*(2), 277–284. doi:10.1016/J.JPBA.2004.06.004

Tamm, A., Bolumar, T., Bajovic, B., & Toepfl, S. (2016). Salt (NaCl) reduction in cooked ham by a combined approach of high pressure treatment and the salt replacer KCl. *Innovative Food Science & Emerging Technologies*, *36*(Supplement C), 294 – 302. doi:10.1016/j.ifset.2016.07.010

Tang, H., Hao, X., & Hu, X. (2019). Spectral enhancement effect of LIBS based on the combination of Au nanoparticles with magnetic field. *Optik*, *179*, 1129 – 1133. doi:10.1016/J.IJLEO.2018.10.146

Tognoni, E., & Cristoforetti, G. (2016). Signal and noise in Laser Induced Breakdown Spectroscopy: An introductory review. *Optics & Laser Technology*, *79*, 164–172. doi:10.1016/j.optlastec.2015.12.010

Tognoni, E., Cristoforetti, G., Legnaioli, S., & Palleschi, V. (2010). Calibration-Free Laser-Induced Breakdown Spectroscopy: State of the art. *Spectrochimica Acta Part B: Atomic Spectroscopy*, *65*(1), 1–14. doi:10.1016/j.sab.2009.11.006

van den Berg, F., Lyndgaard, C. B., Sørensen, K. M., & Engelsen, S. B. (2013). Process Analytical Technology in the food industry. *Trends in Food Science & Technology*, *31*(1), 27–35. doi:10.1016/j.tifs.2012.04.007

Vavrusova, M., & Skibsted, L. H. (2014). Calcium nutrition. Bioavailability and fortification. *LWT - Food Science and Technology*, *59*(2), 1198–1204. doi:10.1016/j.lwt.2014.04.034

WHO. (2009). *Toxicological and Health Aspects of Melamine and Cyanuric Acid*. Geneva, Switzerland: World Health Organization. Retrieved from https://www.who.int/foodsafety/publications/melamine-cyanuric-acid/en

WHO. (2018). *Infant and young child feeding.* https://www.who.int/news-room/fact-sheets/detail/infant-and-young-child-feeding. (Accessed: 2019-04-23)

Yueh, F.-Y., Zheng, H., Singh, J. P., & Burgess, S. (2009). Preliminary evaluation of laser-induced breakdown spectroscopy for tissue classification. *Spectrochimica Acta Part B: Atomic Spectroscopy*, *64*(10), 1059–1067. doi:10.1016/j.sab.2009.07.025